BULLETIN OF RUSSIAN STATE MEDICAL UNIVERSITY

BIOMEDICAL JOURNAL OF PIROGOV RUSSIAN NATIONAL RESEARCH MEDICAL UNIVERSITY

Indexed in Scopus. CiteScore 2018: 0.16

Indexed in WoS. JCR 2018: 0.13

Five-year h-index is 3

Scopus®

WEB OF SCIENCE™

Google scholar

Indexed in RSCI. IF 2017: 0.326

Listed in HAC 27.01.2016 (no. 1760)

Open access to archive

НАУЧНАЯ ЭЛЕКТРОННАЯ БИБЛИОТЕКА
eLIBRARY.RU

ВЫСШАЯ АТТЕСТАЦИОННАЯ КОМИССИЯ (ВАК)

CYBERLENINKA

ВЕСТНИК РОССИЙСКОГО ГОСУДАРСТВЕННОГО МЕДИЦИНСКОГО УНИВЕРСИТЕТА

НАУЧНЫЙ МЕДИЦИНСКИЙ ЖУРНАЛ РНИМУ ИМ. Н. И. ПИРОГОВА

Contents
Содержание

NONINVASIVE PRENATAL TESTING: THE ASPECTS OF ITS INTRODUCTION INTO CLINICAL PRACTICE

Korostin DO[1,2] ✉, Plakhina DA[2], Belova VA[1,2]

[1] Pirogov Russian National Research Medical University, Moscow, Russia

[2] Genotek Ltd., Moscow, Russia

The last couple of years have witnessed the rapid development of prenatal molecular-based screening for fetal aneuploidies that utilizes the analysis of cell-free DNA circulating in the bloodstream of a pregnant woman. The present review looks at the potential and limitations of such testing and the possible causes of false-positive and false-negative results. The review also describes the underlying principles of data acquisition and analysis the testing involves. In addition, we talk about the opinions held by the expert community and some aspects of legislation on the use of noninvasive prenatal testing (NIPT) in clinical practice in the countries where NIPT is much more widespread than in Russia.

✉ **Correspondence should be addressed:** Dmitry O. Korostin
Nastavnichesky per. 17, str. 1, Moscow, 105120; d.korostin@gmail.com

НЕИНВАЗИВНЫЙ ПРЕНАТАЛЬНЫЙ МОЛЕКУЛЯРНЫЙ СКРИНИНГ: ОСОБЕННОСТИ ВНЕДРЕНИЯ В КЛИНИЧЕСКУЮ ПРАКТИКУ

Д. О. Коростин[1, 2] ✉, Д. А. Плахина[2], В. А. Белова[1,2]

[1] Российский национальный исследовательский медицинский университет имени Н. И. Пирогова, Москва, Россия

[2] ООО «Генотек», Москва, Россия

Развитие пренатального молекулярного скрининга анеуплоидий плода, основанного на анализе внеклеточной ДНК, циркулирующей в крови беременной, происходит бурно, особенно в последние 2–3 года. В обзоре представлены возможности и ограничения использования этой методики в клинической практике, а также причины ложноположительных и ложноотрицательных результатов скрининга. Описаны принципы, лежащие в основе технологий как получения, так и анализа данных. Рассмотрены мнения профессиональных сообществ, а также особенности законодательного регулирования применения неинвазивного пренатального скрининга (НИПС) в клинической практике в странах, где уровень использования НИПС существенно превышает отечественный.

✉ **Для корреспонденции:** Дмитрий Олегович Коростин
Наставнический переулок, д. 17, к. 1, г. Москва, 105120; d.korostin@gmail.com

Fetal chromosomal aneuploidy is one of the primary causes of spontaneous abortion, accountable for 35% of all miscarriages [1] and occurring in 0.3% of all births [2, 3]. The most common aneuploidies are trisomies 13, 18, 21 and XXY.

Trisomy 21, or Down syndrome (DS), is observed in 1 in 800 births [4]. The risk of fetal DS increases with maternal age, starting to grow exponentially once a woman turns 34 and approximating an incidence rate of 1 case per 35 births in women over 40 [5].

Until the 1980s, a woman's age was the only reliable prognostic criterion for the risk of aneuploidy; all pregnant women over 35 were recommended to undergo an invasive diagnostic test aimed to identify the karyotype of the fetus. For younger women, the only indication for invasive diagnostic procedures was a family history [6].

Today, the 1st trimester combined ultrasound and biochemical screening test proposed back in 1997 [7] is considered to be the most reliable prognostic tool with its sensitivity of 90% for Down syndrome and the false positive rate of 5% [8].

At present, only invasive diagnostic techniques are employed to diagnose hereditary pathologies of the fetus, including chorionic villus and amniotic fluid sampling. The obtained specimens of fetal cells are analyzed by QF-PCR, MLPA, G-banding, FISH, and molecular karyotyping [9].

Origin of cell-free fetal DNA

Cell-free fetal DNA (cffDNA) transcends the placental barrier and enters the maternal bloodstream [10]. Modern technologies can detect cffDNA in the maternal blood plasma as early as the 4th week of gestation. Its concentration increases throughout pregnancy, peaking in the last 8 weeks before delivery and then dropping abruptly to almost 0 in the first hours after birth [11–15]. Cell-free fetal DNA originates in the placental trophoblast and

leaks into the maternal bloodstream following the apoptosis of trophoblast cells [16]. The placental origin of cffDNA is corroborated by its presence in anembryonic pregnancies in which no embryo is formed, but placental tissue is in place [17], as well as in women with meiotic placental mosaicism (PM).

PM, which is essentially a discrepancy between the karyotypes of a fetus and a maternal placenta, strikes 0.6–1% of women who previously underwent invasive diagnostic procedures [18]. PM can be broken down into mitotic and meiotic types. Mitotic PM results from the chromosomal nondisjunction during one of the divisions of a diploid zygote that gives rise to an aneuploid cell line and leads to confined PM. As a rule, confined PM affects only a limited region of the placenta and can be defined as a low-level mosaicism. Meiotic PM originates from an initially trisomic zygote in which a rescue event occurs: the loss of an extra chromosome copy in the early stages of fetal development. Thus, even if the placenta is partially or fully aneuploid, the fetus can still have a normal karyotype, and vice versa.

Cell-free fetal DNA characteristics

Cell-free DNA molecules circulating in the maternal blood are chopped fragments of 166 bp (maternal cfDNA) or 143 bp (fetal cfDNA) in length [19]. Such size distribution is the result of nonrandom DNA fragmentation [20]. DNA is degraded by various enzymes that cut at the sites they can access. Nucleosomes represent the first level of DNA compaction. They are histone spools with DNA wound around them, spaced 20 base pairs apart. These linker regions can be easily accessed by nucleases. Therefore, we can assume that a 143 bp-long cffDNA fragment corresponds to a "linkerless" DNA coil wound around a nucleosome, whereas a 166 bp-long maternal cfDNA fragment corresponds to a DNA coil containing a linker region. The nonrandom fragmentation pattern can be explained by the difference in histone H1 isoforms determined by the placental or hematopoietic origin of nucleosomes. The main function of histone H1 is to bind to a linker; apparently, the binding does not occur in the case of cffDNA, and the linker is chopped off [19, 21].

The "sawtooth"-like size distribution of shorter DNA fragments with a peak periodicity of ~10 bp suggests that cell-free DNA undergoes further nuclease cleavage in apoptotic bodies at the position of approximately every 10th nucleotide directly attached to a histone protein [19, 22]. No similar size distribution is observed during the analysis of short reads mapped onto a mitochondrial genome that lacks histones.

It has been established that hypo- and hypermethylated regions of fetal and placental genomes do not match those of the maternal genome because of epigenetic difference between tissues [23, 24]. It is hypothesized [25] that unmethylated DNA regions are more accessible for cutting. Maternal cfDNA is hypermethylated, which means tighter DNA wrapping around histones, increased compaction and nucleosome stability, and longer average cfDNA fragment lengths in comparison with fetal DNA.

NIPT aided by MPS

Fetal cells, fetal cell-free RNA and fetal cell-free DNA are potential targets for liquid biopsy. Fetal cell-free DNA has a number of advantages that allow it to be used as a basis for noninvasive prenatal testing (NIPT).

On average, the fetal fraction amounts to 10% of total cell-free DNA at the gestational age when prenatal testing is performed. This value exceeds the number of fetal cells circulating in the maternal blood by 3–4 orders of magnitude.

The contribution of maternal microchimerism is normally negligible in comparison with the fetal DNA fraction. Cell-free DNA is more stable than cell-free RNA, and the methods used for its analysis are better reproducible.

NIPT can be described as a statistical examination aimed at estimating how well each chromosome is represented in a studied sample. Normally, the number of short reads per each chromosome of a nonpregnant woman is proportional to the length of this chromosome. The same is true for women who carry a child with a normal karyotype. However, in trisomies, as is the case with trisomy 21, the proportion of reads needed to cover all copies of the chromosome of interest will be increased relative to other chromosomes. The length of chromosome 21 amounts to about 1.5% of the entire genome. Given that the cffDNA fraction makes 10% of total cfDNA present in the sample, the extra chromosome 21 will cause a 0.08% rise in this value. To assess the reliability of NIPT results, different statistical methods are used, the most common being Fisher's Z test. It is employed to investigate whether an increase in the read count per chromosome of interest is accidental. The actual coverage is compared to the expected precalculated value with due account of the standard error. Z is calculated by the formula:

$$Z = (x - \mu)/\delta ,$$

where A is the studied chromosome; x is the number of reads mapped to A in the analyzed sample; μ is the mean read count needed to cover A in the reference sample (normal control); δ is the standard deviation. The resulting Z score > 3 suggests trisomy; $Z < -3$ suggests monosomy, whereas a range of values from −3 to 3 are indicative of a normal karyotype [26].

The expected value is calculated based on the analysis of a cell-free DNA sample obtained from a diagnosed child.

During the analysis, maternal cfDNA is not separated physically from fetal DNA. This means that if a woman carries multiples, NIPT will be able to detect aneuploidy but will not point to the affected fetus.

NIPT outcomes are largely determined by the fetal DNA fraction. The higher is the proportion of fetal DNA, the higher is the Z value yielded by the analysis in the case of aneuploidy. The minimum fetal fraction needed for reliable NIPT results is 4% [27–29].

Although methods for estimating the proportion of fetal DNA vary, they all share the same underlying principle, searching for significant differences between fetal and maternal cell-free DNA fractions. Such differences involve the presence of Y chromosome, which amounts to half of total cell-free DNA. This approach, however, can only be applied to women carrying male fetuses.

The universal and widespread SNP-based approach to estimating the fetal DNA fraction exploits a simple idea: one should look for those polymorphic loci where the mother is homozygous and the baby is heterozygous (due to the presence of the paternal allele). The polymorphic regions should be sequenced multiple times, and then the number of reads covering the paternal allele should be counted [30–32]. The cffDNA fraction is then calculated by multiplying the proportion of such reads by 2. The following criteria are applied to SNP selection:
• minor allele frequency (MAF) of about 50%;
• SNP should be constituents of different linkage groups;
• SNP should not be under natural selection pressure.

By expanding the panel of target SNPs, one can even detect aneuploidies through comparing read counts per fetal and maternal polymorphic loci in a chromosome of interest. This idea was adopted by Natera to design a noninvasive prenatal test based on the analysis of almost 20,000 SNP [33].

Fetal DNA fraction can also be reliably estimated by calculating the proportion of differentially methylated genome regions in the analyzed cell-free methylome [34].

Because the lengths of fetal and maternal DNA molecules are distributed nonuniformly, the fetal DNA fraction can be determined from the ratio of fragments sized 100–150 bp to those sized 163–169 bp, since they correspond to the fetal and maternal DNA fractions, respectively [35]. This approach is effective in paired-end sequencing [36].

Another novel "nucleosome track" method of quantifying the fetal DNA fraction is underway. The idea behind it is that fetal DNA fragmentation is not random and follows a certain pattern determined by DNA packaging into nucleosomes, as described above [37].

Researchers are also starting to harness neuronal networks to estimate the fetal DNA fraction. Using large training samples (thousands of specimens with a known fetal DNA fraction), one can get reliable results by analyzing a number of certain sequencing parameters [38].

NIPT potential

NIPT is mostly used to screen for chromosomal aneuploidies, but massively parallel sequencing (MPS) technologies are capable of detecting other genome abnormalities as well.

Low and ultra-low (< ×1.0) coverage genome sequencing does not allow point mutations to be detected, but can be employed to screen for deletions and duplications [39]. Such strategy is used to perform prenatal genetic screening aided by high-throughput sequencing [40]. In most cases, NIPT data resolution is not sufficient to capture medium-sized (up to 5 billion bp) deletions and duplications; this problem can be solved by improving data yield per studied sample [41–44]. Unfortunately, this adds to the costs of testing. More complex bioinformatic methods of data processing are a bit less effective [45, 46]. The amount of sequencing data yielded from the sites of interest can be significantly increased through targeted enrichment of genomic DNA regions. For example, the Panorama test [47] targets about 20,000 polymorphic loci densely located in the regions prone to microdeletions. The developers believe that the detection accuracy of the test is 97.8% or higher [48].

Since the moment cffDNA was discovered, the world has seen the emergence of various approaches to the diagnosis of genetic abnormalities of the fetus. The very first of them were capable of determining the sex of the fetus [49] and its Rh factor [50]; they were designed to screen for the sequences that do not typically occur in the maternal genome and exploited different PCR types, including qPCR, ddPRC, and QF-PCR. Later, the development of methods for detecting genetic traits inherited from the father became a routine practice: X-STR markers [51], markers of autosomal dominant conditions, such as Huntington's disease [52] and myotonic dystrophy [53] were soon discovered. However, the majority of monogenic diseases are autosomal-recessive and their development is driven by the mutations in both maternal and paternal copies of the genome. Because of that, prenatal screening typically includes 3 sequencing procedures: sequencing of maternal and paternal genomic DNA required to identify parental haplotypes and locate the mutations of interest followed by cfDNA sequencing in order to see what chromosomes the baby has inherited [54].

The analysis of the cffDNA methylome has revealed the pattern of methylation that can serve as an aneuploidy marker [55, 56]. It has been shown that the placental methylome, which is what NIPT analyzes, is dynamic; the methylation pattern can change depending on the condition of the fetus and the mother. For example, the analysis of cfDNA methylation can be used to diagnose preeclampsia [57–59].

Although there are a few disadvantages to using cell-free RNA as an analyte in screening tests (contamination by noninformative rRNA, poor preservation in the sample, low reproducibility of test results in comparison with cfDNA), changes in the expression of some RNA transcripts in the fetus can be a reliable predictor of preeclampsia long before a woman develops its symptoms [60].

NIPT validation

Like any other diagnostic technique, NIPT had to undergo clinical trials to prove its efficacy.

In 2014, a study conducted in 1,914 pregnant women from 21 US medical centers demonstrated that for NIPT the false-positive rate was significantly lower than for the standard biochemistry screening (0.3% vs. 3.6%, $p < 0.001$ for trisomy 21 and 0.2% vs. 0.6%, $p < 0.03$ for trisomy 18). The test failed in 0.9% of the participants [61].

A study published in 2015 compared the efficacy of NIPT with that of conventional diagnostic techniques [62]. It was conducted in 35 medical centers using the samples collected from 15,841 pregnancies. NIPT was able to detect all cases (38) of true aneuploidy in patients with fetal trisomy 21; in 9 patients the results were false-positive. For trisomy 21, DR was 100%, FPR was 0.06%, and PPV was 80.9% (the standard screening test used in the study returned 78.9%, 5.4%, and 3.4% for DR, FPR and PPV, respectively). NIPT performance was significantly better than that of standard screening in pregnant women with fetal trisomies 13 and 18. This means that NIPT can be used for detecting fetal trisomies in the clinical setting because it has better resolution and higher accuracy in comparison with conventional diagnostic tools.

Causes of false-positive results in NIPT

NIPT has a number of limitations that can cause false-positive results.

Maternal weight and gestational age

The amount of cffDNA correlates positively with the gestational age and is reversely proportional to the body mass index of a pregnant woman. Too few cffDNA fragments at 9–10 weeks into pregnancy do not allow NIPT results to be reliable. For women with high BMI, the test can turn to be ineffective as well, because the probability of a false-positive result remains high [15, 63] if cffDNA fraction is not estimated.

Placental mosaicism

Women who tested positive for aneuploidy by NIPT are advised to undergo an invasive diagnostic procedure to rule out placental mosaicism. Here, amniocentesis should be preferred over chorion villus sampling because the DNA in the villi has the same placental origin as cffDNA [64–67]. It is absolutely not recommended to base the decision of pregnancy termination on NIPT results solely (see below).

Twins

Although NIPT can detect aneuploidies in twin pregnancies, it is unable to identify which of the twins has a chromosomal abnormality. Here, invasive diagnostic techniques should be

employed. Despite the fact that the total cffDNA fraction is higher than in singleton pregnancies [68] and it is possible to estimate the fetal fraction for each of the twins, the accuracy of NIPT is lower than in the case with singleton pregnancies [69].

A vanishing twin syndrome occurs in multiple pregnancies when one of the fetuses dies in the first trimester. The frequency of aneuploidies among vanishing twins is higher than in healthy twins. Because NIPT analyzes total cell-free DNA and in the majority of cases cannot detect the presence of additional haplotypes in the samples, a vanishing twin can contribute to false-positive test results, being an aneuploid fetus itself; it can also mask the aneuploidy of the second twin, causing false-negative results and interfering with sex determination. The study that analyzed data yielded by over 30, 000 noninvasive prenatal tests demonstrates that vanishing twins with aneuploidies occur in 0.11% of the total sample [70]. This is quite close to the false-positive rate reported by an extensive meta-analysis of the literature on NIPT [71]. To avoid errors associated with vanishing twins and to timely detect the second fetus, ultrasound examinations performed in the 1st trimester should be more meticulous.

CNV in parents

It is reported that 17% of all false-positive NIPT results are associated with CNV 0.5 to 14 billion bp in size present in maternal cells [72].

Just like placental mosaicism, parental mosaicism can skew test results. For example, the frequency of monosomy X directly correlates with a woman's age [74]; 16% of sex chromosome aneuploidies detected by NIPT are linked to the abnormalities of the maternal chromosome X [65]. The frequency of monosomy X varies from 1 : 3,300 (the proportion of mosaic cells is above 34%) [74] to 1 : 300 (the proportion of mosaic cells is 4% and above) [75], depending on the low detection threshold for mosaicism.

Tumors

NIPT results can be unreliable in pregnant women with cancer because cancer cells have an unstable genome, tumors usually produce a vast network of blood vessels and release a lot of cfDNA into the bloodstream [76].

Myths about the dangers of invasive diagnostic tests

Among the arguments for a more vigorous clinical promotion of NIPT lobbied by NIPT manufacturers is the risk of complications (including pregnancy loss) associated with invasive diagnostic tests: both amniocentesis and chorionic villus sampling are reported to result in pregnancy loss in 1% of cases [4, 77, 78]. However, other authors provide different figures on pregnancy loss following an invasive diagnostic porcedure: 1 : 200 for chorionic villus sampling and 1 : 300 for amniocentesis [79, 80]. These values are lower than the rate of spontaneous abortions [81].

Legislation and guidelines for NIPT

At present, there are two major models of NIPT incorporation into clinical practice practiced in many countries.

1. The cohort model: the test is recommended to women at risk based on the results of a 1st trimester screening procedure. In this case, the expenses are fully or partially covered by the federal budget.

2. The commercial model: the test is offered to those pregnant women who can afford it (personal funds or health insurance).

At the moment, vast TRIDENT-2 studies are being carried out in Holland and Denmark to investigate the aspects of NIPT introduction in clinical practice (http://www.meerovernipt.nl); the participants are offered to undergo NIPT instead of 1st trimester screening tests.

Below we provide examples of how NIPT is used in different countries and talk about the regulatory legislation.

United Kingdom

In the UK, 800,000 pregnancies are reported annually. In January 2016, the National Screening Committee operating in the UK [82] recommended to incorporate NIPT into the Fetal Anomaly Screening Program [83]. The guidelines suggest that NIPT should be offered to all women at a high risk for aneuploidy (> 1 : 150) revealed by a combined ultrasound and biochemistry test between weeks 10 and 14 of pregnancy. The efficacy report will be released in 2018–2019. If the test proves to be effective, the number of invasive screening procedures will be reduced and the saved money will be used to subsidize NIPT.

Sweden

In Sweden, 120,000 pregnancies are reported annually. In June 2016, the Swedish Society of Obstetrics and Gynecology issued guidelines [84] recommending NIPT to all women whose risk for aneuploidies inferred from the combined ultrasound and biochemistry test ranges between 1 : 51 and 1 : 1,000 and to those who cannot undergo an invasive diagnostic procedure because of HIV or hepatitis. Caution should be exercised when ordering NIPT for a woman carrying multiples. A high risk for aneuploidy means that invasive diagnostic tests should be performed, whereas for women at low risk standard checkup examinations would be enough. The Society does not recommend NIPT to every pregnant woman because there is no sufficient evidence of the test's efficacy in every cohort of pregnant patients and because of its high costs.

France

In France, the number of annual pregnancies reaches 800,000. The French Ministry of Health issued its guidelines for prenatal testing in 2017 [85]. Before the advent of NIPT, screening

Table. Leading US manufacturers of commercial NIPT

NIPR trade name	Manufacturer	Location
MaterniT21Plus™	Sequenom, subsidiary of LabCorp, Inc.	San Diego, CA
Verifi™	Verinata Health, now Illumina	Redwood City, CA
Harmony™	Ariosa Diagnostics	San Jose, CA
Panorama™	Natera	San Carlos, CA

for aneuploidies relied on FMF standards [29]. If the risk for aneuploidy was high (> 1 : 250), invasive diagnostic testing was carried out followed by karyotyping. The expenses were covered by health insurance. According to the recommendations published in 2017, the analysis of circulating cell-free DNA is recommended to women at high risk (from 1 : 1,000 to 1 : 51) for fetal trisomy 21 revealed by 1st trimester ultrasound and biochemistry screening. Pregnant women whose risk for aneuploidy is 1 : 50 or higher should undergo an invasive diagnostic procedure but still can opt for molecular screening first. It is emphasized that NIPT should not be regarded as a substitute for invasive diagnostic testing. The guidelines outline the need for developing a quality control and lab accreditation system. The screening strategy is to be revised in 3 years; among other things, the revision will cover the issues of screening for other aneuploidies and microdeletions.

USA

About 6.35 million pregnancies are reported annually in the USA. The NIPT market is divided between a few major players (see the Table) [86].

NIPT expenses are covered by health insurance or a patient's personal funds. No funding is received from the state.

So far, 4 medical associations have proposed guidelines for NIPT:
 • the American College of Obstetricians and Gynecologists (ACOG), May 2016 [87];
 • the International Society for Prenatal Diagnosis, April 2015 [80];
 • the National society of Genetic Counselors, October 2016 [88];
 • the American College of Medical Genetics and Genomics (ACMG) [89].

The ACMG notes that the evolution of NIPT methods and techniques is so rapid that any currently existing clinical recommendations will become obsolete in just a couple of years. Similar to ACOG, the ACMG guidelines emphasize that all pregnant women should be informed about the possibility of undergoing NIPT and its relative advantages over conventional screening for trisomies 13, 18 and 21. Some experts and manufacturers consider these guidelines as a signal for ordering NIPT for all pregnant women regardless of the results of 1st trimester screening. This interpretation is wrong. ACMG only recommends that pregnant women should be informed of the possibility of undergoing NIPT and provided with all relevant information about the test [86]. Unfortunately, many physicians are unaware of NIPT limitations, tend to misinterpret its results or take wrong decisions. Knowing that, NIPT manufacturers provide their own genetic counseling, which raises a number of questions since the counsellors involved can be biased.

Recently, there has been a rise in the number of patients who test false-positive for sex chromosome aneuploidies. It is imperative that patients should be informed of the situation and explained that clinical outcomes for children with such aneuploidies vary. For example, although the X0 karyotype is a common cause of pregnancy loss, the quality of life of women with Turner syndrome is relatively high.

The guidelines stress that NIPT results should provide accurate information about NIPT specificity, sensitivity, PPV, NPV, and fetal DNA fraction for all types of analyzed mutations (aneuploidies of autosomes, sex chromosomes, CNV).

The most common cause of NIPT failure is low fetal DNA fraction. The low fDNA fraction correlates with a number of fetal aneuploidies [62, 72], meaning that in the case of NIPT failure, the patient should be immediately offered to undergo an invasive diagnostic test instead of repeating NIPT. ACMG does not recommend to use NIPT for detecting microdeletions because no reliable assessment of its specificity and sensitivity has been made so far.

Russia

In Russia, the number of annually reported pregnancies is about 1.8 million. Screening for genetic pathology of the fetus includes biochemistry tests and ultrasound examinations conducted in the 1st trimester. If the revealed risk is 1 : 100, the woman is offered to consult a geneticist and undergo an invasive diagnostic test. All expenses are covered by health insurance and regional budgets [90]. Clinical recommendations on NIPT were published in 2016 [91]; they are largely consistent with the ACMG guidelines mentioned above.

A few obstacles impede NIPT promotion on the Russian market: NIPT is not certified in Russia and almost all MPS reagents and equipment have no marketing authorization in our country.

CONCLUSION

Incorporation of NIPT into clinical practice poses a serious dilemma. If we raise the risk threshold signaling the need for NIPT to a higher value, the doctors who perform invasive testing may lose their skills due to the lack of clients, which will lead to diagnostic inaccuracy. In this case, the detection rate may even become lower than it is now. If we start to offer NIPT to every pregnant woman, the total expenses will soar and become unacceptable even for the most affluent and developed countries. This means that the optimum risk value should be defined at which the balance between the aneuploidy detection rate and the incurred costs will be harmonious.

References

1. Hassold T, Hall H, Hunt P. The origin of human aneuploidy: where we have been, where we are going. Human molecular genetics. 2007; 16 (2): 203–8.
2. Driscoll DA, Gross S. Prenatal screening for aneuploidy. New England Journal of Medicine. 2009; 360 (24): 2556–62.
3. Nagaoka SI, Hassold TJ, Hunt PA. Human aneuploidy: mechanisms and new insights into an age-old problem. Nature Reviews Genetics. 2012; 13 (7): 493–504.
4. Ehrich M, Deciu C, Zwiefelhofer T, Tynan JA, Cagasan L, Tim R, et al. Noninvasive detection of fetal trisomy 21 by sequencing of DNA in maternal blood: a study in a clinical setting. American journal of obstetrics and gynecology. 2011; 204 (3): 205–e1.
5. Morris JK, Mutton DE, Alberman E. Revised estimates of the maternal age specific live birth prevalence of Down's syndrome. Journal of medical screening. 2002; 9 (1): 2–6.
6. Buckley F, Buckley S. Wrongful deaths and rightful lives-screening for Down syndrome. Down Syndrome Research and Practice. 2008; 12 (2): 79–86.
7. Wald NJ, Hackshaw AK. Combining ultrasound and biochemistry in first-trimester screening for Down's syndrome. Prenatal diagnosis. 1997; 17 (9): 821–9.
8. Sillence KA, Madgett TE, Roberts LA, Overton TG, Avent ND. Non-invasive screening tools for Down's syndrome: a review. Diagnostics. 2013; 3 (2): 291–314.

9. Choy KW, Kwok YK, Cheng YKY, Wong KM, Wong HK, Leung KO, et al. Diagnostic accuracy of the BACs-on-Beads™ assay versus karyotyping for prenatal detection of chromosomal abnormalities: a retrospective consecutive case series. BJOG: An International Journal of Obstetrics & Gynaecology. 2014; 121 (10): 1245–52.

10. Lo YD, Corbetta N, Chamberlain PF, Rai V, Sargent IL, Redman CW, et al. Presence of fetal DNA in maternal plasma and serum. The lancet. 1997; 350 (9076): 485–7.

11. Lo YD, Hjelm NM, Fidler C, Sargent IL, Murphy MF, Chamberlain PF, et al. Prenatal diagnosis of fetal RhD status by molecular analysis of maternal plasma. New England Journal of Medicine. 1998; 339 (24): 1734–8.

12. Farina A, Caramelli E, Concu M, Sekizawa A, Ruggeri R, Bovicelli L, et al. Testing normality of fetal DNA concentration in maternal plasma at 10–12 completed weeks' gestation: a preliminary approach to a new marker for genetic screening. Prenatal Diagnosis: Published in Affiliation With the International Society for Prenatal Diagnosis. 2002; 22 (2): 148–52.

13. Bischoff FZ, Lewis DE, Simpson JL. Cell-free fetal DNA in maternal blood: kinetics, source and structure. Human reproduction update. 2005; 11 (1): 59–67.

14. Wang E, Batey A, Struble C, Musci T, Song K, Oliphant A. Gestational age and maternal weight effects on fetal cell-free DNA in maternal plasma. Prenatal diagnosis. 2013; 33 (7): 662–6.

15. Curnow KJ, Gross SJ, Hall MP, Stosic M, Demko Z, Zimmermann B, et al. Clinical experience and follow-up with large scale single-nucleotide polymorphism–based noninvasive prenatal aneuploidy testing. American journal of obstetrics and gynecology. 2014; 211 (5): 527–e1.

16. Tjoa ML, Cindrova-Davies T, Spasic-Boskovic O, Bianchi DW, Burton GJ. Trophoblastic oxidative stress and the release of cell-free feto-placental DNA. The American journal of pathology. 2006; 169 (2): 400–4.

17. Alberry M, Maddocks D, Jones M, Abdel Hadi M, Abdel-Fattah S, Avent N, Soothill PW. Free fetal DNA in maternal plasma in anembryonic pregnancies: confirmation that the origin is the trophoblast. Prenatal Diagnosis: Published in Affiliation With the International Society for Prenatal Diagnosis. 2007; 27 (5): 415–8.

18. Gardner RM, Sutherland GR, Shaffer LG. Chromosome abnormalities and genetic counseling. Oxford University Press USA. 2011; (61).

19. Lo YD, Chan KA, Sun H, Chen EZ, Jiang P, Lun FM, et al. Maternal plasma DNA sequencing reveals the genome-wide genetic and mutational profile of the fetus. Science translational medicine. 2010; 2 (61): 61ra91–61ra91.

20. Ivanov M, Baranova A, Butler T, Spellman P, Mileyko V. Non-random fragmentation patterns in circulating cell-free DNA reflect epigenetic regulation. BMC genomics. 2015; 16 (13): S1.

21. Sancho M, Diani E, Beato M, Jordan A. Depletion of human histone H1 variants uncovers specific roles in gene expression and cell growth. PLoS genetics. 2008; 4 (10): e1000227.

22. Jiang P, Lo YMD. The long and short of circulating cell-free DNA and the ins and outs of molecular diagnostics. Trends in Genetics. 2016; 32 (6): 360–71.

23. Geiman TM, Muegge K. DNA methylation in early development. Molecular Reproduction and Development: Incorporating Gamete Research. 2010; 77 (2): 105–13.

24. Sun K, et al. Plasma DNA tissue mapping by genome-wide methylation sequencing for noninvasive prenatal, cancer, and transplantation assessments. Proceedings of the National Academy of Sciences. 2015; 112 (40): E5503–E5512.

25. Sun K, Jiang P, Wong AI, Cheng YK, Cheng SH, Zhang H, et al. Size-tagged preferred ends in maternal plasma DNA shed light on the production mechanism and show utility in noninvasive prenatal testing. Proceedings of the National Academy of Sciences. 2018; 115 (22): E5106–E5114.

26. Tamminga S, van Maarle M, Henneman L, Oudejans CB, Cornel MC, Sistermans EA. Maternal plasma DNA and RNA sequencing for prenatal testing. Advances in clinical chemistry. 2016; (74): 63–102.

27. Ashoor G, Poon L, Syngelaki A, Mosimann B, Nicolaides KH. Fetal fraction in maternal plasma cell-free DNA at 11–13 weeks' gestation: effect of maternal and fetal factors. Fetal diagnosis and therapy. 2012; 31 (4): 237–43.

28. Canick JA, et al. The impact of maternal plasma DNA fetal fraction on next generation sequencing tests for common fetal aneuploidies. Prenatal diagnosis. 2013; 33 (7): 667–74.

29. Wright D, Syngelaki A, Bradbury I, Akolekar R, Nicolaides KH. First-trimester screening for trisomies 21, 18 and 13 by ultrasound and biochemical testing. Fetal diagnosis and therapy. 2014; 35 (2): 118–26.

30. Kim SK, Hannum G, Geis J, Tynan J, Hogg G, Zhao C, et al. Determination of fetal DNA fraction from the plasma of pregnant women using sequence read counts. Prenatal diagnosis. 2015; 35 (8): 810–15.

31. Jiang P, Peng X, Su X, Sun K, Stephanie CY, Chu WI, et al. FetalQuant SD: accurate quantification of fetal DNA fraction by shallow-depth sequencing of maternal plasma DNA. NPJ genomic medicine. 2016; (1): 16013.

32. Peng XL, Jiang P. Bioinformatics approaches for fetal DNA fraction estimation in noninvasive prenatal testing. International journal of molecular sciences. 2017; 18 (2): 453.

33. Zimmermann B, Hill M, Gemelos G, Demko Z, Banjevic M, Baner J, et al. Noninvasive prenatal aneuploidy testing of chromosomes 13, 18, 21, X, and Y, using targeted sequencing of polymorphic loci. Prenatal diagnosis. 2012; 32 (13): 1233–41.

34. Lun FM, Chiu RW, Sun K, Leung TY, Jiang P, Chan KA, et al. Noninvasive prenatal methylomic analysis by genomewide bisulfite sequencing of maternal plasma DNA. Clinical chemistry. DOI: 10.1373/clinchem.2013.212274.

35. Yu SC, et al. Size-based molecular diagnostics using plasma DNA for noninvasive prenatal testing. Proceedings of the National Academy of Sciences. 2014; 111 (23): 8583–8.

36. Cirigliano V, Ordoñez E, Rueda L, Syngelaki A, Nicolaides KH. Performance of the neoBona test: a new paired-end massively parallel shotgun sequencing approach for cell-free DNA-based aneuploidy screening. Ultrasound in Obstetrics & Gynecology. 2017; 49 (4): 460–4.

37. Straver R, Oudejans C, Sistermans EA, Reinders MJ. Calculating the fetal fraction for noninvasive prenatal testing based on genome-wide nucleosome profiles. Prenatal diagnosis. 2016; 36 (7): 614–21.

38. Kim SK, Hannum G, Geis J, Tynan J, Hogg G, Zhao C, Boom D. Determination of fetal DNA fraction from the plasma of pregnant women using sequence read counts. Prenatal diagnosis. 2015; 35 (8): 810–5.

39. Chen S, Lau TK, Zhang C, Xu C, Xu Z, Hu P, et al. A method for noninvasive detection of fetal large deletions/duplications by low coverage massively parallel sequencing. Prenatal diagnosis. 2013; 33 (6): 584–90.

40. Van den Veyver IB. Recent advances in prenatal genetic screening and testing. F1000 Research. 2016; 5 (F1000 Faculty Rev): 2591.

41. Peters D, Chu T, Yatsenko SA, Hendrix N, Hogge WA, Surti U, et al. Noninvasive prenatal diagnosis of a fetal microdeletion syndrome. New England Journal of Medicine. 2011; 365 (19): 1847–8.

42. Jensen TJ, Dzakula Z, Deciu C, van den Boom D, Ehrich M. Detection of microdeletion 22q11. 2 in a fetus by next-generation sequencing of maternal plasma. Clinical chemistry. 2012; 58 (7): 1148–51.

43. Srinivasan A, Bianchi DW, Huang H, Sehnert AJ, Rava RP. Noninvasive detection of fetal subchromosome abnormalities via deep sequencing of maternal plasma. The American Journal of Human Genetics. 2013; 92 (2): 167–76.

44. Lefkowitz RB, Tynan JA, Liu T, Wu Y, Mazloom AR, Almasri E, et al. Clinical validation of a noninvasive prenatal test for genomewide detection of fetal copy number variants. American journal of obstetrics and gynecology. 2016; 215 (2): 227–e1.

45. Straver R, Sistermans EA, Holstege H, Visser A, Oudejans CB, Reinders MJ. WISECONDOR: detection of fetal aberrations from shallow sequencing maternal plasma based on a within-sample comparison scheme. Nucleic acids research. 2013; 42 (5): e31–e31.

46. Zhao C, Tynan J, Ehrich M, Hannum G, McCullough R, Saldivar JS, Deciu C. Detection of fetal subchromosomal abnormalities by sequencing circulating cell-free DNA from maternal plasma. Clinical chemistry. 2015.

47. Nicolaides KH, Syngelaki A, Gil M, Atanasova V, Markova D. Validation of targeted sequencing of single-nucleotide

polymorphisms for non-invasive prenatal detection of aneuploidy of chromosomes 13, 18, 21, X, and Y. Prenatal diagnosis. 2013; 33 (6): 575–9.

48. Wapner RJ, Babiarz JE, Levy B, Stosic M, Zimmermann B, Sigurjonsson S, Hu J. Expanding the scope of noninvasive prenatal testing: detection of fetal microdeletion syndromes. American journal of obstetrics and gynecology. 2015; 212 (3): 332–e1.

49. Costa JM, Benachi A, Gautier E. New strategy for prenatal diagnosis of X-linked disorders. New England Journal of Medicine. 2002; 346 (19): 1502.

50. Lo YD, Hjelm NM, Fidler C, Sargent IL, Murphy MF, Chamberlain PF, et al. Prenatal diagnosis of fetal RhD status by molecular analysis of maternal plasma. New England Journal of Medicine. 1998; 339 (24): 1734–8.

51. Tang NL, Leung TN, Zhang J, Lau TK, Lo YD. Detection of fetal-derived paternally inherited X-chromosome polymorphisms in maternal plasma. Clinical chemistry. 1999; 45 (11): 2033–5.

52. Bustamante-Aragonés A, de Alba MR, Perlado S, Trujillo-Tiebas MJ, Arranz JP, Díaz-Recasens J, et al. Non-invasive prenatal diagnosis of single-gene disorders from maternal blood. Gene. 2012; 504 (1): 144–9.

53. Amicucci P, Gennarelli M, Novelli G, Dallapiccola B. Prenatal diagnosis of myotonic dystrophy using fetal DNA obtained from maternal plasma. Clinical chemistry. 2000; 46 (2): 301–2.

54. Vermeulen C, Geeven G, de Wit E, Verstegen MJ, Jansen RP, van Kranenburg M, et al. Sensitive monogenic noninvasive prenatal diagnosis by targeted haplotyping. The American Journal of Human Genetics. 2017; 101 (3): 326–39.

55. Tong YK, Jin S, Chiu RW, Ding C, Chan KA, Leung TY, et al. Noninvasive prenatal detection of trisomy 21 by an epigenetic–genetic chromosome-dosage approach. Clinical chemistry. 2010; 56 (1): 90–8.

56. Tsui DW, Lam YD, Lee WS, Leung TY, Lau TK, Lau ET, et al. Systematic identification of placental epigenetic signatures for the noninvasive prenatal detection of Edwards syndrome. PloS one. 2010; 5 (11): e15069.

57. Yuen RK, Penaherrera MS, Von Dadelszen P, McFadden DE, Robinson WP. DNA methylation profiling of human placentas reveals promoter hypomethylation of multiple genes in early-onset preeclampsia. European Journal of Human Genetics. 2010; 18 (9): 1006.

58. Blair JD, Yuen RK, Lim BK, McFadden DE, von Dadelszen P, Robinson WP. Widespread DNA hypomethylation at gene enhancer regions in placentas associated with early-onset pre-eclampsia. Molecular human reproduction. 2013; 19 (10): 697–708.

59. Chu T, Bunce K, Shaw P, Shridhar V, Althouse A, Hubel C, et al. Comprehensive analysis of preeclampsia-associated DNA methylation in the placenta. PLoS One. 2014; 9 (9): e107318.

60. Hahn S, Rusterholz C, Hösli I, Lapaire O. Cell-free nucleic acids as potential markers for preeclampsia. Placenta. 2011; (32): S17–S20.

61. Bianchi DW, Parker RL, Wentworth J, Madankumar R, Saffer C, Das AF, et al. DNA sequencing versus standard prenatal aneuploidy screening. New England journal of medicine. 2014; 370 (9): 799–808.

62. Norton ME, Jacobsson B, Swamy GK, Laurent LC, Ranzini AC, Brar H, et al. Cell-free DNA analysis for noninvasive examination of trisomy. New England Journal of Medicine. 2015; 372 (17): 1589–97.

63. Wataganara T, Peter I, Messerlian GM, Borgatta L, Bianchi DW. Inverse correlation between maternal weight and second trimester circulating cell-free fetal DNA levels. Obstetrics & Gynecology. 2004; 104 (3): 545–50.

64. Rumyantsev AG, Kurcer MA, Mareeva JM, Misjurin AV, Roumiantsev SA, Ustjugov AJ. Clinical significance of the fetal microchimerism for mother. Cellular Transplantation & Tissue Engineering. 2012; 7 (2): 103–111.

65. Wang Y, et al. Maternal mosaicism is a significant contributor to discordant sex chromosomal aneuploidies associated with noninvasive prenatal testing. Clinical chemistry. 2014; 60 (1): 251–9.

66. Bianchi DW. Cherchez la femme: maternal incidental findings can explain discordant prenatal cell-free DNA sequencing results. Genetics in Medicine. 2017; DOI: 10.1038/gim.2017.219.

67. Hartwig TS, Ambye L, Sørensen S, Jørgensen FS. Discordant non-invasive prenatal testing (NIPT)–a systematic review. Prenatal diagnosis. 2017; 37 (6): 527–39.

68. Attilakos G, Maddocks DG, Davies T, Hunt LP, Avent ND, Soothill PW, et al. Quantification of free fetal DNA in multiple pregnancies and relationship with chorionicity. Prenatal diagnosis. 2011; 31 (10): 967–72.

69. Bevilacqua E, Gil MM, Nicolaides KH, Ordoñez E, Cirigliano V, Dierickx H, et al. Performance of screening for aneuploidies by cell-free DNA analysis of maternal blood in twin pregnancies. Ultrasound in Obstetrics & Gynecology. 2015; 45 (1): 61–6.

70. Curnow KJ, Wilkins-Haug L, Ryan A, Kırkızlar E, Stosic M, Hall MP, et al. Detection of triploid, molar, and vanishing twin pregnancies by a single-nucleotide polymorphism–based noninvasive prenatal test. American journal of obstetrics and gynecology. 2015; 212 (1): 79–e1.

71. Gil MM, Quezada MS, Revello R, Akolekar R, Nicolaides KH. Analysis of cell-free DNA in maternal blood in screening for fetal aneuploidies: updated meta-analysis. Ultrasound in obstetrics & gynecology. 2015; 45 (3): 249–66.

72. Zhang H, Gao Y, Jiang F, Fu M, Yuan Y, Guo Y, et al. Non-invasive prenatal testing for trisomies 21, 18 and 13: clinical experience from 146 958 pregnancies. Ultrasound in Obstetrics & Gynecology. 2015; 45 (5): 530–8.

73. Russell LM, Strike P, Browne CE, Jacobs PA. X chromosome loss and ageing. Cytogenetic and genome research. 2007; 116 (3): 181–5.

74. Samango-Sprouse C, Kırkızlar E, Hall MP, Lawson P, Demko Z, Zneimer SM, et al. Incidence of X and Y chromosomal aneuploidy in a large child bearing population. PloS One. 2016; 11 (8): e0161045.

75. Shubina J, Trofimov DY, Barkov IY, Stupko OK, Goltsov AY, Mukosey IS, et al. In silico size selection is effective in reducing false positive NIPS cases of monosomy X that are due to maternal mosaic monosomy X. Prenatal diagnosis. 2017; 37 (13): 1305–10.

76. Bianchi DW, Chudova D, Sehnert AJ, Bhatt S, Murray K, Prosen TL, et al. Noninvasive prenatal testing and incidental detection of occult maternal malignancies. Jama. 2015; 314 (2): 162–9.

77. Ferguson-Smith MA. Placental mRNA in maternal plasma: prospects for fetal screening. Proceedings of the National Academy of Sciences. 2003; 100 (8): 4360–2.

78. Chiu RW, Cantor CR, Lo YD. Non-invasive prenatal diagnosis by single molecule counting technologies. Trends in genetics. 2009; 25 (7): 324–31.

79. ACOG Practice Bulletin # 77: screening for fetal chromosomal abnormalities. Obstet Gynecol. 2007; (109): 217–27.

80. Benn P, Borrell A, Chiu RW, Cuckle H, Dugoff L, Faas B, et al. Position statement from the Chromosome Abnormality Screening Committee on behalf of the Board of the International Society for Prenatal Diagnosis. Prenatal diagnosis. 2015; 35 (8): 725–34.

81. Kascheeva TK, Kuznetzova TV, Baranov VS. New technologies and trends of prenatal diagnostics. Journal of obstetrics and woman disease. 2017; 66 (2): 33–39.

82. UK National Screening Committee. www.gov.uk URL. Available from: https://www.gov.uk/government/groups/uk-national-screening-committee-uk-nsc (data obrashhenija: 20.07.2018).

83. Screening in the UK: making effective recommendations 2015 to 2016. Public Health England hosts the UK National Screening Committee URL. Available from: https://assets.publishing.service.gov.uk/government/uploads/system/uploads/attachment_data/file/538524/Screening_in_the_UK___making_effective_recommendations_2015_to_2016_180716_final.pdf (data obrashhenija: 20.07.2018).

84. Analysis of foetal DNA in the woman's blood: non-invasive prenatal testing (NIPT) for trisomy 13, 18 and 21. SFOG Guidelines URL. Available from: http://www.nfog.org/files/guidelines/NIPT%202016%2006%2005%20.pdf (data obrashhenija: 20.07.2018).

85. Trisomie 21 : la HAS actualise ses recommandations concernant le dépistage prénatal de la trisomie 21. www.has-sante.fr URL. Available from: https://www.has-sante.fr/portail/jcms/c_2768535/fr/trisomie-21-la-has-actualise-ses-recommandations-concernant-le-depistage-prenatal-de-la-trisomie-21 (data obrashhenija: 20.07.2018).

86. Allyse M, Wick MJ. What do the new American College of Medical

Genetics and Genomics (ACMG) guidelines mean for the provision of non-invasive prenatal genetic screening? Journal of Obstetrics and Gynaecology. 2017; 37 (6): 795–8.

87. American College of Obstetricians and Gynecologists: Screening for fetal aneuploidy. Obstet Gynecol. 2016; 127 (5): e123–137.

88. Prenatal cell-free DNA screening. National Society of Genetic Counselors. Available from: http://www.nsgc.org/p/bl/et/blogaid=805#.WCTELTNRftw.linkedin.

89. Gregg AR, Skotko BG, Benkendorf JL, Monaghan KG, Bajaj K, Best RG, et al. Noninvasive prenatal screening for fetal aneuploidy, 2016 update: a position statement of the American College of

Medical Genetics and Genomics. Genetics in medicine. 2016; 18 (10): 1056–65.

90. Informacionno-metodicheskoe pis'mo Minzdrava RF ot 19.03.2015 # 15-4/607. Available from: http://www.consultant.ru/document/cons_doc_LAW_177689/.

91. Sukhikh GT, Trofimov DYu, Barkov IYu, Donnikov AE, Shubina ES, Korostin DO, et al. Non-invasive prenatal DNA-screening of fetus aneuploidies using maternal blood based on high-throuhgput sequencing. Clinical recommendations. Obstetrics and gynecology. 2016; (6): 3–22.

Литература

1. Hassold T, Hall H, Hunt P. The origin of human aneuploidy: where we have been, where we are going. Human molecular genetics. 2007; 16 (2): 203–8.

2. Driscoll DA, Gross S. Prenatal screening for aneuploidy. New England Journal of Medicine. 2009; 360 (24): 2556–62.

3. Nagaoka SI, Hassold TJ, Hunt PA. Human aneuploidy: mechanisms and new insights into an age-old problem. Nature Reviews Genetics. 2012; 13 (7): 493–504.

4. Ehrich M, Deciu C, Zwiefelhofer T, Tynan JA, Cagasan L, Tim R, et al. Noninvasive detection of fetal trisomy 21 by sequencing of DNA in maternal blood: a study in a clinical setting. American journal of obstetrics and gynecology. 2011; 204 (3): 205–e1.

5. Morris JK, Mutton DE, Alberman E. Revised estimates of the maternal age specific live birth prevalence of Down's syndrome. Journal of medical screening. 2002; 9 (1): 2–6.

6. Buckley F, Buckley S. Wrongful deaths and rightful lives-screening for Down syndrome. Down Syndrome Research and Practice. 2008; 12 (2): 79–86.

7. Wald NJ, Hackshaw AK. Combining ultrasound and biochemistry in first-trimester screening for Down's syndrome. Prenatal diagnosis. 1997; 17 (9): 821–9.

8. Sillence KA, Madgett TE, Roberts LA, Overton TG, Avent ND. Non-invasive screening tools for Down's syndrome: a review. Diagnostics. 2013; 3 (2): 291–314.

9. Choy KW, Kwok YK, Cheng YKY, Wong KM, Wong HK, Leung KO, et al. Diagnostic accuracy of the BACs-on-Beads™ assay versus karyotyping for prenatal detection of chromosomal abnormalities: a retrospective consecutive case series. BJOG: An International Journal of Obstetrics & Gynaecology. 2014; 121 (10): 1245–52.

10. Lo YD, Corbetta N, Chamberlain PF, Rai V, Sargent IL, Redman CW, et al. Presence of fetal DNA in maternal plasma and serum. The lancet. 1997; 350 (9076): 485–7.

11. Lo YD, Hjelm NM, Fidler C, Sargent IL, Murphy MF, Chamberlain PF, et al. Prenatal diagnosis of fetal RhD status by molecular analysis of maternal plasma. New England Journal of Medicine. 1998; 339 (24): 1734–8.

12. Farina A, Caramelli E, Concu M, Sekizawa A, Ruggeri R, Bovicelli L, et al. Testing normality of fetal DNA concentration in maternal plasma at 10–12 completed weeks' gestation: a preliminary approach to a new marker for genetic screening. Prenatal Diagnosis: Published in Affiliation With the International Society for Prenatal Diagnosis. 2002; 22 (2): 148–52.

13. Bischoff FZ, Lewis DE, Simpson JL. Cell-free fetal DNA in maternal blood: kinetics, source and structure. Human reproduction update. 2005; 11 (1): 59–67.

14. Wang E, Batey A, Struble C, Musci T, Song K, Oliphant A. Gestational age and maternal weight effects on fetal cell-free DNA in maternal plasma. Prenatal diagnosis. 2013; 33 (7): 662–6.

15. Curnow KJ, Gross SJ, Hall MP, Stosic M, Demko Z, Zimmermann B, et al. Clinical experience and follow-up with large scale single-nucleotide polymorphism–based noninvasive prenatal aneuploidy testing. American journal of obstetrics and gynecology. 2014; 211 (5): 527–e1.

16. Tjoa ML, Cindrova-Davies T, Spasic-Boskovic O, Bianchi DW, Burton GJ. Trophoblastic oxidative stress and the release of cell-free feto-placental DNA. The American journal of pathology. 2006; 169 (2): 400–4.

17. Alberry M, Maddocks D, Jones M, Abdel Hadi M, Abdel-Fattah S, Avent N, Soothill PW. Free fetal DNA in maternal plasma in anembryonic pregnancies: confirmation that the origin is the trophoblast. Prenatal Diagnosis: Published in Affiliation With the International Society for Prenatal Diagnosis. 2007; 27 (5): 415–8.

18. Gardner RM, Sutherland GR, Shaffer LG. Chromosome abnormalities and genetic counseling. Oxford University Press USA. 2011; (61).

19. Lo YD, Chan KA, Sun H, Chen EZ, Jiang P, Lun FM, et al. Maternal plasma DNA sequencing reveals the genome-wide genetic and mutational profile of the fetus. Science translational medicine. 2010; 2 (61): 61ra91–61ra91.

20. Ivanov M, Baranova A, Butler T, Spellman P, Mileyko V. Non-random fragmentation patterns in circulating cell-free DNA reflect epigenetic regulation. BMC genomics. 2015; 16 (13): S1.

21. Sancho M, Diani E, Beato M, Jordan A. Depletion of human histone H1 variants uncovers specific roles in gene expression and cell growth. PLoS genetics. 2008; 4 (10): e1000227.

22. Jiang P, Lo YMD. The long and short of circulating cell-free DNA and the ins and outs of molecular diagnostics. Trends in Genetics. 2016; 32 (6): 360–71.

23. Geiman TM, Muegge K. DNA methylation in early development. Molecular Reproduction and Development: Incorporating Gamete Research. 2010; 77 (2): 105–13.

24. Sun K, et al. Plasma DNA tissue mapping by genome-wide methylation sequencing for noninvasive prenatal, cancer, and transplantation assessments. Proceedings of the National Academy of Sciences. 2015; 112 (40): E5503–E5512.

25. Sun K, Jiang P, Wong AI, Cheng YK, Cheng SH, Zhang H, et al. Size-tagged preferred ends in maternal plasma DNA shed light on the production mechanism and show utility in noninvasive prenatal testing. Proceedings of the National Academy of Sciences. 2018; 115 (22): E5106–E5114.

26. Tamminga S, van Maarle M, Henneman L, Oudejans CB, Cornel MC, Sistermans EA. Maternal plasma DNA and RNA sequencing for prenatal testing. Advances in clinical chemistry. 2016; (74): 63–102.

27. Ashoor G, Poon L, Syngelaki A, Mosimann B, Nicolaides KH. Fetal fraction in maternal plasma cell-free DNA at 11–13 weeks' gestation: effect of maternal and fetal factors. Fetal diagnosis and therapy. 2012; 31 (4): 237–43.

28. Canick JA, et al. The impact of maternal plasma DNA fetal fraction on next generation sequencing tests for common fetal aneuploidies. Prenatal diagnosis. 2013; 33 (7): 667–74.

29. Wright D, Syngelaki A, Bradbury I, Akolekar R, Nicolaides KH. First-trimester screening for trisomies 21, 18 and 13 by ultrasound and biochemical testing. Fetal diagnosis and therapy. 2014; 35 (2): 118–26.

30. Kim SK, Hannum G, Geis J, Tynan J, Hogg G, Zhao C, et al. Determination of fetal DNA fraction from the plasma of pregnant women using sequence read counts. Prenatal diagnosis. 2015; 35 (8): 810–15.

31. Jiang P, Peng X, Su X, Sun K, Stephanie CY, Chu WI, et al. FetalQuant SD: accurate quantification of fetal DNA fraction by shallow-depth sequencing of maternal plasma DNA. NPJ genomic medicine. 2016; (1): 16013.

32. Peng XL, Jiang P. Bioinformatics approaches for fetal DNA fraction estimation in noninvasive prenatal testing. International journal of

molecular sciences. 2017; 18 (2): 453.

33. Zimmermann B, Hill M, Gemelos G, Demko Z, Banjevic M, Baner J, et al. Noninvasive prenatal aneuploidy testing of chromosomes 13, 18, 21, X, and Y, using targeted sequencing of polymorphic loci. Prenatal diagnosis. 2012; 32 (13): 1233–41.

34. Lun FM, Chiu RW, Sun K, Leung TY, Jiang P, Chan KA, et al. Noninvasive prenatal methylomic analysis by genomewide bisulfite sequencing of maternal plasma DNA. Clinical chemistry. DOI: 10.1373/clinchem.2013.212274.

35. Yu SC, et al. Size-based molecular diagnostics using plasma DNA for noninvasive prenatal testing. Proceedings of the National Academy of Sciences. 2014; 111 (23): 8583–8.

36. Cirigliano V, Ordoñez E, Rueda L, Syngelaki A, Nicolaides KH. Performance of the neoBona test: a new paired-end massively parallel shotgun sequencing approach for cell-free DNA-based aneuploidy screening. Ultrasound in Obstetrics & Gynecology. 2017; 49 (4): 460–4.

37. Straver R, Oudejans C, Sistermans EA, Reinders MJ. Calculating the fetal fraction for noninvasive prenatal testing based on genome-wide nucleosome profiles. Prenatal diagnosis. 2016; 36 (7): 614–21.

38. Kim SK, Hannum G, Geis J, Tynan J, Hogg G, Zhao C, Boom D. Determination of fetal DNA fraction from the plasma of pregnant women using sequence read counts. Prenatal diagnosis. 2015; 35 (8): 810–5.

39. Chen S, Lau TK, Zhang C, Xu C, Xu Z, Hu P, et al. A method for noninvasive detection of fetal large deletions/duplications by low coverage massively parallel sequencing. Prenatal diagnosis. 2013; 33 (6): 584–90.

40. Van den Veyver IB. Recent advances in prenatal genetic screening and testing. F1000 Research. 2016; 5 (F1000 Faculty Rev): 2591.

41. Peters D, Chu T, Yatsenko SA, Hendrix N, Hogge WA, Surti U, et al. Noninvasive prenatal diagnosis of a fetal microdeletion syndrome. New England Journal of Medicine. 2011; 365 (19): 1847–8.

42. Jensen TJ, Dzakula Z, Deciu C, van den Boom D, Ehrich M. Detection of microdeletion 22q11. 2 in a fetus by next-generation sequencing of maternal plasma. Clinical chemistry. 2012; 58 (7): 1148–51.

43. Srinivasan A, Bianchi DW, Huang H, Sehnert AJ, Rava RP. Noninvasive detection of fetal subchromosome abnormalities via deep sequencing of maternal plasma. The American Journal of Human Genetics. 2013; 92 (2): 167–76.

44. Lefkowitz RB, Tynan JA, Liu T, Wu Y, Mazloom AR, Almasri E, et al. Clinical validation of a noninvasive prenatal test for genomewide detection of fetal copy number variants. American journal of obstetrics and gynecology. 2016; 215 (2): 227–e1.

45. Straver R, Sistermans EA, Holstege H, Visser A, Oudejans CB, Reinders MJ. WISECONDOR: detection of fetal aberrations from shallow sequencing maternal plasma based on a within-sample comparison scheme. Nucleic acids research. 2013; 42 (5): e31–e31.

46. Zhao C, Tynan J, Ehrich M, Hannum G, McCullough R, Saldivar JS, Deciu C. Detection of fetal subchromosomal abnormalities by sequencing circulating cell-free DNA from maternal plasma. Clinical chemistry. 2015.

47. Nicolaides KH, Syngelaki A, Gil M, Atanasova V, Markova D. Validation of targeted sequencing of single-nucleotide polymorphisms for non-invasive prenatal detection of aneuploidy of chromosomes 13, 18, 21, X, and Y. Prenatal diagnosis. 2013; 33 (6): 575–9.

48. Wapner RJ, Babiarz JE, Levy B, Stosic M, Zimmermann B, Sigurjonsson S, Hu J. Expanding the scope of noninvasive prenatal testing: detection of fetal microdeletion syndromes. American journal of obstetrics and gynecology. 2015; 212 (3): 332–e1.

49. Costa JM, Benachi A, Gautier E. New strategy for prenatal diagnosis of X-linked disorders. New England Journal of Medicine. 2002; 346 (19): 1502.

50. Lo YD, Hjelm NM, Fidler C, Sargent IL, Murphy MF, Chamberlain PF, et al. Prenatal diagnosis of fetal RhD status by molecular analysis of maternal plasma. New England Journal of Medicine. 1998; 339 (24): 1734–8.

51. Tang NL, Leung TN, Zhang J, Lau TK, Lo YD. Detection of fetal-derived paternally inherited X-chromosome polymorphisms in maternal plasma. Clinical chemistry. 1999; 45 (11): 2033–5.

52. Bustamante-Aragonés A, de Alba MR, Perlado S, Trujillo-Tiebas MJ, Arranz JP, Díaz-Recasens J, et al. Non-invasive prenatal diagnosis of single-gene disorders from maternal blood. Gene. 2012; 504 (1): 144–9.

53. Amicucci P, Gennarelli M, Novelli G, Dallapiccola B. Prenatal diagnosis of myotonic dystrophy using fetal DNA obtained from maternal plasma. Clinical chemistry. 2000; 46 (2): 301–2.

54. Vermeulen C, Geeven G, de Wit E, Verstegen MJ, Jansen RP, van Kranenburg M, et al. Sensitive monogenic noninvasive prenatal diagnosis by targeted haplotyping. The American Journal of Human Genetics. 2017; 101 (3): 326–39.

55. Tong YK, Jin S, Chiu RW, Ding C, Chan KA, Leung TY, et al. Noninvasive prenatal detection of trisomy 21 by an epigenetic–genetic chromosome-dosage approach. Clinical chemistry. 2010; 56 (1): 90–8.

56. Tsui DW, Lam YD, Lee WS, Leung TY, Lau TK, Lau ET, et al. Systematic identification of placental epigenetic signatures for the noninvasive prenatal detection of Edwards syndrome. PloS one. 2010; 5 (11): e15069.

57. Yuen RK, Penaherrera MS, Von Dadelszen P, McFadden DE, Robinson WP. DNA methylation profiling of human placentas reveals promoter hypomethylation of multiple genes in early-onset preeclampsia. European Journal of Human Genetics. 2010; 18 (9): 1006.

58. Blair JD, Yuen RK, Lim BK, McFadden DE, von Dadelszen P, Robinson WP. Widespread DNA hypomethylation at gene enhancer regions in placentas associated with early-onset pre-eclampsia. Molecular human reproduction. 2013; 19 (10): 697–708.

59. Chu T, Bunce K, Shaw P, Shridhar V, Althouse A, Hubel C, et al. Comprehensive analysis of preeclampsia-associated DNA methylation in the placenta. PLoS One. 2014; 9 (9): e107318.

60. Hahn S, Rusterholz C, Hösli I, Lapaire O. Cell-free nucleic acids as potential markers for preeclampsia. Placenta. 2011; (32): S17–S20.

61. Bianchi DW, Parker RL, Wentworth J, Madankumar R, Saffer C, Das AF, et al. DNA sequencing versus standard prenatal aneuploidy screening. New England journal of medicine. 2014; 370 (9): 799–808.

62. Norton ME, Jacobsson B, Swamy GK, Laurent LC, Ranzini AC, Brar H, et al. Cell-free DNA analysis for noninvasive examination of trisomy. New England Journal of Medicine. 2015; 372 (17): 1589–97.

63. Wataganara T, Peter I, Messerlian GM, Borgatta L, Bianchi DW. Inverse correlation between maternal weight and second trimester circulating cell-free fetal DNA levels. Obstetrics & Gynecology. 2004; 104 (3): 545–50.

64. Румянцев А. Г., Курцер М. А., Мареева Ю. М., Мисюрин А. В., Румянцев С. А., Устюгов А. Ю. Клиническое значение фетального микрохимеризма у матери. Гены и клетки. 2012; 7 (2): 103–111.

65. Wang Y, et al. Maternal mosaicism is a significant contributor to discordant sex chromosomal aneuploidies associated with noninvasive prenatal testing. Clinical chemistry. 2014; 60 (1): 251–9.

66. Bianchi DW. Cherchez la femme: maternal incidental findings can explain discordant prenatal cell-free DNA sequencing results. Genetics in Medicine. 2017; DOI: 10.1038/gim.2017.219.

67. Hartwig TS, Ambye L, Sørensen S, Jørgensen FS. Discordant non-invasive prenatal testing (NIPT)–a systematic review. Prenatal diagnosis. 2017; 37 (6): 527–39.

68. Attilakos G, Maddocks DG, Davies T, Hunt LP, Avent ND, Soothill PW, et al. Quantification of free fetal DNA in multiple pregnancies and relationship with chorionicity. Prenatal diagnosis. 2011; 31 (10): 967–72.

69. Bevilacqua E, Gil MM, Nicolaides KH, Ordoñez E, Cirigliano V, Dierickx H, et al. Performance of screening for aneuploidies by cell-free DNA analysis of maternal blood in twin pregnancies. Ultrasound in Obstetrics & Gynecology. 2015; 45 (1): 61–6.

70. Curnow KJ, Wilkins-Haug L, Ryan A, Kırkızlar E, Stosic M, Hall MP, et al. Detection of triploid, molar, and vanishing twin pregnancies by a single-nucleotide polymorphism–based noninvasive prenatal test. American journal of obstetrics and gynecology. 2015; 212 (1): 79–e1.

71. Gil MM, Quezada MS, Revello R, Akolekar R, Nicolaides KH. Analysis of cell-free DNA in maternal blood in screening for fetal

aneuploidies: updated meta-analysis. Ultrasound in obstetrics & gynecology. 2015; 45 (3): 249–66.

72. Zhang H, Gao Y, Jiang F, Fu M, Yuan Y, Guo Y, et al. Non-invasive prenatal testing for trisomies 21, 18 and 13: clinical experience from 146 958 pregnancies. Ultrasound in Obstetrics & Gynecology. 2015; 45 (5): 530–8.

73. Russell LM, Strike P, Browne CE, Jacobs PA. X chromosome loss and ageing. Cytogenetic and genome research. 2007; 116 (3): 181–5.

74. Samango-Sprouse C, Kırkızlar E, Hall MP, Lawson P, Demko Z, Zneimer SM, et al. Incidence of X and Y chromosomal aneuploidy in a large child bearing population. PloS One. 2016; 11 (8): e0161045.

75. Shubina J, Trofimov DY, Barkov IY, Stupko OK, Goltsov AY, Mukosey IS, et al. In silico size selection is effective in reducing false positive NIPS cases of monosomy X that are due to maternal mosaic monosomy X. Prenatal diagnosis. 2017; 37 (13): 1305–10.

76. Bianchi DW, Chudova D, Sehnert AJ, Bhatt S, Murray K, Prosen TL, et al. Noninvasive prenatal testing and incidental detection of occult maternal malignancies. Jama. 2015; 314 (2): 162–9.

77. Ferguson-Smith MA. Placental mRNA in maternal plasma: prospects for fetal screening. Proceedings of the National Academy of Sciences. 2003; 100 (8): 4360–2.

78. Chiu RW, Cantor CR, Lo YD. Non-invasive prenatal diagnosis by single molecule counting technologies. Trends in genetics. 2009; 25 (7): 324–31.

79. ACOG Practice Bulletin № 77: screening for fetal chromosomal abnormalities. Obstet Gynecol. 2007; (109): 217–27.

80. Benn P, Borrell A, Chiu RW, Cuckle H, Dugoff L, Faas B, et al. Position statement from the Chromosome Abnormality Screening Committee on behalf of the Board of the International Society for Prenatal Diagnosis. Prenatal diagnosis. 2015; 35 (8): 725–34.

81. Кащеева Т. К., Кузнецова Т. В., Баранов В. С. Новые технологии и тенденции развития пренатальной диагностики. Журнал акушерства и женских болезней. 2017; 66 (2): 33–39.

82. UK National Screening Committee. www.gov.uk URL. Available from: https://www.gov.uk/government/groups/uk-national-screening-committee-uk-nsc (дата обращения: 20.07.2018).

83. Screening in the UK: making effective recommendations 2015 to 2016. Public Health England hosts the UK National Screening Committee URL. Available from: https://assets.publishing.service.gov.uk/government/uploads/system/uploads/attachment_data/file/538524/Screening_in_the_UK___making_effective_recommendations_2015_to_2016_180716_final.pdf (дата обращения: 20.07.2018).

84. Analysis of foetal DNA in the woman's blood: non-invasive prenatal testing (NIPT) for trisomy 13, 18 and 21. SFOG Guidelines URL: http://www.nfog.org/files/guidelines/NIPT%202016%2006%2005%20.pdf (дата обращения: 20.07.2018).

85. Trisomie 21 : la HAS actualise ses recommandations concernant le dépistage prénatal de la trisomie 21. www.has-sante.fr URL. Available from: https://www.has-sante.fr/portail/jcms/c_2768535/fr/trisomie-21-la-has-actualise-ses-recommandations-concernant-le-depistage-prenatal-de-la-trisomie-21 (дата обращения: 20.07.2018).

86. Allyse M, Wick MJ. What do the new American College of Medical Genetics and Genomics (ACMG) guidelines mean for the provision of non-invasive prenatal genetic screening? Journal of Obstetrics and Gynaecology. 2017; 37 (6): 795–8.

87. American College of Obstetricians and Gynecologists: Screening for fetal aneuploidy. Obstet Gynecol. 2016; 127 (5): e123–137.

88. Prenatal cell-free DNA screening. National Society of Genetic Counselors. Available from: http://www.nsgc.org/p/bl/et/blogaid=805#.WCTELTNR ftw.linkedin.

89. Gregg AR, Skotko BG, Benkendorf JL, Monaghan KG, Bajaj K, Best RG, et al. Noninvasive prenatal screening for fetal aneuploidy, 2016 update: a position statement of the American College of Medical Genetics and Genomics. Genetics in medicine. 2016; 18 (10): 1056–65.

90. Информационно-методическое письмо Минздрава РФ от 19.03.2015 № 15-4/607. Доступно по ссылке: http://www.consultant.ru/document/cons_doc_LAW_177689/.

91. Сухих Г. Т., Трофимов Д. Ю., Барков И. Ю., Донников А. Е., Шубина Е. С., Коростин Д. О. и др. Неинвазивный пренатальный ДНК-скрининг анеуплоидий плода по крови матери методом высокопроизводительного секвенирования. Клинические рекомендации. Акушерство и гинекология. 2016; (6): 3–22.

DETECTION OF CHROMOSOMAL REARRANGEMENTS IN THE SHORT ARMS OF CHROMOSOMES 4 AND 12 AS AN EXAMPLE OF A WHOLE-GENOME APPROACH TO NONINVASIVE PRENATAL TESTING

Goltsov AYu ✉, Mukosey IS, Kochetkova TO, Shubina J, Kuznetsova MV, Stupko OK, Barkov IYu, Rebrikov DV, Trofimov DYu

Kulakov National Medical Research Center for Obstetrics, Gynecology and Perinatology, Moscow, Russia

Timely detection of fetal aneuploidy is an important aspect of clinical practice. At present, analytical techniques involving high-throughput sequencing are on the rise. Noninvasive prenatal testing (NIPT) ensures reliable results as early as week 9–11 into pregnancy. This article describes a clinical case of NIPT application and further verification of its results. Using next-generation sequencing, the microarray analysis of cell-free DNA in the amniotic fluid and the cytogenetic analysis of fetal chromosomes, a high risk of chromosomal rearrangements was detected in the short arms of chromosomes 4 and 12. This prediction was verified by molecular karyotyping conducted in both parents. The mother was found to be a balanced carrier of translocations between chromosomes 4 and 12. This case demonstrates the advantages of a whole-genome approach to NIPT over targeted-based.

Keywords: aneuploidy, noninvasive prenatal testing, syndrome, invasive diagnostic test, combined screening

ДЕТЕКЦИЯ ХРОМОСОМНЫХ ПЕРЕСТРОЕК В КОРОТКОМ ПЛЕЧЕ 4-Й И 12-Й ХРОМОСОМ КАК ПРИМЕР ПОЛНОГЕНОМНОГО ПОДХОДА ПРИ ПРОВЕДЕНИИ НЕИНВАЗИВНОГО ДНК-СКРИНИНГА

А. Ю. Гольцов ✉, И. С. Мукосей, Т. О. Кочеткова, Е. Шубина, М. В. Кузнецова, О. К. Ступко, И. Ю. Барков, Д. В. Ребриков, Д. Ю. Трофимов

Национальный медицинский исследовательский центр акушерства, гинекологии и перинатологии имени В. И. Кулакова, Москва, Россия

Своевременное обнаружение анеуплоидий плода очень важно в клинической практике. В настоящее время идет активное развитие аналитических методов с применением высокопроизводительного секвенирования. Благодаря неинвазивному пренатальному ДНК-скринингу (НИПС) достоверные результаты можно получать на сроке 9–11 недель. Описан клинический случай применения НИПС и дальнейшей верификации полученных результатов. С помощью методов высокопроизводительного секвенирования, микроматричного анализа амниотической жидкости и цитогенетического кариотипирования у плода обнаружен высокий риск хромосомных перестроек в коротком плече 4-й и 12-й хромосом. Результаты были подтверждены с помощью молекулярного кариотипирования. Проверка родителей позволила выявить у матери сбалансированные хромосомные перестройки в 4-й и 12-й хромосомах. Данный случай демонстрирует преимущества полногеномного подхода перед таргетным при проведении НИПС.

Ключевые слова: анеуплоидии, неинвазивный пренатальный ДНК-скрининг, синдром, инвазивная диагностика, комбинированный скрининг

Chromosomal aneuploidy (CA) is a common cause of perinatal death and abnormal fetal development. CA is diagnosed in one in 3 pregnancies ended in missed or spontaneous abortions. The incidence rate of CA in newborn infants is 1 : 300. The most common aneuploidies are trisomies 21, 18 and 13 [1] and sex chromosome aneuploidy. Maternal age is one of the risk factors for CA.

For timely detection of fetal CA, Russia has adopted 1st trimester screening that combines an ultrasound scan and blood biochemistry tests [2]. It has limited specificity and sensitivity because biochemical parameters of the blood are determined by a number of factors that also include the hormonal status of the mother apart from the chromosomal status of the fetus. Women at high risk for aneuploidy are recommended to undergo additional, more accurate tests. CA is confirmed in about 13 to 15% of these women. The tests are invasive (amniocentesis, cordocentesis, chorionic villus sampling) and can cause pregnancy loss in 0.5-2% of

patients; therefore, they are contraindicated for women at high risk for pregnancy loss. Noninvasive prenatal testing (NIPT) is an alternative to invasive procedures in cases when gestational age does not exceed 18–19 weeks [3]. NIPT does not have contraindications for high-risk women and can be performed as early as 9–10 weeks into pregnancy. Noninvasive prenatal tests vary in the number of chromosomes they target, which is usually limited to chromosomes 13, 18 and 21 [4,5]. Even in whole-genome-based NIPT, other chromosomes are rarely analyzed (Prenetix, Panorama). There is a test that only looks for trisomy 21 (Down syndrome); it is also referred to as NIPT.

Case study

Below, we describe a case of a 30-year-old pregnant female patient P. The patient already had a 3-year-old daughter diagnosed with disseminated intravascular coagulation and high-pressure hydrocephalus. The patient's BMI was 17.6 kg/m².

The patient was pregnant for the third time; the pregnancy was spontaneous. An ultrasound scan performed as part of combined first trimester screening was not suggestive of chromosomal abnormalities or congenital defects. NFT was 1.3 mm; the nasal bone could be visualized. β-HCG = 0.508 MoM; PAPP-A = 0.314 MoM.

The following risks were identified based on the results of first trimester screening:

trisomy 21 — 1 : 10 084 (baseline risk 1 : 585);
trisomy 18 — 1 : 1073 (baseline risk 1 : 1396);
trisomy 13 — 1 : 1372 (baseline risk 1 : 4389).

A blood sample for NIPT was collected at 13 weeks 4 days gestational age. Whole-genome sequencing of the cell-free DNA library was carried out using Ion S5XL (ThermoFisher Scientific; USA); the yielded data were analyzed following a protocol proposed in [6]. The obtained reads were mapped onto the reference genome; CG content was bias-corrected, and uniquely mapped reads were counted. The risk for CA was estimated using the original software developed by the authors of this work [7].

Based on the results of our analysis, the following conclusions were drawn. The prepared whole-genome library was covered by 7.5 million reads; the sex of the fetus was determined as male. Y chromosome sequences made 16% of the total cell-free DNA. No aneuploidy was detected for chromosomes 13, 18 and 21. However, the analysis revealed a high risk of a p16-p14 deletion on the short arm of chromosome with an estimated size of 35 Mb (Fig. 1A) and a high risk of a p13.3–p12.1 duplication (25 Mb in size) on the short arm of chromosome 12 (Fig. 1B). The obtained data had to be further verified using invasive techniques [8, 9].

To verify NIPT results [10], a microarray analysis of the amniotic fluid was performed using CytoScan Optima Array microchips (Affimetrics; USA). Sampling was done at 16 weeks into pregnancy.

Results are presented in Fig. 2 and 3.
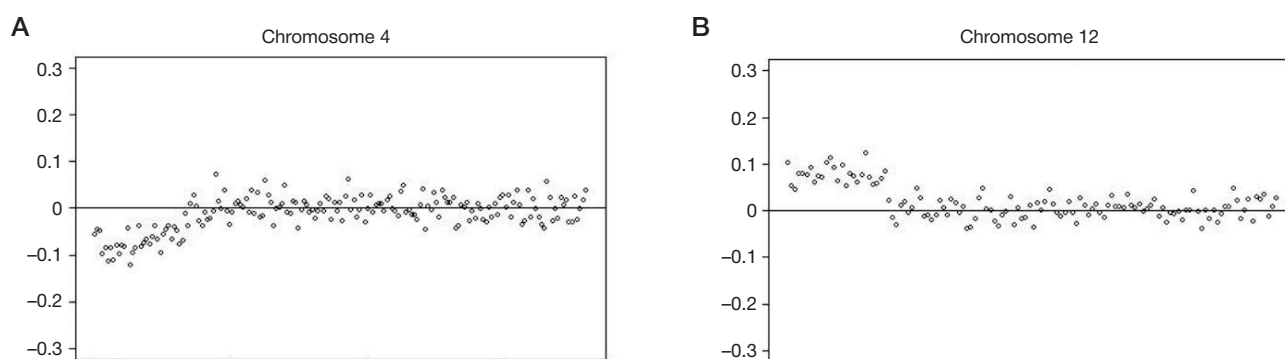
Fig. 1. A visual representation of distribution of reads along the chromosome. The Y axis shows deviations in the read count from the reference values for the normal genotype. **A**. Distribution of reads for chromosome 4. **B**. Distribution of reads for chromosome 12

Fig. 2. Results of the analysis of the amniotic fluid collected from patient P. showing a deletion on the short arm of chromosome 4

Fig. 3. Results of the analysis of the amniotic fluid collected from patient P. showing a duplication on the short arm of chromosome 12

Specimen type: peripheral blood

Staining type: G-banding

Karyotype: 46,XX,t(4;12)(p15.1;p11.2)

Conclusion: Balanced female carrier of a reciprocal translocation between chromosomes 4 and 12 with breakpoints at 4p15.1 and 12p11.2
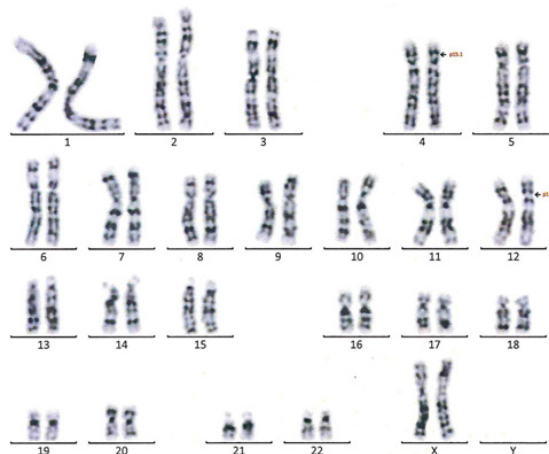
Fig. 4. Patient P.'s karyotype

The embryonic karyotype is described below:

arr[hg19] 4p16.3(68,345-35,195,686)x1 — a 35 million b.p.-long partial deletion of the short arm of chromosome 4 causing the Wolf–Hirschhorn syndrome (OMIM# 194190);

arr[hg19] 12p13.33p11.22(173,786-28,183,286)x3 — a 28 million b.p.-long duplication on the short arm of chromosome 12 causing the Pallister–Killian syndrome (OMIM# 601803) also known as tetrasomy 12p.

The patient was recommended to terminate pregnancy. Pregnancy was terminated at 18 weeks.

DISCUSSION

The analysis revealed detrimental chromosomal rearrangements in the fetus. Therefore, it was recommended that both parents undergo karyotyping. The mother was found to carry a balanced translocation involving chromosomes 4 and 12, the underlying cause of the abnormalities in the fetus (Fig. 4).

We were able to detect such rare chromosomal aberrations only due to the use of whole-genome sequencing during NIPT.

There are a few varieties of NIPT. Some of them are based either on the targeted sequencing of chromosomes 13, 18 and 21 or on the selective analysis of only certain chromosomes [11, 12]. Obviously, such approaches do not allow detection of those chromosomal rearrangements that are present on other, untargeted chromosomes. There have been clinical reports of missed partial deletions (22q11, known as DiGeorge syndrome), as well as deletions of the entire short arm of chromosome 5 (cat's cry syndrome), that went unnoticed by NIPT and eventually led to the birth of an unhealthy child.

CONCLUSION

This clinical case had a few minor and major implications. First, due to the high risk of chromosomal abnormalities in future pregnancies, the patient and her husband were recommended to undergo preimplantation genetic profiling. Second, whole-genome NIPT has a few advantages over targeted-based since it covers all chromosomes and does not result in the loss of data from clinically important genome regions.

References

1. Ehrich M, Deciu C, Zwiefelhofer T, Tynan JA, Cagasan L, Tim R, et al. Noninvasive detection of fetal trisomy 21 by sequencing of DNA in maternal blood: a study in a clinical setting. American journal of obstetrics and gynecology. 2011; 204 (3): 205–e1.
2. Wald NJ, Hackshaw AK. Combining ultrasound and biochemistry in first-trimester screening for Down's syndrome. Prenatal diagnosis. 1997; 17 (9): 821–9.
3. Zhang H, Gao Y, Jiang F, Fu M, Yuan Y, Guo Y, et al. Non-invasive prenatal testing for trisomies 21, 18 and 13: Clinical experience from 146 958 pregnancies. Ultrasound Obstet. Gynecol. 2015; 45 (5): 530–8.
4. Hartwig TS, Ambye L, Sørensen S, Jørgensen FS. Discordant non-invasive prenatal testing (NIPT) — a systematic review. Prenat Diagn. 2017; 37 (6): 527–39.
5. Canick JA, Palomaki GE, Kloza EM, Lambert-Messerlian GM, Haddow JE. The impact of maternal plasma DNA fetal fraction on next generation sequencing tests for common fetal aneuploidies. Prenat Diagn. 2013; 33 (7): 667–74.
6. Sukhikh GT, Karetnikova NA, Baranova EE, Shubina E,

Korostin DO, Ekimov A, et al. Noninvasive prenatal diagnosis of aneuploidies by next- generation sequencing (ngs) in a group of high-risk women. Obstetrics and Gynecology. 2015; (4): 5–10.
7. Noninvasive prenatal DNA-scrining fetal aneuploidy in maternal blood by next-generation sequencing (ngs) method. Clinical recommendation. Obstetrics and Gynecology. 2016; (6): 1–22.
8. Lo YM, Chan KC, Sun H, Chen EZ, Jiang P, Lun FM, et al. Maternal plasma DNA sequencing reveals the genome-wide genetic and mutational profile of the fetus. Sci Transl Med. 2010; 2 (61): 61–91.
9. Fiorentino F, Bono S, Pizzuti F, Mariano M, Polverari A, Duca S, et al. The importance of determining the limit of detection of non invasive prenatal testing methods. Prenat Diagn. 2016; 36 (4): 304–11.
10. Juneau K, Bogard PE, Huang S, Mohseni M, Wang ET, Ryvkin P, et al. Microarray-Based Cell-Free DNA Analysis Improves Noninvasive Prenatal Testing. Fetal Diagn Ther. 2014; 36 (4): 282–6.
11. Wang J-C, Sahoo T, Schonberg S, Kopita K, Ross L, Patek K, et al. Discordant noninvasive prenatal testing and cytogenetic results: a study of 109 consecutive cases. Genet Med. 2015; 17 (3): 234–6.

12. Ma J, Cram DS, Zhang J, Shang L, Yang H, Pan H. Birth of a child with trisomy 9 mosaicism syndrome associated with paternal isodisomy 9: case of a positive noninvasive prenatal test result unconfirmed by invasive prenatal diagnosis. Mol Cytogenet. 2015; (8): 44.

Литература

1. Ehrich M, Deciu C, Zwiefelhofer T, Tynan JA, Cagasan L, Tim R, et al. Noninvasive detection of fetal trisomy 21 by sequencing of DNA in maternal blood: a study in a clinical setting. American journal of obstetrics and gynecology. 2011; 204 (3): 205–e1.
2. Wald NJ, Hackshaw AK. Combining ultrasound and biochemistry in first-trimester screening for Down's syndrome. Prenatal diagnosis. 1997; 17 (9): 821–9.
3. Zhang H, Gao Y, Jiang F, Fu M, Yuan Y, Guo Y, et al. Non-invasive prenatal testing for trisomies 21, 18 and 13: Clinical experience from 146 958 pregnancies. Ultrasound Obstet. Gynecol. 2015; 45 (5): 530–8.
4. Hartwig TS, Ambye L, Sørensen S, Jørgensen FS. Discordant non-invasive prenatal testing (NIPT) — a systematic review. Prenat Diagn. 2017; 37 (6): 527–39.
5. Canick JA, Palomaki GE, Kloza EM, Lambert-Messerlian GM, Haddow JE. The impact of maternal plasma DNA fetal fraction on next generation sequencing tests for common fetal aneuploidies. Prenat Diagn. 2013; 33 (7): 667–74.
6. Сухих Г. Т., Каретникова Н. А., Баранова Е. Е., Шубина Е. С., Коростин Д. О., Екимов А. Н. и др. Неинвазивная пренатальная диагностика анеуплоидий методом высокопроизводительного секвенирования (NGS) в группе женщин высокого риска. Акушерство и гинекология. 2015; (4): 5–10.
7. Неинвазивный пренатальный ДНК-скрининг анеуплоидий плода по крови матери методом высокопроизводительного секвенирования. Клинические рекомендации. Акушерство и гинекология. 2016; (6): 1–22.
8. Lo YM, Chan KC, Sun H, Chen EZ, Jiang P, Lun FM, et al. Maternal plasma DNA sequencing reveals the genome-wide genetic and mutational profile of the fetus. Sci Transl Med. 2010; 2 (61): 61–91.
9. Fiorentino F, Bono S, Pizzuti F, Mariano M, Polverari A, Duca S, et al. The importance of determining the limit of detection of non invasive prenatal testing methods. Prenat Diagn. 2016; 36 (4): 304–11.
10. Juneau K, Bogard PE, Huang S, Mohseni M, Wang ET, Ryvkin P, et al. Microarray-Based Cell-Free DNA Analysis Improves Noninvasive Prenatal Testing. Fetal Diagn Ther. 2014; 36 (4): 282–6.
11. Wang J-C, Sahoo T, Schonberg S, Kopita K, Ross L, Patek K, et al. Discordant noninvasive prenatal testing and cytogenetic results: a study of 109 consecutive cases. Genet Med. 2015; 17 (3): 234–6.
12. Ma J, Cram DS, Zhang J, Shang L, Yang H, Pan H. Birth of a child with trisomy 9 mosaicism syndrome associated with paternal isodisomy 9: case of a positive noninvasive prenatal test result unconfirmed by invasive prenatal diagnosis. Mol Cytogenet. 2015; (8): 44.

TOXICITY OF ^{13}C-LABELED LINOLEIC AND LINOLENIC ACIDS FOR DIAGNOSTIC BREATH TESTS

Tynio YaYa[1], Morozova GV[2], Biryukova YuK[3,4] ✉, Trubnikova EV[3], Zylkova MV[4], Sivokhin DA[5], Ivanov KP[6], Pozdniakova NV[7], Kazakova EA[8], Mutnykh ES[9], Shevelev AB[9,10]

[1] Russian State University of Physical Education, Sport, Youth and Tourism, Moscow, Russia

[2] Skryabin Moscow State Academy of Veterinary Medicine and Biotechnology, Moscow, Russia

[3] Kursk State University, Kursk, Russia

[4] Chumakov Federal Scientific Center for Research and Development of Immune and Biological Products, Russian Academy of Sciences, Moscow, Russia

[5] Sechenov First Moscow State Medical University (Sechenov University), Moscow, Russia

[6] Bakulev Center for Cardiovascular Surgery Moscow, Russia

[7] Blokhin National Medical Research Center of Oncology, Moscow, Russia

[8] National Research University Higher School of Economics, Moscow, Russia

[9] Vavilov Institute of General Genetics, Moscow, Russia

[10] Plekhanov Russian University of Economics, Moscow, Russia

Noninvasive stable isotope breath tests allow highly accurate and safe estimation of liver and biliary tract function. The aim of this study was to test ^{13}C-labeled linoleic and linolenic acids intended for diagnostic use for acute and subchronic toxicity. The acids were synthesized using the patented method. A single intragastric administration of the tested compounds to experimental BALB/c mice and Wistar rats in the amounts exceeding clinical doses 500 to 2500-fold did not cause animal death. In the subchronic toxicity test, the rats received 5 to 25 times higher doses than recommended for clinical use in humans. In a 14-day follow-up period, no significant differences were observed between the main and the control groups in terms of weight, blood count (red blood cells, white blood cells, platelets), and blood biochemistry (hemoglobin, total protein, alkaline phosphatase, alanine aminotransferase, aspartate aminotransferase, lactate dehydrogenase, bilirubin). The studied compounds are safe at doses intended for oral administration and are recommended for further preclinical and clinical trials.

Keywords: breath test, linoleic acid, linolenic acid, carbon-13

✉ **Correspondence should be addressed:** Yulia K. Biryukova
Kosygina 4, Moscow, 119334; biriukova-ula@mail.ru

ИССЛЕДОВАНИЕ ТОКСИЧНОСТИ [13]C-МЕЧЕНЫХ ЛИНОЛЕВОЙ И ЛИНОЛЕНОВОЙ КИСЛОТ, ПРЕДНАЗНАЧЕННЫХ ДЛЯ ПРОВЕДЕНИЯ ДИАГНОСТИЧЕСКИХ ДЫХАТЕЛЬНЫХ ТЕСТОВ

Я. Я. Тыньо[1], Г. В Морозова[2], Ю. К. Бирюкова[3,4] ✉, Е. В. Трубникова[3], М. В. Зылькова[4], Д. А. Сивохин[5], К. П. Иванов[6], Н. В. Позднякова[7], Е. А. Казакова[8], Е. С. Мутных[9], А. Б. Шевелев[9,10]

[1] Российский государственный университет физической культуры, спорта, молодежи и туризма, Москва, Россия

[2] Московская государственная академия ветеринарной медицины и биотехнологии имени К. И. Скрябина, Москва, Россия

[3] Курский государственный университет, Курск, Россия

[4] Федеральный научный центр исследований и разработки иммунологических препаратов имени М. П. Чумакова, Москва, Россия

[5] Первый Московский государственный медицинский университет имени И. М. Сеченова (Сеченовский Университет), Москва, Россия

[6] Национальный медицинский исследовательский центр сердечно-сосудистой хирургии имени А. Н. Бакулева, Москва, Россия

[7] Национальный медицинский исследовательский центр онкологии имени Н. Н. Блохина, Москва, Россия

[8] Национальный исследовательский университет Высшая школа экономики, Москва, Россия

[9] Институт общей генетики имени Н. И. Вавилова, Москва, Россия

[10] Российский экономический университет имени Г. В. Плеханова, Москва, Россия

Неинвазивные дыхательные тесты с применением изотопно-меченых соединений представляют собой новый высокоточный и безопасный метод функционального исследования печени и билиарной системы. Целью работы было провести биологические испытания острой и субхронической токсичности [13]C-меченых линолевой и линоленовой кислот, синтезированных по оригинальной методике и предназначенных для проведения диагностических дыхательных тестов. При однократном внутрижелудочном введении изучаемых соединений лабораторным мышам линии BALB/c и крысам Wistar в дозах, превышающих диагностические в 500–2500 раз, образцы соединений не вызывали смертности экспериментальных животных. При проведении субхронического эксперимента на крысах при дозировках испытываемых соединений, в 5 и 25 раз превышающих терапевтическую дозу для человека, в течение 14 суток было выявлено отсутствие достоверных изменений у животных в экспериментальных группах по сравнению с контрольной по массе тела, гематологическим показателям (содержанию эритроцитов, лейкоцитов и тромбоцитов в крови) и биохимическим показателям сыворотки крови (уровню гемоглобина, общего белка, щелочной фосфатазы, аланинаминотрансферазы, аспартатаминотрансферазы, лактатдегидрогеназы, билирубина). Исследованные меченые кислоты безвредны в дозах, планируемых для перорального введения, и могут быть рекомендованы к доклиническим и клиническим испытаниям.

Ключевые слова: дыхательный тест, линолевая кислота, линоленовая кислота, углерод-13

✉ **Для корреспонденции:** Юлия Константиновна Бирюкова
ул. Косыгина, д. 4, г. Москва, 119334; biriukova-ula@mail.ru

Breath tests are safe and effective tools that provide diagnostic information about the internal organs of the human body. The stable ^{13}C [1] and minimally radioactive ^{14}C [2] breath tests were introduced into clinical practice in the late 20th century. Since then, they have become the gold standard in detecting *Helicobacter pylori* infection [3]. Urease abundantly produced by *H. pylori* breaks down the urea taken in by the patient into $^{13}CO_2$ or $^{14}CO_2$ and ammonia. These products of urea hydrolysis are absorbed into the bloodstream and then excreted by the lungs [4]. The exhaled isotope-labeled CO_2 can be measured using mass spectrometry or a Geiger-Mueller counter [5]. In the absence of *H. pylori* infection, the reaction described above does not occur, and the concentrations of the exhaled $^{13}CO_2$ or $^{14}CO_2$ do not fall outside the reference range.

Non-invasive breath tests are highly accurate, cheap, easy, and safe for both the doctor and the patient. They provide valuable information about a number of parameters needed to choose a treatment strategy [6].

So far, carbon isotopes have been employed as tracers in a variety of breath tests for assessing insulin resistance (those are based on ^{13}C-glucose [7], ^{13}C-metacetin [8], ^{13}C-galactose and ^{13}C-aminopyrine [9]) and in the diagnosis of chronic liver diseases, including hepatitis B and C, cirrhosis, toxic hepatitis, alcoholic hepatitis, etc. ^{13}C-octanoic acid is used to measure the rate of gastric emptying [10], and (^{13}C3-glyceryl) tri-octanoate helps in detecting exocrine pancreatic insufficiency [4].

We believe that extensive efforts taken to increase production output of carbon isotopes and create cost-effective equipment for measuring the isotopic composition of the exhaled breath will expedite introduction of such tests into clinical routine.

Linoleic and linolenic acids are the main active components used in breath tests designed to assess liver and biliary tract function. They are fatty acids with a carbon chain consisting of 18 carbon atoms. The acids are unsaturated: linoleic acid has two carbon-carbon bonds, whereas linolenic acid has three [11].

Tetrasodium pyrophosphate widely used in the production of radiopharmaceutical agents both in Russia and abroad serves as an excipient. In Russia, it was approved for medical applications by Order 507 of the Ministry of Healthcare dated April 14, 1985 (Certificate 85/507/13) and is now marketed as Pyrphotech ^{99m}Tc [12]. Pyrphotech has demonstrated good performance in bone scintigraphy, imaging of acute myocardial infarction, imaging of the choroid, angiocardiography, etc. [12, 13].

Patent 2630691 registered in Russia describes the original *Method of synthesis of ^{13}C and ^{14}C linoleic and linolenic acids* [14]; these fatty acids labeled with carbon isotopes are intended for use in breath tests that assess liver and biliary tract function. It is essential that therapeutic and diagnostic agents undergo a safety trial prior to being introduced into clinical practice. The aim of this work was to study acute and subchronic toxicity of ^{13}C-labeled linoleic and linolenic acids.

METHODS

The acute toxicity test of linoleic and linolenic acids labeled with ^{13}C at position 1 was conducted in strict compliance with the *Guidelines on the study of general toxicity of pharmacological agents* [15]. The test was carried out in 95 male and female BALB/C mice weighing 18 to 20 g and 45 male and female Wistar rats weighing 180 to 210 g.

The tested ^{13}C-labeled acids were synthesized as described in the *Method of synthesis of ^{13}C and ^{14}C linoleic and linolenic acids* (Patent 2630691) [14]. The structure and purity of the intermediate and end products were assessed with nuclear magnetic resonance spectroscopy using an AM 300 spectrometer operating at 300 MHz (Bruker; Germany) and a DRX-500 spectrometer operating at 500 MHz (Bruker; Germany). Mass spectra were acquired using a direct-infusion Finnigan MAT Model Incos 50, 70 eV (Finnigan MAT; UK) and a high-resolution mass spectrometer MicrOTOFII (BrukerDaltonics; Germany) (ESI).

The animals selected for the study were kept in T3 cages. Animal housing met the *Sanitary and Epidemiological Requirements for Laboratory Animal Facilities*. The animals had unlimited access to tap water supplied via 500 ml glass bottles with stainless steel stoppers. The animals had a fixed meal schedule and were fed with pellets containing a balanced composition of amino acids, minerals and vitamins. Throughout the experiment, their physical activity, body weight, appetite, hair condition, and behavior were closely monitored.

For the acute toxicity test, the samples of the tested compounds were dissolved in olive oil and the freshly prepared solutions were administered to the animals by gavage. The rats received a single dose of 100 to 500 mg; the mice, a single dose of 10 to 50 mg. The follow-up period was 3 days. The lethal dose (LD_{50}) was determined for both BALB/c mice and Wistar rats using the Deichmann–LeBlanc method [15].

The subacute toxicity test of the synthesized isotope-labeled acids was conducted in 180 Wistar rats weighing 110–135 g. The test was performed in strict compliance with the *Guidelines on the study of general toxicity of pharmacological agents* [15]. The freshly prepared solutions of the tested compounds were fed to the animals by gavage at doses specified above every day for 2 weeks. The animals were distributed into several groups consisting of 15 males and 15 females each. Group 1 was the control group. The controls received olive oil that did not contain any of the tested acids. Group 2 received 5 mg/kg ^{13}C-labeled linoleic acid, which is 5 times higher than the clinical dose in humans. Group 3 received 25 mg/kg ^{13}C-labeled linoleic acid, which is 25 times higher than the human clinical dose. Group 4 received 5 mg/kg ^{13}C-labeled linolenic acid; this dose exceeds the human clinical dose 5-fold. Group 5 received 25 mg/kg ^{13}C-labeled linolenic acid, which exceeds the human clinical dose 5-fold.

In rats, blood samples (2.0–2.5 ml) were collected from the tail vein before the subchronic toxicity test, one week after the first administration of the tested compounds and 2 weeks after the first administration. Blood count was aided by a Picoscale PS-4M automated analyzer (Medicor-Elektromedika; Hungary).

Concentration of blood glucose, total protein, creatinine, cholesterol, total bilirubin, alkaline phosphatase, alanine aminotransferase, aspartate aminotransferase, and lactate dehydrogenase were determined using a discrete FP 901 analyzer (Labsystems; Finland).

The rats were sacrificed on day 14 of the subchronic toxicity experiment. Necropsy was performed straight away in order to avoid self-digestion of tissue by intracellular enzymes. A detailed report was prepared for each necropsy.

Specimens of organs and tissues were fixed in 10% neutral buffered formalin, then dehydrated, cleared, and embedded in paraffin wax. Serial sections were prepared using a sliding MS-1 microtome (Ambimed; Russia). Upon deparaffinization, the sections were stained with hematoxylin-eosin, mounted in Canada balsam and covered with a coverslip. The obtained slides were examined under a Leica CM E microscope (Leica Microsystems; German) and photographed using a Micromed DCM-510 SCOPE eyepiece camera (Nabludatelnye pribory; Russia) at ×40, ×100, ×200, and ×400 magnification. Images

were processed in the Future Win Joe software (Future Optics; Chine) supplied with the eyepiece camera. Necropsy data were compared between the rats who had received ^{13}C-labeled linoleic and linolenic acids and the controls.

The null hypothesis was tested using the nonparametric Mann–Whitney U and Fisher exact tests in *Statistica 8.0 for Windows* (Dell; USA). Means, the median, maximum and minimum values and interquartile ranges were calculated [16]. For qualitative variables, the sampling fraction was calculated and expressed as percentage, as well as the sampling error.

RESULTS

Study of acute single-dose toxicity of ^{13}C-labeled linoleic and linoleic acids

No signs of intoxication or gastric irritation were noticed in the animals following single administration of the tested compounds at the highest dose of 2.632 mg/kg for mice and 2.564 mg/kg for rats. No death cases were observed in both rats and mice. We found no differences in sensitivity to the compounds between the animals of different sex and species.

Thus, intragastric administration of ^{13}C-labeled linoleic and ^{13}C-labeled linolenic acids to small animal species at doses 2,500 times higher than the clinical dose in humans did not cause intoxication or animal death during the entire follow-up period (3 days). The manufacturer of ^{13}C-labeled linoleic acid (Science Lab; USA) specifies that its LD_{50} is 3.2 g/kg. This value was obtained after administering a significantly higher dose of the tested fatty acid to experimental animals. Therefore, we

conclude that our acute toxicity test revealed no difference in toxicity between the acid synthesized by us and its commercially available analogue.

Study of subchronic toxicity of ^{13}C-labeled linoleic and linolenic acids in rats

Two-week daily administration of 5 and 25 mg/kg ^{13}C-labeled linoleic and linolenic acids did not cause any significant changes in the animals' behavior and appearance, as compared to the controls. The animals were active, their hair was smooth and appetite was good.

Body weight dynamics monitored in all experimental and control groups throughout the experiment are presented in Tables 1 and 2.

On the whole, no significant differences were observed between the experimental and control groups except for the male group that was receiving 5 and 25 mg/kg ^{13}C-linolenic acid for 2 weeks. Those male rats were gaining more weight than the controls, which suggests a stimulatory effect of the tested compound on animal growth. No detrimental effect of the acid was observed on the growth and general health of the laboratory animals.

Results of blood tests in the experimental and control groups are shown in Table 3.

Slight yet significant differences (> 0.95 confidence level) in hemoglobin concentrations were revealed in the male rats who were receiving 5 mg/kg ^{13}C-linolenic acid. In the group of female rats who receiving the same dose of ^{13}C-linolenic acid, the differences were significant for white blood cell and platelet

Table 1. Body weight dynamics of male rats that received ^{13}C-labeled linoleic and linolenic acids by intragastric gavage for 2 weeks

Before the experiment	Controls, g	Experimental group, g	*p*
Linoleic acid, 5 mg/kg	113.3	115.7	> 0.05
Linoleic acid, 25 mg/kg	113.3	114.0	> 0.05
Day 14 of the experiment			
Linoleic acid, 5 mg/kg	132.1	135.3	> 0.05
Linoleic acid, 25 mg/kg	132.1	133.6	> 0.05
Before the experiment			
Linolenic acid, 5 mg/kg	116.4	114.2	> 0.05
Linolenic acid, 25 mg/kg	116.4	117.5	> 0.05
Day 14 of the experiment			
Linolenic acid, 5 mg/kg	130.6	136.3	> 0.001
Linolenic acid, 25 mg/kg	130.6	138.2	< 0.001

Table 2. Body weight dynamics of female rats that received ^{13}C-labeled linoleic and linolenic acids by intragastric gavage for 2 weeks

Before the experiment	Controls, g	Experimental group, g	*p*
Linoleic acid, 5 mg/kg	111.9	112.2	> 0.05
Linoleic acid, 25 mg/kg	111.9	112.9	> 0.05
Day 14 of the experiment			
Linoleic acid, 5 mg/kg	129.3	132.1	> 0.05
Linoleic acid, 25 mg/kg	129.3	131.5	> 0.05
Before the experiment			
Linolenic acid, 5 mg/kg	113.8	115.4	> 0.05
Linolenic acid, 25 mg/kg	113.8	114.6	> 0.05
Day 14 of the experiment			
Linolenic acid, 5 mg/kg	127.2	134.1	> 0.05
Linolenic acid, 25 mg/kg	127.2	130.3	> 0.05

counts. However, on day 14 of the experiment, the differences faded, which may suggest they were accidental.

By contrast, the end of week 1 revealed no significant differences between the groups that were receiving higher (25 mg/kg) doses of ^{13}C-labeled linolenic acid. However, a significant decline in white blood cell count (> 0.999 confidence level) was noticed in the female rats on day 14, as well as a slight decline in platelet count in both males and females

(> 0.95 confidence level). In spite of the differences between the groups, the absolute values of the measured parameters fell within the normal reference range, suggesting safety of the tested doses.

Total protein levels in the blood serum are given in Table 4.

The female rats who were receiving 5 mg/kg of the tested compound had higher total protein concentrations than the controls by the end of week 1 and week 2. A similar situation

Table 3. Blood count in rats that received ^{13}C-linoleic acid for 2 weeks

5 mg/kg			25 mg/kg		
Red blood cells					
	Males	Females		Males	Females
Week 1	$p > 0.05$	$p > 0.05$	Week 1	$p > 0.05$	$p < 0.05$
Week 2	$p > 0.05$	$p > 0.05$	Вторая неделя	$p > 0.05$	$p < 0.05$
White blood cells					
Week 1	$p > 0.05$	$p < 0.05$	Week 1	$p > 0.05$	$p > 0.05$
Week 2	$p > 0.05$	$p > 0.05$	Week 2	$p > 0.05$	$p = 0.001$
Platelets					
Week 1	$p > 0.05$	$p < 0.05$	Week 1	$p > 0.05$	$p > 0.05$
Week 2	$p > 0.05$	$p > 0.05$	Week 2	$p < 0.05$	$p < 0.05$
Hemoglobin					
Week 1	$p < 0.05$	$p > 0.05$	Week 1	$p > 0.05$	$p > 0.05$
Week 2	$p > 0.05$	$p > 0.05$	Week 2	$p > 0.05$	$p > 0.05$

Table 4. Total protein concentrations (g/L) in the blood serum of rats that received ^{13}C-linoleic acid for 2 weeks

5 mg/kg			25 mg/kg		
	Males	Females		Males	Females
Week 1	$p > 0.05$	$p < 0.05$	Week 1	$p > 0.05$	$p < 0.05$
Week 2	$p < 0.05$	$p < 0.05$	Week 2	$p < 0.05$	$p > 0.05$

Table 5. Enzymic activity and total bilirubin levels in the blood serum of male rats that received ^{13}C-linoleic acid for 2 weeks

5 mg/kg			25 mg/kg		
Alkaline phosphatase					
	Males	Females		Males	Females
Week 1	$p > 0.05$	$p < 0.05$	Week 1	$p < 0.01$	$p < 0.01$
Week 2	$p < 0.05$	$p < 0.05$	Week 2	$p < 0.001$	$p < 0.01$
Alanine aminotransferase, un/L					
Week 1	$p > 0.05$	$p < 0.05$	Week 1	$p < 0.001$	$p < 0.001$
Week 2	$p < 0.05$	$p < 0.05$	Week 2	$p > 0.05$	$p > 0.05$
Aspartate aminotransferase, un/L					
Week 1	$p > 0.05$	$p > 0.05$	Week 1	$p < 0.05$	$p > 0.05$
Week 2	$p < 0.001$	$p < 0.01$	Week 2	$p > 0.05$	$p > 0.05$
Lactate dehydrogenase, un/L					
Week 1	$p > 0.05$	$p < 0.001$	Week 1	$p < 0.001$	$p < 0.001$
Week 2	$p < 0.001$	$p < 0.001$	Week 2	$p < 0.001$	$p < 0.001$
Total bilirubin, µM					
Week 1	$p < 0.001$	$p < 0.01$	Week 1	$p < 0.001$	$p < 0.001$
Week 2	$p > 0.05$	$p < 0.001$	Week 2	$p < 0.001$	$p < 0.001$

was observed in the male rats on day 14 of the experiment. As compared to the controls, total protein levels were also higher in the female rats a week after the onset of the experiment and in the male animals on day 14. This suggests that the studied compound stimulates protein synthesis, which cannot be regarded as a sign of its toxic effect.

Hepatotoxicity of candidate drugs is traditionally inferred from elevated aspartate and alanine aminotransferases, alkaline phosphatase, lactate dehydrogenase, and total bilirubin in the blood serum (Table 5).

In week one, we witnessed a slight decline in hepatic enzymes in the animals who were receiving 5 mg/kg ^{13}C-linoleic acid. During week 2, this decline became significant in all the subjects. A drop in alkaline phosphatase was the most pronounced for 25 mg/kg doses. By contrast, the levels of aminotransferases had gone back to normal by the end of week 2.

Administered at 5 and 25 mg/kg, ^{13}C-linoleic acid caused a significant decline in total bilirubin measured in the blood serum during weeks 1 and 2 of the experiment (except for the group of male rats during week 2). This observation suggests that the tested compound is not toxic to the liver and possibly has a hepatoprotective effect.

DISCUSSION

It is hard to assess the feasibility of breath tests in small laboratory animals because collection of exhaled air samples is a technically demanding procedure. Therefore, we plan to conduct the efficacy and safety trials of ^{13}C-linoleic and ^{13}C-linolenic acids in human patients once the acids successfully pass extensive toxicity studies. A similar strategy was adopted

by other researchers who developed a ^{14}C urea breath test for detecting *H. pylori* infection [2].

Acute toxicity tests of ^{13}C-linoleic and ^{13}C-linolenic acids administered to BALB/c mice and Wistar rats as a single oral dose that exceeds the clinical dose in humans 500 to 2,500-fold did not reveal any signs of general toxicity or gastric irritation. No death cases were observed.

The study of subchronic toxicity of ^{13}C-linoleic acid administered to male and female Wistar rats at 5 and 25 mg/kg, which is 5 and 25 times higher than the clinical dose in humans, on a daily basis for 2 weeks did not reveal any pronounced effect of the acids on the general health, activity and behavior of the animals.

Moreover, at such high doses the acids produced a beneficial effect on the animals reflected in their blood count and blood chemistry. White blood cells and platelets underwent a transient decline in their number but the counts were still within the normal reference range. A transient decline was also observed for alkaline phosphatase, alanine aminotransferase, aspartate aminotransferase, lactate dehydrogenase, and bilirubin. Those effects were dose-dependent, suggesting that they will be further reduced to zero at clinical doses. There are reports of similar effects observed for linoleic and linolenic acids not labeled with carbon isotopes [17].

CONCLUSIONS

^{13}C-labeled linoleic and ^{13}C-labeled linolenic acids synthesized following the original method described in Patent 2630691 (Russia) are safe for laboratory animals at doses intended for oral intake and can be recommended for further preclinical and clinical trials.

References

1. Savarino V, Vigneri S, Celle G. The ^{13}C urea breath test in the diagnosis of Helicobacter pylori infection. Gut. 1999; 45 (suppl. 1): 18–23.
2. Balăn H, Gold CA, Dworkin HJ, McCormick VA, Freitas JE. Procedure Guideline for Carbon-14-Urea Breath Test. J Nucl Med. 2016; 39 (11): 2012–14.
3. Zhou Q, Li L, Ai Y, Pan Z, Guo M, Han J. Diagnostic accuracy of the ^{14}C-urea breath test in Helicobacter pylori infections: a meta-analysis. Wien Klin Wochenschr. 2017; 129 (1–2): 38–45.
4. Elman AR, Rapoport SI. Stabil'no-izotopnaja diagnostika v Rossii: itogi i perspektivy. ^{13}S-preparaty, pribory, metody. Klin. med. 2014; 92 (7): 5–11. Russian.
5. Modak AS. Stable isotope breath tests in clinical medicine: A review. J Breath Res. 2007; 1 (1): R1–R13.
6. Musialik J, Jonderko K, Kasicka-Jonderko A, Buschhaus M. $^{13}CO_2$ breath tests in non-invasive hepatological diagnosis. Prz. Gastroenterol. 2015; 10 (1): 1–6.
7. Mizrahi M, Lalazar G, Adar T, Raz I, Ilan Y. Assessment of insulin resistance by a ^{13}C glucose breath test: A new tool for early diagnosis and follow-up of high-risk patients. Nutr J. 2010; (9): 25. DOI:10.1186/1475-2891-9-25.
8. Elman AR, Korneeva GA, Noskov YuG, Khan VN, Shishkina EYu, Negrimovski VM, i dr. Sintez produktov, mechennyh izotopom ^{13}S, dlja medicinskoj diagnostiki. Rossijskij himicheskij zhurnal. 2013; LVII (5-2): 3–24. Rssian.
9. Giannini EG, Alberto F, Paolo B, Federica B, Federica M. ^{13}C-galactose breath test and ^{13}C-aminopyrine breath test for the study of liver function in chronic liver disease. Clin Gastroenterol Hepatol. 2005; 3 (3): 279–85.

10. Horowitz M, O'Donovan D, Jones KL, Feinle C, Rayner CK, Samsom M. Gastric emptying in diabetes: Clinical significance and treatment. Diabet Med. 2002; 19 (3): 177–94.
11. Titov VN. Klinicheskaja biohimija zhirnyh kislot, lipidov i lipoproteinov. Gipolipidemicheskaja terapija i profilaktika ateroskleroza. Kliniko-laboratornyj konsilium. 2014; (1): 4–29. Russian.
12. Malysheva AO, Kodina GE, Voronitckaya NN, Grafskova TA, Semonenko NP. Opredelenie kachestva radiofarmacevticheskogo preparata «Pirfoteh, 99m Tc» v medicinskih uchrezhdenijah. MOBI-HimFarma. 2017; s. 103. Available from: http://mobi-chem.org/arhiv.html. Russian.
13. Sazonova SI, Ilyushenkova YuN, Lishmanov YuB. Metodika radionuklidnogo issledovanija vospalitel'nyh processov v serdce. Sibirskij medicinskij zhurnal 2015; 30 (4): 32–5. Russian.
14. Pozdeev VV, Tyno YYa, Morozova GV, Bychenko AB, Biryukova YuK, Shevelev AB, avtory; OOO «GK NASh MIR»(RU), patentoobladatel'. Synthesis method of linoleum and linolenic acids, marked by carbon compunds ^{13}C and ^{14}C. Patent RF № 2630691. 12.09.2017.
15. Habriev RU. Rukovodstvo po jeksperimental'nomu (doklinicheskomu) izucheniju novyh farmakologicheskih veshhestv. M.: Medicina, 2005. 832 s. Russian
16. Rebrova OYu. Statisticheskij analiz medicinskih dannyh. Primenenie paketa prikladnyh programm STATISTICA. M.: MediaSfera, 2003. 312 s. Russian
17. Teng H, Lin Q, Li K, Yuan B, Song H, Peng H, et al. Hepatoprotective effects of raspberry (Rubus coreanus Miq.) seed oil and its major constituents. Food Chem Toxicol. 2017; (110): 418–24.

Литература

1. Savarino V, Vigneri S, Celle G. The ^{13}C urea breath test in the diagnosis of Helicobacter pylori infection. Gut. 1999; 45 (suppl. 1): 18–23.
2. Balãn H, Gold CA, Dworkin HJ, McCormick VA, Freitas JE. Procedure Guideline for Carbon-14-Urea Breath Test. J Nucl Med. 2016; 39 (11): 2012–14.
3. Zhou Q, Li L, Ai Y, Pan Z, Guo M, Han J. Diagnostic accuracy of the ^{14}C-urea breath test in Helicobacter pylori infections: a meta-analysis. Wien Klin Wochenschr. 2017; 129 (1–2): 38–45.
4. Эльман А. Р., Рапопорт С. И. Стабильно-изотопная диагностика в России: итоги и перспективы. ^{13}C-препараты, приборы, методы. Клин. мед. 2014; 92 (7): 5–11.
5. Modak AS. Stable isotope breath tests in clinical medicine: A review. J Breath Res. 2007; 1 (1): R1–R13.
6. Musialik J, Jonderko K, Kasicka-Jonderko A, Buschhaus M. $^{13}CO_2$ breath tests in non-invasive hepatological diagnosis. Prz. Gastroenterol. 2015; 10 (1): 1–6.
7. Mizrahi M, Lalazar G, Adar T, Raz I, Ilan Y. Assessment of insulin resistance by a ^{13}C glucose breath test: A new tool for early diagnosis and follow-up of high-risk patients. Nutr J. 2010; (9): 25. DOI:10.1186/1475-2891-9-25.
8. Эльман А. Р., Корнеева Г. А., Носков Ю. Г., Хан В. Н., Шишкина Е. Ю., Негримовски В. М. и др. Синтез продуктов, меченных изотопом ^{13}C, для медицинской диагностики. Российский химический журнал. 2013; LVII (5-2): 3–24.
9. Giannini EG, Alberto F, Paolo B, Federica B, Federica M. ^{13}C-galactose breath test and ^{13}C-aminopyrine breath test for the study of liver function in chronic liver disease. Clin Gastroenterol Hepatol. 2005; 3 (3): 279–85.
10. Horowitz M, O'Donovan D, Jones KL, Feinle C, Rayner CK, Samsom M. Gastric emptying in diabetes: Clinical significance and treatment. Diabet Med. 2002; 19 (3): 177–94.
11. Титов В. Н. Клиническая биохимия жирных кислот, липидов и липопротеинов. Гиполипидемическая терапия и профилактика атеросклероза. Клинико-лабораторный консилиум. 2014; (1): 4–29.
12. Малышева А. О., Кодина Г. Е., Вороницкая Н. Н., Графскова Т. А., Семоненко Н. П. Определение качества радиофармацевтического препарата «Пирфотех, 99m Тс» в медицинских учреждениях. МОБИ-ХимФарма. 2017; с. 103. Доступно по ссылке: http://mobi-chem.org/arhiv.html.
13. Сазонова С. И., Ильюшенкова Ю. Н., Лишманов Ю. Б. Методика радионуклидного исследования воспалительных процессов в сердце. Сибирский медицинский журнал 2015; 30 (4): 32–5.
14. Поздеев В. В., Тыньо Я. Я., Морозова Г. В., Быченко А. Б., Бирюкова Ю. К., Шевелев А. Б., авторы; ООО "ГК"НАШ МИР"(RU), патентообладатель. Способ синтеза линолевой и линоленовой кислот, меченных изотопами углерода ^{13}C и ^{14}C. Патент РФ № 2630691. 12.09.2017.
15. Хабриев Р. У. Руководство по экспериментальному (доклиническому) изучению новых фармакологических веществ. М.: Медицина, 2005. 832 с.
16. Реброва О. Ю. Статистический анализ медицинских данных. Применение пакета прикладных программ STATISTICA. М.: МедиаСфера, 2003. 312 с.
17. Teng H, Lin Q, Li K, Yuan B, Song H, Peng H, et al. Hepatoprotective effects of raspberry (Rubus coreanus Miq.) seed oil and its major constituents. Food Chem Toxicol. 2017; (110): 418–24.

METHODS FOR DNA QUANTIFICATION YIELD SIMILAR RELATIVE BUT DIFFERENT ABSOLUTE VALUES

Balanovsky OP[1,2,3] ✉, Kagazezheva ZhA[1,2], Olkova MV[2]

[1] Vavilov Institute of General Genetics, Moscow, Russia

[2] Research Center for Medical Genetics, Moscow, Russia

[3] Biobank of North Eurasia, Moscow, Russia

DNA quantification is a routine yet important procedure that determines the efficacy of long-term sample storage and further manipulations with the sample. There are a few well-established methods for measuring DNA concentrations. However, it still not fully clear how concordant their results are. The aim of this work was to measure DNA concentrations in a set of samples using different quantification methods and to compare the obtained values. In 2 independent experiments, a total of 100 genomic DNA samples were analyzed using 3 different DNA quantification methods, including spectrophotometry (NanoDrop), fluorometry (Qubit) and real-time PCR (Quantifiler). The obtained relative concentrations demonstrated an excellent correlation (the correlation coefficients were as high as 0.98 to 0.99). However, the absolute concentrations showed a considerable variation and even a twofold difference. Spectrophotometry yielded the highest concentrations, whereas fluorometry yielded the lowest. The real-time PCR results were intermediate. The differences were more pronounced for the samples with low DNA concentrations. We recommend that such differences should be accounted for when estimating DNA concentrations using an arsenal of different quantification methods.

Keywords: DNA concentration, measurement method, real-time PCR, spectrophotometry, fluorometry

МЕТОДЫ ИЗМЕРЕНИЯ КОНЦЕНТРАЦИИ ДНК: СОВПАДЕНИЕ ОТНОСИТЕЛЬНЫХ ВЕЛИЧИН И РАЗЛИЧИЯ АБСОЛЮТНЫХ

О. П. Балановский[1,2,3] ✉, Ж. А. Кагазежева[1,2], М. В. Олькова[2]

[1] Институт общей генетики имени Н. И. Вавилова, Москва, Россия

[2] Медико-генетический научный центр, Москва, Россия

[3] Биобанк Северной Евразии, Москва, Россия

Измерение концентрации ДНК является базовым методом, от надежности которого зависит эффективность дальнейшего хранения и использования образцов. Существует несколько широко распространенных и хорошо зарекомендовавших себя способов измерения концентрации ДНК, однако степень их согласованности друг с другом изучена недостаточно. Целью работы было измерить концентрации одних и тех же образцов разными методами и провести сравнительный анализ полученных результатов. В двух независимых экспериментах, суммарно включивших 100 образцов геномной ДНК, сравнивали три метода определения концентрации ДНК: спектрофотометрический (Nanodrop), флуориметрический (Qubit) и ПЦР в реальном времени (Quantifiler). Выявлено, что значения концентрации ДНК, полученные разными методами, хорошо коррелируют друг с другом (коэффициенты корреляции составляют 0,98–0,99). Однако при такой отличной корреляции относительных величин концентрации абсолютные величины, полученные разными методами, варьируют значительно, вплоть до двукратных различий. Спектрофотометрический метод дает наиболее высокие концентрации, ПЦР в реальном времени — промежуточные, а флуориметрический — наиболее низкие. Различия в результатах более выражены для образцов с низкой концентрацией. Мы рекомендуем учитывать наличие этих систематических различий между результатами измерения концентрации ДНК, полученными разными методами.

Ключевые слова: концентрация ДНК, методы измерения, ПЦР в реальном времени, спектрофотометрический метод, флуориметрический метод

DNA quantification is a routine procedure performed by many laboratories. It is an important part of sample preparation for long-term storage, biobanking or NGS. There are a few well-established methods for measuring DNA concentrations that have been conveniently translated into commercially available reagent kits and instrumentation. Still, it is not uncommon that different methods yield different estimates. The available literature [1–6] warns against the limitations and specific characteristics of DNA quantification methods that the end user may not be fully aware of. Genomic DNA and DNA

library concentrations are measured prior to whole-genome sequencing, as part of a sample reception procedure or while monitoring the quality of stored DNA samples. In our lab, we work with extensive sample collections from the Biobank of North Eurasia [7], among other projects; therefore, it is critical for us to find an optimal method for DNA quantification, understand the nuances of its application and compare it to other existing measurement methods. It is highly likely that other laboratories may face a similar task. The aim of this work was to measure DNA concentrations in a series of samples using different quantification methods and compare the obtained values by assessing the repeatability of each method, determining the concordance of the results and identifying the trends of differences between the obtained values.

METHODS

In 2017–2018 we conducted a series of experiments in which we measured DNA concentrations in a set of samples using different quantification methods. The following DNA quantification methods were compared: a) NanoDrop spectrophotometry, which can determine both DNA concentration and DNA quality from the absorbance of a sample at a certain wavelength; b) fluorescence-based measurements using fluorescent dyes (Qubit); c) real-time PCR (Human DNA Quantifiler).

All the experiments gave the same picture, so in this article we will talk about the most elaborately planned experiments (1 and 2) in which the number of controlled variables was the highest. In both experiments, we used DNA samples from the Biobank of North Eurasia obtained through phenol-chloroform extraction.

In experiment #1, 49 DNA samples were analyzed. Prior to the experiment, DNA concentrations were estimated using a Qubit fluorometer and Qubit reagent kits. Highly concentrated samples were diluted down to < 50 ng/μl because the Human Quantifiler kit guarantees accurate measurements only at concentrations below 55 ng/μl, given that standard dilution series are prepared in strict accordance with the manufacturer's guidelines. In those 49 samples, DNA concentrations were measured in 3 ways: spectrophotometrically in 3 replicates per sample using a NanoDrop spectrophotometer; fluorescently in 3 replicates per sample using Qubit instrumentation and reagent kits; using real-time PCR and a Human DNA Quantifiler kit. Due to high costs of the reagents, real-time PCR was conducted in 2 replicates for half of the samples. Because the correlation between the replicates was 0.99, DNA concentrations in the rest of the samples were measured only once per sample.

For spectrophotometry, we used NanoDrop 2000 (Thermo Fisher Scientific; USA) in strict compliance with the manufacturer's protocol. DNA samples were aspirated into an automatic Research Plus pipette (Eppendorf; Germany) that allows adjusting the dispensed volume between 1 and 10 μl. DNA concentrations were measured in 2 μl samples at 20 °C.

Fluorescence measurements were done using a Qubit 4 fluorometer (Thermo Fisher Scientific; USA), compatible 0.5 ml thin-walled assay tubes by the same manufacturer and Qubit™ dsDNA BR Assay Kits (Thermo Fisher Scientific; USA) in strict accordance with the manufacturer's protocol [7]. Samples were aspirated into an 0.1–2.5 μl automatic Research Plus pipette (Eppendorf; Germany). DNA concentrations were measured in 2 μl samples at 20 °C.

Real-time PCR was performed using a 7500 Real-Time PCR System for Human Identification (Applied Biosystems; USA) and a Quantifiler™ Human DNA Quantification Kit (Thermo Fisher Scientific; USA) in strict compliance with the manufacturer's

protocol. Samples were aspirated into an automated 0.1–2.5 μl Research Plus pipette (Eppendorf; Germany). Two μl of each sample were amplified.

In experiment #2, 51 DNA samples were analyzed. Methods, reagent kits and instrumentation applied to measure DNA concentrations were the same as in experiment 1. Fluorescence measurements were done in 2 replicates. Other measurements were performed in one replicate per sample. Prior to the experiment, DNA concentrations were estimated using a Qubit fluorometer and Qubit reagent kits. The range of DNA concentrations measured in experiment 2 was shifted upward to 20–90 ng/μl.

Experiments 1 and 2 were conducted by different researchers at different time points. Initial data processing and graph construction were done in MS Excel; correlation coefficients were computed in *Statistica 7*.

RESULTS

Results of experiments 1 and 2 are shown in Tables 1 and 2, respectively. Because the experiments were of the same type, their results are presented together in the Figure and Tables 3 and 4. First, a more detailed experiment 1 is described and then its results are compared to the results of experiment 2.

We started analyzing the data collected in experiment 1 by calculating the repeatability of the results obtained with one and the same DNA quantification method in a few replicates per sample. The repeatability turned out to be extremely high: the correlation coefficient varied between 0.99 and 1.00, which at the very least suggests the absence of a pipetting error. Therefore, for each sample, mean concentrations of all replicates were used for further analysis.

Since real-time PCR-based DNA quantification (below referred to as Quantifiler) is considered to be the most accurate, we used it as a reference method. Values obtained with other methods were compared to those yielded by Quantifiler. We would like to emphasize that a different choice of a reference method would have led us to the same conclusions. In Figure 1A, DNA concentrations obtained with real-time PCR are plotted on the X-axis. DNA concentrations obtained using all three analyzed methods are plotted on the Y-axis. The Quantifiler curve can only take a form of a 45 degree line (the black line in the picture). It serves as a baseline. The 2 other curves look more interesting.

The NanoDrop curve (Fig. 1A; the orange one) was constructed from the values that on the whole were concordant with Quantifiler estimates. Still, they were a bit higher, with stochastic fluctuations ("beats"). The NanoDrop spectrophotometer returned higher DNA concentrations than the Quantifiler kit for the samples containing 20 ng/μl DNA. For lower DNA concentrations, both methods generated very similar results.

In the Figure, the orange NanoDrop curve lies above the black Quantifiler line, and the blue Qubit curve is below the latter. For all our samples, Qubit generated lower concentration values, as compared to Quantifiler. Unlike the NanoDrop curve, the Qubit curve looks smoother, suggesting better stability of measurements. The first impression of the Qubit curve is that the distance between its every point and every corresponding point of the Quantifiler line is fixed. However, the blue dotted trendline demonstrates that the Qubit curve is not only characterized by lower DNA concentrations but also has a different slope.

The next step was quantitative analysis. Table 3 (specifically, the values above the diagonal) shows correlations between the results obtained with 3 tested DNA quantification methods. The correlation coefficients were very high (at least 0.98),

Table 1. Results of DNA quantification in individual samples (Experiment 1)

SampleID	Quantifiler1	Quantifiler2	Qubit1	Qubit2	Qubit3	Nanodrop1	Nanodrop2	Nanodrop3
21	10.7	10.3	6.1	5.9	5.6	11.6	13.1	12.0
22	18.3	17.6	12.2	11.2	11.4	23.7	25.0	24.1
23	36.6	33.2	24.4	24.1	24.0	51.6	51.2	49.8
24	44.2	47.8	34.0	36.2	31.9	73.7	75.2	73.2
25	64.3	58.4	47.2	45.0	49.6	101.1	104.4	102.8
31	10.2	9.8	5.5	5.4	5.6	8.6	7.9	8.0
32	18.1	18.3	11.2	11.0	10.9	15.7	16.4	17.1
33	37.0	35.7	23.6	24.5	23.4	38.6	37.6	39.5
34	44.7	47.4	32.9	30.1	31.4	51.5	54.4	51.7
35	59.2	54.4	42.1	43.3	42.6	67.8	70.7	69.4
41	10.3	9.7	5.6	6.1	5.2	8.2	7.7	7.5
42	14.8	15.5	11.6	11.0	10.9	16.3	16.9	16.2
43	28.7	27.3	22.3	23.0	22.7	35.8	35.8	36.8
44	40.1	39.8	32.8	32.3	33.5	53.2	51.5	53.4
45	59.0	55.3	45.3	45.7	46.0	70.7	71.9	71.7
51	10.1	10.5	5.9	5.7	5.5	10.0	9.3	9.3
52	20.1	20.2	11.8	11.6	11.5	19.9	19.2	19.5
53	34.2	35.8	23.2	22.0	23.4	38.4	39.4	36.3
54	47.7	44.6	31.9	33.7	34.0	59.5	57.8	58.1
71	9.0	8.8	5.3	5.4	5.1	8.1	8.1	8.4
72	15.5	15.4	9.7	10.3	10.3	17.2	17.5	17.7
73	28.2	30.6	18.5	19.5	19.1	36.3	36.1	36.3
74	42.3	44.6	34.2	27.7	30.3	54.3	52.7	54.1
75	53.0	58.1	40.6	46.3	41.9	75.2	72.1	72.6
81	10.8		5.8	5.7	5.8	9.1	9.0	9.0
82	23.1		11.8	11.6	11.8	20.4	19.3	19.5
83	32.7	32.4	21.9	21.7	21.2	36.5	37.5	36.8
84	48.3		32.0	33.6	33.9	59.7	58.0	58.3
85	63.6		45.6	46.9	47.0	77.1	80.5	80.5
91	10.9		5.7	5.8	5.8	10.2	9.8	9.8
92	19.4		11.7	11.9	10.9	22.4	23.3	23.5
93	33.9		22.2	22.9	23.0	46.2	47.0	46.0
94	51.5		36.0	35.5	36.0	70.3	70.9	69.6
95	62.2		40.3	45.3	46.6	92.3	90.2	91.5
101	10.1		5.6	5.9	5.7	10.7	10.5	11.6
102	22.4		12.5	12.3	12.2	23.8	24.6	21.9
103	39.0		22.0	23.3	22.8	50.3	50.7	50.0
104	51.9		32.2	34.0	34.1	70.4	70.6	68.0
105	63.0		44.7	46.4	46.4	95.0	92.0	95.5
111	8.3		4.5	4.7	4.7	7.0	7.5	7.7
112	17.4		10.1	10.3	10.0	14.9	14.9	16.3
113	30.2		18.0	19.6	20.2	31.5	33.0	29.8
114	43.6		28.8	28.3	30.0	45.6	44.6	46.2
115	56.9		39.3	41.8	40.5	62.8	63.3	61.4
121	9.8		5.3	5.1	4.8	10.3	9.9	10.4
122	20.5		10.4	10.9	11.2	21.0	21.8	21.9
123	36.2		22.3	22.6	23.5	43.9	43.7	42.4
124	49.4		32.6	32.3	32.0	63.0	64.2	63.9
125	56.4		41.9	41.5	42.8	84.0	82.8	81.9

Table 2. Results of DNA quantification in individual samples (Experiment 2)

| SampleID	Nanodrop	Qubit1	Qubit2	Quantifiler
1	67.5	45.4	50.2	56.0
2	71.9	51.2	52	56.2
3	99.1	78	65.1	78.5
4	59.2	47.5	49	48.4
8	97.1	69.7	76.2	83.7
10	76.4	67.2	65.9	68.1
11	58	46.7	43.3	46.6
12	88.7	66.8	63.7	73.1
13	59.8	42.2	40.8	48.9
14	92.4	62.1	66.1	79.8
15	78.6	50.4	51.8	62.7
16	74.3	50.7	51.4	60.5
17	72.5	29.6	48.4	43.6
18	47.5	34.6	35.5	39.0
19	84.5	59.1	59.8	63.7
20	98.5	71.2	77	83.5
21	69.9	56.4	61.3	68.5
26	66.2	45.2	33.8	62.3
27	100.1	54.9	77.9	81.3
28	97	74.1	75	79.5
29	95.6	62.8	68.1	72.4
32	58.5	39.2	40.6	41.5
33	71.3	47.4	44.3	61.1
34	82.6	43	64.1	75.3
35	101.7	69.2	74.1	86.5
37	101.6	73.3	74	84.5
44	101.7	49.8	48.3	70.2
46	99.2	86	63.6	93.9
48	101.7	70.7	78.5	80.1
49	50.9	36.5	37.5	41.2
51	50.8	27.4	29.8	34.8
52	48.1	38.7	42.2	50.3
53	52.6	31.9	46.1	54.4
54	27.2	18.3	15.9	23.1
55	52.5	34.6	36.8	36.7
56	55.8	32.7	34.7	72.3
57	50.2	31.2	35.8	50.1
58	62.7	58.2	50.9	28.5
59	36.3	23.2	26.7	25.7
60	18.5	11.4	11.9	31.9
61	34.8	22.2	25.9	27.1
62	73.3	28.2	55.9	66.6
63	112.5	50	90.2	92.2
65	54.1	21.7	36	42.3
72	63.3	42.9	50.6	53.4
73	66.9	40.1	36.5	50.0
74	68.9	40.2	47.4	50.4
75	41.1	25.4	24.7	29.1
76	75	43.3	51.4	63.8
77	71.7	51.1	50.4	61.2
79	99.7	64.8	64.9	74.9
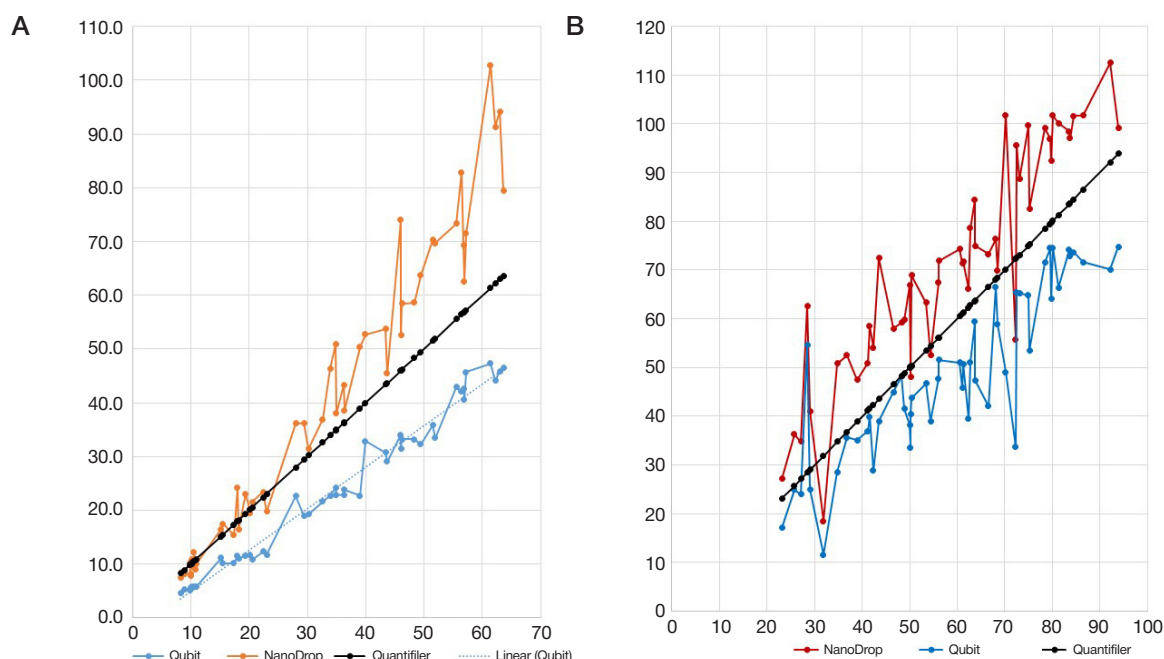
Fig. 1. DNA concentrations in individual samples measured using different methods. **A**: Experiment 1. **B** Experiment 2. The X-axis: concentrations yielded by Quantifiler. The Y-axis: concentrations yielded by Quantifiler (*the black line*), Qubit (the blue line) and NanoDrop (*the red line*).

demonstrating excellent correlation between the values produced by different measurement methods. However, this was not the case with the mean values (Table 4). Most importantly, mean Qubit values were significantly (1.5 times) lower than mean Quantifiler values, whereas mean DNA concentrations measured with NanoDrop were by 25% higher than those measured with Quantifiler. Moreover, the variability of the obtained values depended on a DNA concentration in the studied sample. When the total sample was split into two subsets of equal sample size and different concentrations, the ratio of mean Qubit/Quantifiler values reached 61% for the samples with lower DNA concentrations and 71% for the samples with higher concentrations (Table 4; differences were considered significant at $p = 0.01$; the Mann–Whitney U test was applied). So, in order to study the relationship between DNA concentrations and differences in the values obtained using different quantification methods, we arranged the total sample into 5 subsets in the ascending order of concentrations and

calculated the ratio of Qubit to Quantifiler concentrations (Table 4). Although the size of the subgroups was small (10 samples per subset), we managed to identify a distinct trend: the ratio of Qubit to Quantifiler concentrations increased monotonously from 55% (twofold differences at low concentrations) to 75% (a 25% difference at high concentrations).

The results described above pertain to experiment 1. In experiment 2, the graph (Fig. 1B) demonstrates the same trend for individual samples: in comparison with real-time PCR-derived concentrations (Quantifiler), NanoDrop values (the red curve) are higher and Qubit values (the blue curve) are lower. Statistical noise (the chaotic character of the curves) was more pronounced in experiment 2, which we attributed to the operator effect. Similar to experiment 1, the results yielded by the studied DNA quantification methods were well-correlated. However, they were affected by the operator effect: although the correlation coefficients were high (0.88–0.93) in experiment 2 (Table 3; the values under the diagonal), they

Table 3. Correlation coefficients for DNA concentrations yielded by different quantification methods. Above diagonal: experiment 1. Below diagonal: experiment 2

	Quantifiler	Qubit	Nanodrop
Quantifiler	1	0.99	0.98
Qubit	0.93	1	0.98
Nanodrop	0.91	0.88	1

Table 4. Mean DNA concentrations yielded by different quantification methods

		Quantifiler	Qubit	Nanodrop	Qubit/Quantifiler	Nanodrop/Quantifiler
Experiment 1	All samples	33.1	22.7	41.3	0.68	1.25
	lower conc (*n* = 24)	17.0	10.4	18.0	0.61	1.05
	higher conc (*n* = 25)	48.6	34.5	63.8	0.71	1.31
	conc_range1 (*n* = 10)	9.9	5.5	9.3	0.55	0.94
	conc_range2 (*n* = 10)	19.0	11.2	19.7	0.59	1.04
	conc_range3 (*n* = 10)	33.6	22.2	40.8	0.66	1.22
	conc_range4 (*n* = 10)	46.6	32.6	59.9	0.70	1.29
	conc_range5 (*n* = 10)	59.2	44.2	80.8	0.75	1.36
Experiment 2	All samples	59.0	49.2	71.4	0.83	1.21

were still lower than in experiment 1. Just like in experiment 1, the analysis of mean values revealed that Qubit estimates were by 20% lower than those measured with Quantifiler, whereas NanoDrop estimates were by 20% higher than those generated by Quantifiler. In experiment 2, we could not identify the relationship between the ratio of DNA concentrations measured with different quantification methods and the DNA concentration in the studied sample. We attributed this to a higher rate of experimental error in experiment 2: due to the operator effect, this relationship could not be observed in a studied sample size.

DISCUSSION

The sets of samples analyzed in our experiments were different. The experiments were conducted at different time points by differently experienced researchers. But the observed trends were similar: relative concentration values yielded by different quantification methods were well-correlated whereas absolute DNA concentrations differed significantly. Besides, the lower was the concentration, the more pronounced was the difference. This means that each of the tested quantification methods reliably measures relative concentrations, which can be further used as a reference for other samples measured using the same method. However, a problem arises when we measure DNA concentrations with different quantification methods within one study. Conversion would be a solution here (figures from two rightmost columns in Table 4 could be used as conversion coefficients), but such calculations are complicated because the conversion coefficient depends on concentrations.

Research works cited above report that different DNA quantification methods can produce concordant [1] or different [3, 4] results. We used a large sample set (a total of 100 samples in both experiments), whereas the majority of similar studies are carried out using only 3 to 6 samples. This allowed us to run a statistical analysis on the obtained concentration values and identify the relationship between the measured concentration and the variability of the results depending on the method applied.

Given that each of the tested methods has its own nuances, it was hard to predict the results of the experiments. On the one hand, estimates based on real-time PCR (Quantifiler) can be lower than those yielded by the Qubit fluorometer because real-time PCR measures the effective DNA concentration (i.e., long intact DNA fragments that can be amplified), whereas Qubit analyzes all the fragments. On the other hand, PCR-derived values can be higher than those measured with Qubit instrumentation and dyes because real-time PCR amplifies both double- and single-stranded DNA from each analyzed sample, whereas Qubit assays are selective for double-stranded DNA only. Concentrations returned by the spectrophotometer were higher than those calculated from real-time PCR. This can be explained by the presence of phenol or protein admixtures in the sample. Phenol makes a more significant contribution because its absorbance peak occurs at 270 nm and overlaps with the absorbance peak of DNA at 260 nm wavelength.

Reference standards used (known DNA concentrations included in the reagent kit) may have contributed to the differences in the resulting concentration values. According to the information provided by the manufacturer of the Quantifiler kit, the concentration of the reference standard should be 200 ng/μl. However, when measured with Qubit kits and equipment, this concentration turned out to be by 5–10% lower. Of note, both Qubit and Quantifiler kits are produced by Thermo Fisher Scientific [8]. A similar problem with Quantifiler reference standards was reported in one of early works. But even if a different standard had been used, it would not have solved the problem, because the variability of the results between the methods is unstable and depends on the concentration of DNA in the sample.

Measurement discrepancies between the tested quantification methods might be to some extent determined by a few other factors pertaining to the conditions of the experiment. We worked with low-fragmented DNA obtained through phenol-chloroform extraction that was taken in a range of concentrations between 5 and 100 ng/μl. We think that the trends we discovered will be observed for other DNA samples with a different shelf-life and different extraction methods. However, in this case DNA quantification may be affected by other factors that were not present in our experiment.

Surprisingly, NanoDrop spectrophotometry, which does not have a reputation of a reliable DNA quantification method, performed well in our experiment. Although the rate of error was a bit higher than that of Qubit (see the Figure), correlation coefficients for NanoDrop and Qubit, as well as for NanoDrop and Quantfiler, were quite high (Table 3).

We also noted the so-called operator effect: one and the same method demonstrates different repeatability when applied by different members of staff who use the same equipment and follow the same protocols. This fact is consistent with our previous observations [6].

Although no systemic errors were observed in the work of the researchers who conducted the experiments and the latter were elaborately planned, the error of measurement was different depending on who performed the procedure. We assume that the difference in measurement accuracy will be even more pronounced for routine laboratory tasks

CONCLUSIONS

We found that DNA concentrations measured in a large sample set using different quantification methods were well-correlated but the obtained values differed between the methods applied: NanoDrop spectrophotometry yielded higher concentrations, real-time PCR (Quantifiler), intermediate values, and fluorometry (Qubit), lower values. The differences were more pronounced for the samples with low DNA concentrations. We recommend that such regular differences should be accounted for when estimating DNA concentrations using an arsenal of different quantification methods. It would also be wise to explicitly specify what method and what reagent kit are used to measure DNA concentrations in your experiment even if this method is well-established and reliable.

References

1. Bhat S, Curach N, Mostyn T, Bains GS, Griffiths KR, et al. Comparison of methods for accurate quantification of DNA mass concentration with traceability to the international system of units. Anal Chem. 2010 Sep 1; 82 (17): 7185–92. DOI: 10.1021/ac100845m.
2. Li X, Wu Y, Zhang L, Cao Y, Li Y, Li J, et al. Comparison of

three common DNA concentration measurement methods. Anal Biochem. 2014 Apr 15; (451): 18–24. DOI: 10.1016/j.ab.2014.01.016.

3. Nielsen K, Mogensen HS, Hedman J, Niederstätter H, Parson W, Morling N. Comparison of five DNA quantification methods. Forensic Science International: Genetics. 2008; 2 (3): 226–30.

4. He HJ, Stein EV, DeRose P, Cole KD. Limitations of methods for measuring the concentration of human genomic DNA and oligonucleotide samples. Biotechniques. 2018 Feb 1; 64 (2): 59–68. DOI: 10.2144/btn-2017-0102.

5. Nakayama Y, Yamaguchi H, Einaga N, Esumi M. Pitfalls of DNA Quantification Using DNA Binding Fluorescent Dyes and Suggested Solutions. PLoS ONE. 2016; 11 (3): e0150528. DOI 10.1371/journal.pone.0150528.

6. Belenikin MS, Galahova AA, Balanovskaya EV, Balanovsky OP. Ocenka vosproizvodimosti fluometricheskogo izmereniya koncentracii DNK. Genetika. 2018; (54): 113–6. DOI: 10.1134/S0016675818130040. Russian.

7. Balanovskaya EV, Zhabagin MK, Agdzhoyan AT, Chukhryaeva MI, Markina NV, Balaganskaya OA, et al. Population biobanks: Organizational models and prospects of application in gene geography and personalized medicine. Russian Journal of Genetics. 2016; 52 (12): 1227–43.

8. Qubit dsDNA BR Assay Kits Manual (MAN0002325, Revision: A.0). Available from: https://tools.thermofisher.com/content/sfs/manuals/Qubit_dsDNA_BR_Assay_UG.pdf.

Литература

1. Bhat S, Curach N, Mostyn T, Bains GS, Griffiths KR, et al. Comparison of methods for accurate quantification of DNA mass concentration with traceability to the international system of units. Anal Chem. 2010 Sep 1; 82 (17): 7185–92. DOI: 10.1021/ac100845m.

2. Li X, Wu Y, Zhang L, Cao Y, Li Y, Li J, et al. Comparison of three common DNA concentration measurement methods. Anal Biochem. 2014 Apr 15; (451): 18–24. DOI: 10.1016/j.ab.2014.01.016.

3. Nielsen K, Mogensen HS, Hedman J, Niederstätter H, Parson W, Morling N. Comparison of five DNA quantification methods. Forensic Science International: Genetics. 2008; 2 (3): 226–30.

4. He HJ, Stein EV, DeRose P, Cole KD. Limitations of methods for measuring the concentration of human genomic DNA and oligonucleotide samples. Biotechniques. 2018 Feb 1; 64 (2): 59–68. DOI: 10.2144/btn-2017-0102.

5. Nakayama Y, Yamaguchi H, Einaga N, Esumi M. Pitfalls of DNA Quantification Using DNA Binding Fluorescent Dyes and Suggested Solutions. PLoS ONE. 2016; 11 (3): e0150528. DOI 10.1371/journal.pone.0150528.

6. Беленикин М. С., Галахова А. А., Балановская Е. В., Балановский О. П. Оценка воспроизводимости флуометрического измерения концентрации ДНК. Генетика. 2018; (54): 113–6. DOI: 10.1134/S0016675818130040.

7. Балановская Е. В., Жабагин М. К., Агджоян А. Т., Чухряева М. И., Маркина Н. В., Балаганская О. А. и др. Популяционные биобанки: принципы организации и перспективы применения в геногеографии и персонализированной медицине. Генетика. 2016; (12): 1371–87.

8. Qubit dsDNA BR Assay Kits Manual (MAN0002325, Revision: A.0). Available from: https://tools.thermofisher.com/content/sfs/manuals/Qubit_dsDNA_BR_Assay_UG.pdf.

ELECTROENCEPHALOGRAM-BASED EMOTION RECOGNITION USING A CONVOLUTIONAL NEURAL NETWORK

Savinov VB, Botman SA, Sapunov VV, Petrov VA, Samusev IG, Shusharina NN ✉

Immanuel Kant Baltic Federal University, Kaliningrad, Russia

The existing emotion recognition techniques based on the analysis of the tone of voice or facial expressions do not possess sufficient specificity and accuracy. These parameters can be significantly improved by employing physiological signals that escape the filters of human consciousness. The aim of this work was to carry out an EEG-based binary classification of emotional valence using a convolutional neural network and to compare its performance to that of a random forest algorithm. A healthy 30-year old male was recruited for the experiment. The experiment included 10 two-hour-long sessions of watching videos that the participant had selected according to his personal preferences. During the sessions, an electroencephalogram was recorded. Then, the signal was cleared of artifacts, segmented and fed to the model. Using a neural network, we were able to achieve a F1 score of 87%, which is significantly higher than the F1 score for a random forest model (67%). The results of our experiment suggest that convolutional neural networks in general and the proposed architecture in particular hold great promise for emotion recognition based on electrophysiological signals. Further refinement of the proposed approach may involve optimization of the network architecture to include more classes of emotions and improvement of the network's generalization capacity when working with a large number of participants.

Keywords: machine learning, artificial neural network, electroencephalogram, emotional state, valence, deep learning, convolutional networks

ОПРЕДЕЛЕНИЕ ЭМОЦИОНАЛЬНОГО СОСТОЯНИЯ СВЕРТОЧНОЙ НЕЙРОННОЙ СЕТЬЮ ПО ДАННЫМ ЭЛЕКТРОЭНЦЕФАЛОГРАФИИ

В. Б. Савинов, С. А. Ботман, В. В. Сапунов, В. А. Петров, И. Г. Самусев, Н. Н. Шушарина ✉

Балтийский федеральный университет имени Иммануила Канта, Калининград, Россия

Существующие методы определения эмоционального состояния, основанные на регистрации тональности голоса и мимики, не обладают достаточной точностью и специфичностью. Эти показатели можно повысить с помощью анализа биосигналов, которые не проходят через сознательные фильтры, для чего необходимо создание эффективного алгоритма определения эмоционального состояния на основании анализа электрофизиологических сигналов. Целью работы было провести бинарную классификацию валентности эмоционального состояния по данным электроэнцефалографии с использованием сверточной нейронной сети и сравнить эффективность ее работы с эффективностью метода случайного леса. В качестве подопытного был выбран здоровый 30-летний мужчина. В течение 10 сессий по 2 ч каждая с подопытного производили запись электроэнцефалограммы во время просмотра им специально сформированного набора видеофильмов. Полученный сигнал фильтровали, сегментировали и использовали для обучения классификаторов. При использовании сети удалось достичь значения F1-меры, равного 87%, что превышает показатель, полученный при использовании метода случайного леса с входными данными в виде вектора признаков (67%). Достигнутые результаты свидетельствуют о высокой перспективности применения нейронных сетей сверточного типа в общем, и предложенной архитектуры, в частности, для решения задач по распознаванию эмоционального состояния по данным электрофизиологических сигналов. Дальнейшие работы по развитию подхода могут быть направлены на оптимизацию архитектуры сети для расширения числа идентифицируемых классов, а также повышения обобщающей способности сети при работе с большим количеством испытуемых.

Ключевые слова: машинное обучение, искусственные нейронные сети, электроэнцефалограмма, эмоциональное состояние, валентность, глубокое обучение, сверточные сети

Emotions play a crucial role in our daily lives, affecting our perception, decision-making and social interactions. Emotions can have an outward manifestation, showing in the tone of voice or a facial expression, as well as evoke physiological changes invisible to the naked eye. Although self-assessment studies do yield useful information, there are certain issues with the reliability and validity of the obtained data [1]. Because both voice and facial expression can be mimicked, they can hardly serve as reliable indicators of a person's emotional state [2]. In contrast, the analysis of physiological signals fosters our understanding of basic emotional responses and the underlying biological mechanisms [3].

The following biosignals are commonly used to analyze a person's emotional state: galvanic skin response (GSR), electromyogram (EMG), heart rate (HR), respiratory rate (RR), and electroencephalogram (EEG). Of them, EEG is the most interesting; it reflects the activity of the cerebral cortex that shapes a number of emotional responses. Although EEG has low spatial resolution, its temporal resolution is quite high, meaning that changes to the phase and frequency of the signal can be conveniently measured following exposure to an external emotional stimulus. Besides, electoencephalography is advantageously noninvasive, fast and inexpensive, in comparison with other techniques for the acquisition of biological data.

As a rule, the EEG-based research into emotion recognition involves classification of a relatively small number of discrete states evoked by a specific stimulus. Usually, a raw EEG signal is passed through a filter first, and then features are extracted from it; classification is performed using a machine learning algorithm. The efficacy of this approach is largely determined by how features, which are the mathematically calculated signal attributes, are constructed and selected. Normally, feature construction accounts for the experimental and theoretical data on brain biology and the processes that an emotional stimulus induces in the brain.

The selected features are used to form feature vectors for machine learning models, such as random forests, multilayer perceptrons, support vector machines, *k*-nearest neighbors, etc. [4–6]. Classification accuracy of the listed models varies depending on the quality of input data, task criteria and the choice of a learning algorithm. In the case of an EEG signal, classification accuracy can be as high as 77% [7], whereas for multimodal signals it increases up to 83% [8]. The outcome is largely determined by the choice of a model and its parameters, signal features, and the techniques used to reduce data dimensionality.

Convolutional neural networks and deep learning are an alternative to the aforementioned algorithms for EEG-based emotion recognition. Neural networks are successfully used to process electrophysiological signals [9]. At present, the analysis of EEG signals by convolutional networks is employed to solve a variety of medical tasks and aid brain-computer interactions, including seizure prediction [10], detection of P300 waves [11], and recognition of emotions [12, 13] using DEAP datasets [14]. Such wide range of tasks proves that convolutional neural networks are a versatile and robust tool. Deep learning allows the optimal features to be automatically generated during the training process and, therefore, cancels the need for manual feature selection. Still, some authors use externally computed features [15] and Fourier and wavelet transforms [16, 17] as input data for a neural network.

The aim of this work was to carry out an EEG-based binary classification of emotional valence by creating and training a convolutional neural network and to compare its performance to that of a random forest algorithm with explicitly formed feature vectors.

METHODS

One of the authors of this work, a healthy male aged 30 years without a history of psychiatric disorders, volunteered to be an experimental subject. He underwent multiple sessions that involved exposure to different stimuli and lasted a few weeks. The design of our experiment was an adaptation of a well-known method [18]. It is common to recruit more than one participant and conduct a single session with each of the subjects. In our case, although the data were collected from one subject, the total data amount was quite substantial because the sessions were repeated multiple times. People differ in their emotional response to the same stimulus, and this diversity complicates the identification of physiological patterns that correspond to certain emotional states. When only one participant is engaged in a series of experiments, the interpretability of data improves significantly because the perception style remains unchanged.

The initial set of videos used to elicit a positive or negative emotional state was compiled based on the personal preferences of the study participant. The participant was familiar with the selected videos, therefore his emotional state during the sessions was largely determined by his inner psychic life, memories, etc. and not by the external stimulus as such. Later, the set was expanded to include additional videos that were categorized as emotionally positive or negative based on their resemblance to the original films. Data acquisition took 2 weeks. Ten two-hour long sessions were conducted. During a session that also included breaks, the participant watched six 15-min long videos (two from each category). Each video was played only once. A positive video was always followed by a negative.

EEG signals were recorded using a previously developed neurodevice [19]. Ag/AgCl electrodes with a conductive gel were attached to a special cap for EEG at positions F3, F4, C3, C4, P3, P4, O1, O2 (the 10–20 system), as required by the monopolar recording technique. The electrode at position Fpz was used as a ground and reference. The sampling rate was 250 Hz. Second-order Butterworth filters were applied to cut off 1 and 50 Hz frequencies; additionally, a notch filter was used to remove a 50 Hz noise.

Once filtered, the data were standardized per channel and segmented into the sliding windows of 2 s with a 0.2 s overlap. Then, the resulting dataset was fed to the neural network. A filtered nonstandardized segmented signal was used to calculate features. The selected features included those recommended in the literature [20]: high-order crossings up to the 6-th order, band power for delta, theta, alpha, beta and gamma frequency ranges and power asymmetry ratio.

All models were trained as follows: the EEG data obtained during each of the sessions were assigned to one of the two classes depending on what type of stimulus was used to evoke the signal. The assignment was binary: positive stimuli were assigned to class 1, whereas negative, to class 2. The network was trained using a minibatch stochastic gradient descent method (the learning rate optimization algorithm Adam [21], the minibatch size of 64, the learning rate of 0.001, 30 epochs) and categorical cross-entropy as a loss function. Thus, the input tensor had 3 dimensions [64, 8, 500], where 64 was the minibatch size, 8 was the number of EEG channels, 500 was the length of an EEG segment with an overlap of 50 time points.

All stages of the experiment, including signal recording and processing, as well as model training, involved the use of *Python* and *scikit-learn* and *Keras* libraries.

RESULTS

We have created a neural network with the following architecture: 2 convolutional layers of 64 kernels each, a batch normalization layer, an ELU (exponential linear unit) layer, an average pooling layer (window size 4, stride 1), 2 convolutional layers of 64 kernels each, a batch normalization layer, a ReLU (rectifier linear unit) layer, a max-pooling layer (window size 2, stride 1), 2 convolutional layers of 128 kernels each, a batch normalization layer, a ReLU layer, a max-pooling layer (window size 2, stride 1),
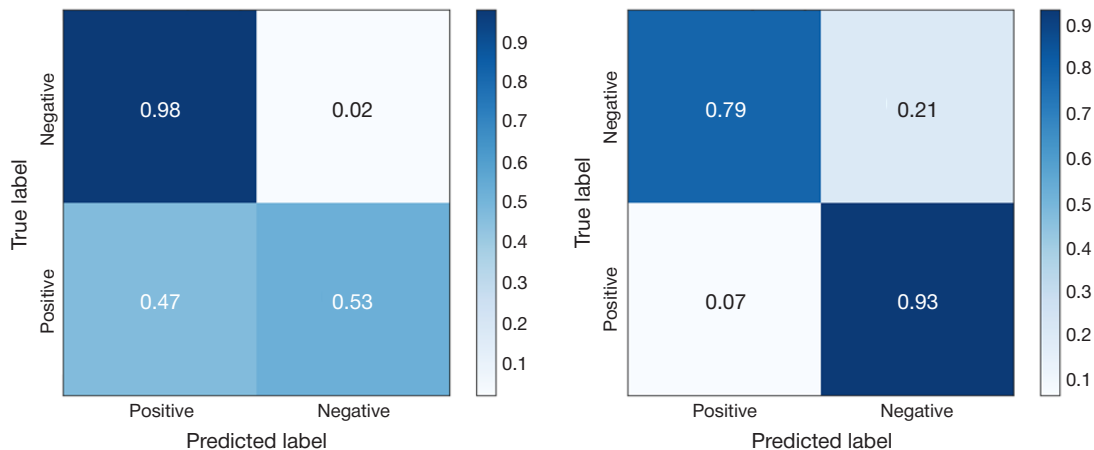
Fig. Confusion matrices for the random forest algorithm (*left panel*) and the convolutional neural network (*right panel*)

a fully connected layer consisting of 256 neurons with a ReLU activation function. The following parameters were used in all convolutional layers: size 3, stride 1, padding 0. *Softmax* (normalized exponential function) was used as an activation function for the output layer.

The use of a neural network allowed us to achieve a F1 score of 87% on a validation sample, which is significantly higher than an F1 score for a random forest model (67%). Confusion matrices (see the Figure) demonstrate that the random forest model successfully identifies positive states, outperforming the neural network slightly, but has low specificity to negative states. By contrast, the performance of the deep learning model in identifying and differentiating between the two studied states is equally accurate.

When testing the performance of our convolutional neural network using a dataset cleared of noise (electrooculography, EOG), we did not observe any significant changes to classification accuracy. The analysis of neural network activations demonstrated that EOG artifacts did not significantly skew classification results.

DISCUSSION

Today, neural networks are gradually replacing the well-established approaches to the analysis of electrophysiological signals involving manual selection of features and classical models of machine learning. Unsurprisingly, this trend is observed in the field of emotion recognition. One of the major differences between the approach proposed in this paper and its counterparts that also exploit convolutional networks is the use of an input signal without converting it into frequency domain representation (Fourier or wavelet transform).

Given that our model was trained and tested using the data obtained in the course of this particular experiment, we cannot compare its performance to that of its counterparts. However, it definitely outperforms classical models. The use of a neural network cancels the need for manual optimization of feature selection.

CONCLUSIONS

The proposed approach to emotion recognition is based on the use of a convolutional neural network and does not require signal conversion into frequency domain representation. Our model has demonstrated higher accuracy in comparison with a random forest algorithm. Further refinement of the approach will aim to improve its generalization capacity and include more classes of emotions into the algorithm. Effective techniques for emotion recognition could be potentially used for solving practical tasks in the field of psychology and marketing.

References

1. Calvo RA, D'Mello S. Affect detection: An interdisciplinary review of models, methods, and their applications. IEEE Transactions on affective computing. 2010; 1 (1): 18–37.
2. Jerritta S, Murugappan M, Nagarajan R, Wan K. Physiological signals based human emotion recognition: a review. Signal Processing and its Applications (CSPA), 2011 IEEE 7th International Colloquium on. IEEE. 2011; p. 410–5.
3. Li Q, Yang Z, Liu S, Dai Z, Liu Y. The study of emotion recognition from physiological signals. Advanced Computational Intelligence (ICACI). 2015 Seventh International Conference on. IEEE. 2015; p. 378–82.
4. Soroush MZ, Maghooli K, Setarehdan SK, Nasrabadi AM. Emotion classification through nonlinear EEG analysis using machine learning methods. International Clinical Neuroscience Journal. 2018; 5 (4): 135–49.
5. Liu J, Meng H, Nandi A, Li M. Emotion detection from EEG recordings. The 2016 12th International Conference on Natural Computation, Fuzzy Systems and Knowledge Discovery (ICNC–FSKD). IEEE. 2016; p. 1722–7.
6. Ackermann P, Kohlschein C, Bitsch JA, Wehrle K, Jeschke S. EEG-based automatic emotion recognition: Feature extraction, selection and classification methods. 2016 IEEE 18th international conference on e-health networking, applications and services (Healthcom). IEEE. 2016; p. 1–6.
7. Mehmood RM, Du R, Lee HJ. Optimal feature selection and deep learning ensembles method for emotion recognition from human brain EEG sensors. IEEE Access. 2017; (5): 14797–806.
8. Yin Z, Zhao M, Wang Y, Yang J, Zhang J. Recognition of emotions using multimodal physiological signals and an ensemble deep learning model. Computer methods and programs in biomedicine. 2017; (140): 93–110.
9. Min S, Lee B, Yoon S. Deep learning in bioinformatics. Briefings in bioinformatics. 2017; 18 (5): 851–69.
10. Page A, Shea C, Mohsenin T. Wearable seizure detection using convolutional neural networks with transfer learning. 2016 IEEE International Symposium on Circuits and Systems (ISCAS). IEEE. 2016; p. 1086–9.
11. Cecotti H, Graser A. Convolutional neural networks for P300

detection with application to brain-computer interfaces. IEEE transactions on pattern analysis and machine intelligence. 2011; 33 (3): 433–45.

12. Gao Y, Lee HJ, Mehmood RM. Deep learninig of EEG signals for emotion recognition. 2015 IEEE International Conference on Multimedia & Expo Workshops (ICMEW). IEEE. 2015; p. 1–5.

13. Tripathi S, Acharya S, Sharma RD, Mittal S, Bhattacharya S. Using Deep and Convolutional Neural Networks for Accurate Emotion Classification on DEAP Dataset. Twenty-Ninth IAAI Conference. 2017.

14. Koelstra S, Muhl C, Soleymani M, Lee JS, Yazdani A, Ebrahimi T et al. Deap: A database for emotion analysis; using physiological signals. IEEE transactions on affective computing. 2012; 3 (1): 18–31.

15. Li J, Zhang Z, He H. Hierarchical convolutional neural networks for EEG-based emotion recognition. Cognitive Computation. 2018; 10 (2): 368–80.

16. Kwon YH, Shin SB, Kim SD. Electroencephalography based fusion two-dimensional (2D)-convolution neural networks (CNN) model for emotion recognition system. Sensors. 2018; 18 (5): 1383.

17. Yuan L, Cao J. Patients' eeg data analysis via spectrogram image with a convolution neural network. International Conference on Intelligent Decision Technologies. Cham: Springer, 2017; p. 13–21.

18. Picard RW, Vyzas E, Healey J. Toward machine emotional intelligence: Analysis of affective physiological state. IEEE transactions on pattern analysis and machine intelligence. 2001; 23 (10): 1175–91.

19. Shusharina NN, Borchevkin DA, Sapunov VV, Petrov VA, Patrushev MV. A Wireless Portable Platform for Physiological Potentials Registration and Processing: A Unified Approach. Journal of Pharmaceutical Sciences and Research. 2017; 9 (7): 1178.

20. Jenke R, Peer A, Buss M. Feature extraction and selection for emotion recognition from EEG. IEEE Transactions on Affective Computing. 2014; 5 (3): 327–39.

21. Kingma DP, Ba J. Adam: A method for stochastic optimization. arXiv:1412.6980. [Preprint]. 2014 [cited 2014 Dec 22]. Available from: https://arxiv.org/abs/1412.6980.

Литература

1. Calvo RA, D'Mello S. Affect detection: An interdisciplinary review of models, methods, and their applications. IEEE Transactions on affective computing. 2010; 1 (1): 18–37.

2. Jerritta S, Murugappan M, Nagarajan R, Wan K. Physiological signals based human emotion recognition: a review. Signal Processing and its Applications (CSPA), 2011 IEEE 7th International Colloquium on. IEEE. 2011; p. 410–5.

3. Li Q, Yang Z, Liu S, Dai Z, Liu Y. The study of emotion recognition from physiological signals. Advanced Computational Intelligence (ICACI). 2015 Seventh International Conference on. IEEE. 2015; p. 378–82.

4. Soroush MZ, Maghooli K, Setarehdan SK, Nasrabadi AM. Emotion classification through nonlinear EEG analysis using machine learning methods. International Clinical Neuroscience Journal. 2018; 5 (4): 135–49.

5. Liu J, Meng H, Nandi A, Li M. Emotion detection from EEG recordings. The 2016 12th International Conference on Natural Computation, Fuzzy Systems and Knowledge Discovery (ICNC–FSKD). IEEE. 2016; p. 1722–7.

6. Ackermann P, Kohlschein C, Bitsch JA, Wehrle K, Jeschke S. EEG-based automatic emotion recognition: Feature extraction, selection and classification methods. 2016 IEEE 18th international conference on e-health networking, applications and services (Healthcom). IEEE. 2016; p. 1–6.

7. Mehmood RM, Du R, Lee HJ. Optimal feature selection and deep learning ensembles method for emotion recognition from human brain EEG sensors. IEEE Access. 2017; (5): 14797–806.

8. Yin Z, Zhao M, Wang Y, Yang J, Zhang J. Recognition of emotions using multimodal physiological signals and an ensemble deep learning model. Computer methods and programs in biomedicine. 2017; (140): 93–110.

9. Min S, Lee B, Yoon S. Deep learning in bioinformatics. Briefings in bioinformatics. 2017; 18 (5): 851–69.

10. Page A, Shea C, Mohsenin T. Wearable seizure detection using convolutional neural networks with transfer learning. 2016 IEEE International Symposium on Circuits and Systems (ISCAS). IEEE. 2016; p. 1086–9.

11. Cecotti H, Graser A. Convolutional neural networks for P300

12. Gao Y, Lee HJ, Mehmood RM. Deep learninig of EEG signals for emotion recognition. 2015 IEEE International Conference on Multimedia & Expo Workshops (ICMEW). IEEE. 2015; p. 1–5.

13. Tripathi S, Acharya S, Sharma RD, Mittal S, Bhattacharya S. Using Deep and Convolutional Neural Networks for Accurate Emotion Classification on DEAP Dataset. Twenty-Ninth IAAI Conference. 2017.

14. Koelstra S, Muhl C, Soleymani M, Lee JS, Yazdani A, Ebrahimi T et al. Deap: A database for emotion analysis; using physiological signals. IEEE transactions on affective computing. 2012; 3 (1): 18–31.

15. Li J, Zhang Z, He H. Hierarchical convolutional neural networks for EEG-based emotion recognition. Cognitive Computation. 2018; 10 (2): 368–80.

16. Kwon YH, Shin SB, Kim SD. Electroencephalography based fusion two-dimensional (2D)-convolution neural networks (CNN) model for emotion recognition system. Sensors. 2018; 18 (5): 1383.

detection with application to brain-computer interfaces. IEEE transactions on pattern analysis and machine intelligence. 2011; 33 (3): 433–45.

17. Yuan L, Cao J. Patients' eeg data analysis via spectrogram image with a convolution neural network. International Conference on Intelligent Decision Technologies. Cham: Springer, 2017; p. 13–21.

18. Picard RW, Vyzas E, Healey J. Toward machine emotional intelligence: Analysis of affective physiological state. IEEE transactions on pattern analysis and machine intelligence. 2001; 23 (10): 1175–91.

19. Shusharina NN, Borchevkin DA, Sapunov VV, Petrov VA, Patrushev MV. A Wireless Portable Platform for Physiological Potentials Registration and Processing: A Unified Approach. Journal of Pharmaceutical Sciences and Research. 2017; 9 (7): 1178.

20. Jenke R, Peer A, Buss M. Feature extraction and selection for emotion recognition from EEG. IEEE Transactions on Affective Computing. 2014; 5 (3): 327–39.

21. Kingma DP, Ba J. Adam: A method for stochastic optimization. arXiv:1412.6980. [Preprint]. 2014 [cited 2014 Dec 22]. Available from: https://arxiv.org/abs/1412.6980.

COMPLEX DECUBITUS ULCER THERAPY IN A PATIENT IN CHRONIC CRITICAL CONDITION: A CASE REPORT

Yakovleva AV[1] ✉, Yakovlev AA[1], Petrova MV[1,2], Krylov KYu[3]

[1] Federal Research and Clinical Center of Intensive Care Medicine and Rehabilitology, Moscow, Russia

[2] Peoples Friendship University of Russia, Moscow, Russia

[3] Pirogov Russian National Research Medical University, Moscow, Russia

76.72% of patients admitted to the ICU of the Federal Research and Clinical Center of Intensive Care Medicine and Rehabilitology (FRCC ICMR) in a chronic critical condition (CCC) associated with various types of damage to the brain were diagnosed with decubitus ulcers (DU), or bedsores, of 3rd and/or 4th stage. 33.41% of them were planned to undergo invasive rehabilitation procedures (neurosurgical intervention) that cannot be done while the patient has DU. This report describes a complex technique used to treat a 4th-stage sacrum DU in a CCC patient that needed ventriculoperitoneal shunting. We have covered contraindications to the exclusively surgical DU closing and the successful and rapid healing of the 4th-stage sacrum DU after application of the treatment technique.

СЛУЧАЙ ПРИМЕНЕНИЯ КОМПЛЕКСНОГО СПОСОБА ЛЕЧЕНИЯ ДЕКУБИТАЛЬНОЙ ЯЗВЫ У ПАЦИЕНТА В ХРОНИЧЕСКОМ КРИТИЧЕСКОМ СОСТОЯНИИ

А. В. Яковлева[1] ✉, А. А. Яковлев[1], М. В. Петрова[1,2], К. Ю. Крылов[3]

[1] Федеральный научно-клинический центр реаниматологии и реабилитологии, Москва, Россия

[2] Российский университет дружбы народов, Москва, Россия

[3] Российский национальный исследовательский медицинский университет имени Н. И. Пирогова, Москва, Россия

У 76,72% пациентов, поступивших в реанимационные отделения Федерального научно-клинического центра реаниматологии и реабилитологии (ФНКЦ РР) в хроническом критическом состоянии (ХКС), обусловленном различными поражениями головного мозга, были диагностированы декубитальные язвы (ДЯ), или пролежни, 3-й и/или 4-й стадии. Из них 33,41% пациентов было необходимо плановое прохождение этапа инвазивной реабилитации (нейрохирургическое вмешательство), противопоказанием к которому служило наличие ДЯ. В работе описано применение комплексного способа лечения ДЯ крестца 4-й стадии у пациента в ХКС, которому требовалось выполнение вентрикуло-перитонеального шунтирования. Описаны противопоказания к исключительно хирургическому способу закрытия ДЯ и результаты быстрого и успешного заживления ДЯ крестца 4-й стадии путем использования комплексного способа лечения.

Pressure ulcers, or bedsores, or decubitus ulcers (DU) are ulcerative-necrotic damage to the skin that develops in weakened bedridden patients with impaired microcirculation. Constant pressure, shear and friction forces [1] are the main causes of DU.

Pain, anti-DU procedures and extended stay in the hospital worsen the quality of life of DU patients. Pressure ulcers pave the way to chronic infection; larger bedsores can cause plasma loss with traumatic discharge and generally contribute to the premature death of patients. Therefore, any intervention aimed at DU prevention and/or treatment once such have appeared aids to reduce the cost of treatment and improve the patient's quality of life [2].

The data describing the frequency of DU occurrence in Russian medical organizations is scarce [1]; in European hospitals, the prevalence ranges from 8.3 to 23%, and in Canadian medical institutions the figure goes up to 26% [3].

According to the British researchers, 15 to 20% of patients in hospitals and other types of medical facilities develop bedsores. In the US, 17% of all hospitalized patients run the risk of developing pressure ulcers or already have them [1].

ICU of the Federal Research and Clinical Center of Intensive Care Medicine and Rehabilitology (FRCC ICMR) receives patients in chronic critical conditions (CCC) resulting from various damage to the brain. 76.2% of them have 3rd- and/or 4th-stage DU, localization of which varies. There are certain

peculiarities to the pathological processes (and their treatment) in such patients. A critical condition is an extreme stage of any pathology that calls for external support, full or partial, of vital body functions due to disruption of their autoregulation [4]. CCC is peculiar to ICU patients that survived the acute phase of their disease but remain dependent on intensive care procedures for a long period of time, neither dying nor recovering [5].

Having searched national and foreign databases, we failed to find any data on the frequency of DU development in CCC patients with brain injuries. Various authors report DU healing time of 1 year and longer in patients with other pathologies, following a conservative therapy combining drugs and physiological procedures [6–8]; this healing time is long enough to hinder proper care and rehabilitation of paralyzed patients [6–8]. Outside of surgery, the common approach to treating bedsores is to apply therapeutic dressings to them, like a biologically active dressing for treatment of hard-to-heal wounds [9]. Another solution is to freeze the sores with an applicator cooled down with liquid nitrogen to the temperature of –180 °C [10]. There was also developed a separate treatment technique for patients with spinal cord injuries: soft tissues on the opposite sides of the bedsore are pierced with 2 spokes running at the depth of 0.5–0.8 mm, their ends fixed and gradually brought together [11].

This report describes a complex surgery-free DU therapy technique, its application to a 4th-stage DU in a CCC brain injury patient and the resulting fast healing of the DU.

Case description

Patient D., 23 years old, was admitted to FRCC ICMR for rehabilitation.

Diagnosis: sequelae of concomitant car accident injuries (closed chest injury and contused right lung, closed fracture and displacement of the left clavicle's middle third, closed fracture and displacement of L4–L5 (right), closed fracture of pubic and sciatic bones, comminuted fracture of body and wing of the left iliac bone and right lateral sacrum masses (with displacement), open comminuted fracture and displacement of the left femur's upper third, closed fracture and displacement of the right femur's middle third, 3rd-degree trauma shock). Bleeding from acute gastric and duodenal ulcers (finished), complicated by posthypoxic encephalopathy. Post-sepsis (catheter-associated) condition. 3rd-degree DU on the right lateral malleolus, 3rd-degree DU on the left calcaneal region, 4th-degree DU on the sacrum.

Anamnesis: the patient underwent a series of reconstructive surgeries on his musculoskeletal system (11 months) before being admitted to FRCC ICMR. Postsurgery complications — massive bleeding from acute gastric and duodenal ulcers, which led to the development of posthypoxic encephalopathy and consciousness reduction to the level of coma. Further on, the patient stabilized in CCC, vegetative state. In the background, DU developed on various areas of the patient's body within the first month of hospitalization. There were two plastic surgery attempts on the sacrum DU (autologous tissue), one of them made abroad, but both, through purulent-necrotic complications, led to aggravation of the wound.

At admission, the patient's condition was regarded as severe, level of his consciousness vegetative. He was breathing through a tracheostomy cannula, feed through a gastrostoma, urinated through a catheter. We have registered a deep stage of tetraparesis with increased muscle tone (spastic type), flexion contractures of elbow, wrist, knee and ankle joints, severe protein-energy deficiency. The patient's nutritional status was as

follows: height — 180 cm, weight — 51 kg, BMI — 15.74 kg/sq m, mid-arm circumference (MC) — 17.5 cm (norm — 29 cm), triceps skin fold thickness (TSFT) — 6 mm (norm — 10.5 mm), mid-arm muscle circumference (MMC) — 15.6 cm (norm — 23–25.5 cm). His Nutric score was 2 points, which is low. The results of the Laboratory studies were as follows: transferrin — 52 mg/dL (norm — 200 mg/dL), cholinesterase — 0.81 U/l, albumin — 18 g/l.

Additional examination during the first week yielded indications for the planned ventriculoperitoneal shunt (VPS) — severe hydrocephalus with periventricular edema.

Description of the sacrum DU: area — 114 sq cm (planimetry data); complete skin necrosis and extensive damage to the underlying tissue; well-defined fibrous cicatrizing edges; 3 cm deep pocket along the lower edge; at the bottom of the ulcer — fragments of bone tissue, loose yellow substance covering the area of about 79% of the wound surface; the wound is wet, with yellow exudate evenly distributed over it. The tissue around the DU was pale gray, there was an ulcerated edema with pseudinoma up to 2 cm around the wound; the granulation tissue was dull, it was found at the bottom, covered about 17% of the total DU surface; there were no signs of epithelialization. The Bates–Jensen assessment tool score was 51 points.

This kind of DU prevented the planned VPS and thus needed to be healed as quickly as possible. The patient's medical history and somatic status ruled out radical surgery.

It was decided to apply the patented DU treatment technique [12]. The ulcer was mechanically cleaned daily even if the necrosis area was less than 1 sq cm, followed by laser therapy: 904 nm, four 18 W LEDs, pulse frequency — 2–5000 Hz, maximum average power — 4 • 13.5 mW, load — 3.5 J/sq cm, 1.12 minutes at each point (Combi 400 V system, GymnaUniphy; Belgium–Germany). We have selected six exposure points along the wound's edge and three points along the wound's vertical diameter. After the procedures the wound was covered with an Atrauman dressing. The nutritionist controlled the patient's nutrition (quality and quantity) and adjusted it depending on the anthropometric parameters and laboratory test results. To assess the DU healing dynamics, we used the S.Y.R. scale, a derivative of Bates–Jensen assessment tool. The scale's Y axis is for Bates–Jensen points (increment — 5 points), its X axis is for time (increment — 7 days). The points were put on the graph once every 7 days (Fig. 1).

Seven days of therapy yielded positive results and dynamics: the DU area shrunk to 86 sq cm, the wound's edges grew clearer, the pocket closed, the necrotic tissue patches turned white-gray, viscous, their area decreased to 37% of the total DU area. The exudate became serous and hemorrhagic. Scar tissue formed along the wound's edges; there appeared the signs of epithelialization. The edema around the DU grew smaller, ulceration healed (Fig. 2). Bates-Jensen score — 40 points. It was decided to not change the dressing material composition since the signs of active infection in the DU persisted.

Fourteen days of therapy decreased the DU to 39 sq cm, and the necrotic tissue's area shrunk to no more than 13% of the wound's area. The amount of exudate decreased significantly, down to complete absence of free-flowing exudate. Bates–Jensen score — 36 points. Given the significantly reduced exudation and infection arrest, it was decided to apply Branolind dressing to the wound after procedures.

After 28 days of therapy, the DU area was 23 sq cm, its bottom lined with granulations, edge undergoing active epithelialization. The wound was wet and without free-flowing exudate and edema; the tissue around the wound was pale

pink. Dense scar tissue lined its edge (Fig. 3). Bates–Jensen score — 26 points.

After 35 days of therapy, the DU area was 8 sq cm, its bottom lined with massive granulations, edge undergoing active epithelialization (67% of the total DU area). Bates–Jensen score — 23 points.

The DU was completely cicatrized on the 46th day of therapy (Fig. 4). Bates-Jensen score — 13 points (healed). The patient's nutritional status: weight — 55 kg, BMI — 16.98 kg/sq m, MC — 18.5 cm, TSFT — 6 mm, MMC — 16.6 cm. Nutric score — 3 points (low); transferrin — 173 mg/dl, cholinesterase — 2.66 U/l, albumin — 32 g/l.

The patient received the VPS, with no purulent-septic complications expected immediately after surgery and later. The rehabilitation program was completed with pool activities and extra therapeutic exercises through reduction of the spastic component.

Case discussion

The characteristics of the patient's DU implied that the only treatment option available was surgery. However, his physical condition and medical history suggested that such an operation would likely bring wound complications and delay healing.

Compared to conservative treatment, radical surgery is a fast remedy, but the likelihood of postoperative complications in such a case directly depends on the somatic condition of the patient at the time of surgery. In our experience, DU closing surgery in a brain-injury CCC patient is almost never a success,

since such patient's somatic condition is significantly different from the "ideal" needed for planned operations. We believe that the risk of postoperative complications in such patients is extremely high when closing the DU surgically. Many of such patients are incapable of restoring self-movement capabilities to a sufficient level within a relatively short period of time, which means that time and quality of DU contact with surfaces are defined solely by standard anti-decubital measures. Therefore, we consider it inappropriate and unsafe to close DU in such patients solely by surgical methods.

Reducing the bedsore healing time is crucial for the overall rehabilitation of many brain-injury CCC patients. The patented complex DU therapy method [9] allowed healing the DU within a short period of time and, consequently, performing the planned neurosurgical intervention.

In CCC patients, it is necessary to accurately measure the scale of the surgery against the patient's indicators and to take into account all the circumstances, i.e. not only the possibility to prepare the wound for surgery but also the consequent rehabilitation forecasts, short and long-term.

CONCLUSIONS

The improvement of conservative treatment and its combination with modern surgical and physical therapies allow significant reduction of DU healing time in brain-injury CCC patients while excluding the risks associated with single-step surgery. The patented method is an effective option of DU treatment in brain-injury CCC patients when there are contraindications to its single-step surgical closure.
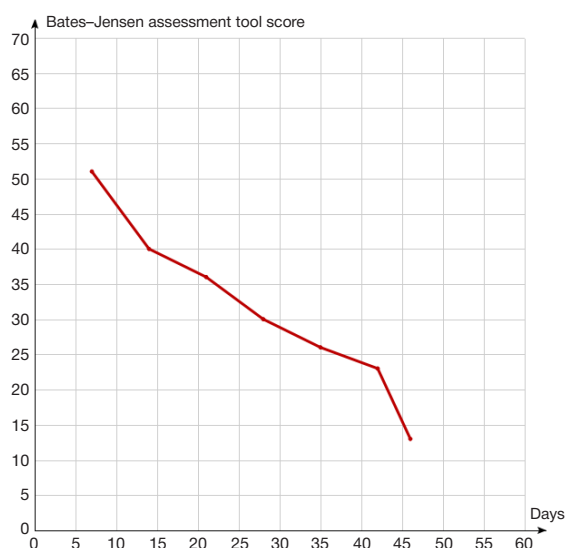

Fig. 1. S.Y.R graphic model

Fig. 2. Sacrum decubitus ulcer, 7th day of treatment

Fig. 3. Sacrum decubitus ulcer, 28th day of treatment

Fig. 4. Sacrum decubitus ulcer, 46th day of treatment

References

1. GOST R 56819-2015. Nacionalnyj standart Rossijskoj Federacii. Nadlezhashhaya medicinskaya praktika. Infologicheskaya model. Profilaktika prolezhnej (utv. i vveden v dejstvie Prikazom Rosstandarta ot 30.11.2015 № 2089-st) Available from: http://www.consultant.ru/cons/cgi/online.cgi?req=doc&base=OTN&n=11348#018678300170008422.
2. Pressure Sore Statistics (Decubitus Ulcer Stats) [Internet] [cited 2013 Mar 11]. Available from: http://decubitusulcervictims.com/pressure-sore-statistics.
3. McInnes E, Jammali-Blasi A, Bell-Syer SEM, Dumville JS, Middleton V, Cullum N. Support surfaces for pressure ulcer prevention. The Cochrane Database of Systematic Reviews (9): CD001735.
4. Zilber AP. E'tyudy' kriticheskoj mediciny'. M.: MED-press-inform, 2006.
5. Girard K, Raffin TA. The chronically critically ill: to save or let die? Respir Care. 1985; (30): 339–47.
6. Baskov AB. Xirurgicheskoe lechenie prolezhnej u bolnyx so spinomozgovoj travmoj. Zhurn. Voprosy nejroxirurgii. 2000; (1): 7–10.
7. Garkavi AB, Elizarov PM. Nekotorye osobennosti techeniya prolezhnevogo processa u spinalnyx bolnyx. Sovremenny'e podxody v diagnostike i lechenie patologii pozvonochnika i spinnogo mozga. M., 1993.
8. Ryabuxa NP, Kasumov RD, Davydov EA, Musixin VN. K voprosu o lechenii prolezhnej pri pozvonochno-spinomozgovoj travme. Sbornik statej. Ekaterinburg, 1995; s. 120–125.
9. Baindurashvili AG, Kagan AV, Brazol MA, Tsvetaev EV, Mitrofanova EV, Melnikov MR, inventor; Federal State Budgetary Institution The Turner scientific research institute for children's orthopedics under the Ministry of Health of the Russian Federation, Komitet po zdravookhraneniyu administratsii Sankt-Peterburga Gosudarstvennoe uchrezhdenie zdravookhraneniya «Detskaya gorodskaya bolnitsa №1», assignee. Biologicheski aktivnaya povyazka dlya lecheniya dlitelno ne zazhivayushhikh ran (troficheskie yazvy, prolezhni, glubokie dermal'nye ozhogi). Patent RF № 2450833. 2010 Dec 23.
10. Glukhov AA, Aralova MV, inventor; Glukhov AA, Aralova MV, assignee. Sposob kompleksnogo lecheniya prolezhnej u patsientov s dlitel'noj immobilizatsiej. Patent RF № 2578382. 2014 Jun 05.
11. Chirkov AA, inventor; The Loginov Moscow Clinical Scientific Center is State Institution funded by Moscow Health Department, assignee. Sposob korrektsii prolezhnej u spinal'nykh bol'nykh. Patent RF № 2620019. 2015 Oct 05.
12. Grechko AV, Danilets VV, Rebrov KS, Sidorov IB, SHajbak AA, Shhelkunova IG, Yakovlev AA, inventor; Federal Research and Clinical Center of Intensive Care Medicine and Rehabilitology, assignee. Sposob kompleksnogo lecheniya prolezhnej u patsientov s dlitel'noj immobilizatsiej. Patent RF № 2661084. 2017 Jul 21.

Литература

1. ГОСТ Р 56819-2015. Национальный стандарт Российской Федерации. Надлежащая медицинская практика. Инфологическая модель. Профилактика пролежней (утв. и введен в действие Приказом Росстандарта от 30.11.2015 № 2089-ст). Доступно по ссылке: http://www.consultant.ru/cons/cgi/online.cgi?req=doc&base=OTN&n=11348#018678300170008422.
2. Pressure Sore Statistics (Decubitus Ulcer Stats) [Internet] [cited 2013 Mar 11]. Available from: http://decubitusulcervictims.com/pressure-sore-statistics.
3. McInnes E, Jammali-Blasi A, Bell-Syer SEM, Dumville JS, Middleton V, Cullum N. Support surfaces for pressure ulcer prevention. The Cochrane Database of Systematic Reviews (9): CD001735.
4. Зильбер А. П. Этюды критической медицины. М.: МЕД-пресс-информ, 2006.
5. Girard K, Raffin TA. The chronically critically ill: to save or let die? Respir Care. 1985; (30): 339–47.
6. Басков А. В. Хирургическое лечение пролежней у больных со спиномозговой травмой. Вопросы нейрохирургии. 2000; (1): 7–10.
7. Гаркави А. В., Елизаров П. М. Некоторые особенности течения пролежневого процесса у спинальных больных. Современные подходы в диагностике и лечение патологии позвоночника и спинного мозга. М., 1993.
8. Рябуха Н. П., Касумов Р. Д., Давыдов Е. А., Мусихин В. Н. К вопросу о лечении пролежней при позвоночно-спиномозговой травме. Сборник статей. Екатеринбург, 1995; с. 120–125.
9. Баиндурашвили А. Г., Каган А. В., Бразоль М. А., Цветаев Е. В., Митрофанова Е. В., Мельников М. Р., авторы; Федеральное государственное учреждение «Научно-исследовательский детский ортопедический институт имени Г. И. Турнера» Министерства здравоохранения и социального развития РФ, Комитет по здравоохранению администрации Санкт-Петербурга Государственное учреждение здравоохранения «Детская городская больница №1», патентообладатели. Биологически активная повязка для лечения длительно не заживающих ран (трофические язвы, пролежни, глубокие дермальные ожоги). Патент РФ № 2450833 23.12.2010.
10. Глухов А. А., Аралова М. В., авторы; Глухов А.А., Аралова М. В., патентообладатель. Способ лечения больных с трофическими язвами. Патент РФ № 2578382 05.06.2014.
11. Чирков А. А., автор; Государственное бюджетное учреждение здравоохранения города Москвы Московский клинический научно-практический центр А. С. Логинова Департамента здравоохранения города Москвы, патентообладатель. Способ коррекции пролежней у спинальных больных. Патент РФ № 2620019 05.10.2015.
12. Гречко А. В., Данилец В. В., Ребров К. С., Сидоров И. Б., Шайбак А. А., Щелкунова И. Г., Яковлев А. А., авторы; Федеральное государственное бюджетное научное учреждение «Федеральный научно-клинический центр реаниматологии и реабилитологии», патентообладатель. Способ комплексного лечения пролежней у пациентов с длительной иммобилизацией. Патент РФ № 2661084 21.07.2017.

PROBLEMS OF MEDICAL REHABILITATION IN PATIENTS AFTER A TRANSIENT ISCHEMIC ATTACK

Kostenko EV ✉, Eneeva MA, Kravchenko VG

Moscow Centre for Research and Practice in Medical Rehabilitation, Restorative and Sports Medicine, Moscow, Russia

The efficacy of rehabilitation in post-TIA patients still remains a clinical challenge, considering the combined burden of the primary disease and comorbidities. The aim of this study was to provide a rationale for introducing psychological counseling into post-TIA rehabilitation programs after studying the presentations of cognitive and emotional impairments developed after this cerebrovascular event. We analyzed in- and outpatient medical records of 351 participants (the mean age was 58.6 ± 2.2 years) who had experienced a TIA. Data was collected from forms 0.25/y and 003/y, medical/social questionnaires and also included MMSE and HADS scores. We found that CI and MD ranked second after cardiovascular diseases among the comorbidities in post-TIA patients (186.8 cases per 100 patients). We conclude that rehabilitation of post-TIA patients should involve a multidisciplinary team of experts including a psychotherapist or a clinical psychologist who will provide psychological counselling.

Keywords: transient ischemic attack, neuropsychological disorders, cognitive impairment, mood disorders, medical rehabilitation

✉ **Correspondence should be addressed:** Elena V. Kostenko
Baumanskaya 70, Moscow, 105007; ekostenko58@mail.ru

АКТУАЛЬНЫЕ ВОПРОСЫ ОРГАНИЗАЦИИ МЕДИЦИНСКОЙ РЕАБИЛИТАЦИИ ПАЦИЕНТОВ, ПЕРЕНЕСШИХ ТРАНЗИТОРНУЮ ИШЕМИЧЕСКУЮ АТАКУ

Е. В. Костенко ✉, М. А. Энеева, В. Г. Кравченко

Московский научно-практический центр медицинской реабилитации, восстановительной и спортивной медицины, Москва, Россия

Повышение эффективности реабилитационных мероприятий у пациентов, перенесших транзиторную ишемическую атаку (ТИА), с учетом особенностей основного и ведущих сопутствующих заболеваний остается актуальной задачей. Целью исследования было на основании изучения особенностей когнитивных и эмоциональных нарушений обосновать значение психокоррекции в комплексе реабилитационных мероприятий у пациентов, перенесших ТИА. Была изучена и проанализирована заболеваемость у 351 пациента, перенесшего ТИА. Средний возраст обследованных пациентов составил 58,6 ± 2,2 года. Для сбора информации проводили выкопировку данных из медицинских карт амбулаторных больных (форма 0.25/у) и медицинских карт стационарных больных (форма 003/у), в том числе данных опроса пациентов по Анкете медико-социальной характеристики пациентов, учитывали также данные шкал MMSE, HADS. Выявлено, что второе место по уровню заболеваемости у пациентов, перенесших ТИА, после заболеваний сердечно-сосудистой системы занимают психические расстройства, распространенность которых составила 186,8 случая на 100 пациентов. Важное место в программах медико-социальной реабилитации пациентов, перенесших ТИА, должна занимать коррекция психических расстройств с участием психотерапевта, медицинского психолога в составе мультидисциплинарной бригады.

Ключевые слова: транзиторная ишемическая атака, нейропсихологические расстройства, когнитивные нарушения, эмоциональные расстройства, медицинская реабилитация

✉ **Для корреспонденции:** Елена Владимировна Костенко
ул. Бауманская, д. 70, г. Москва, 105007; ekostenko58@mail.ru

A transient ischemic attack (TIA) is a type of an acute cerebrovascular syndrome that is not accompanied by persistent neurological symptoms characteristic of a focal brain injury. Because TIA symptoms rapidly resolve on their own, patients often ignore them as insignificant and do not seek immediate medical help; for the same reason, doctors may not recognize the short-lived symptoms as TIA [1].

TIA can be a harbinger of a much more devastating acute vascular event; therefore, its clinical importance and prognostic value should not be underestimated. Post-TIA patients are at a higher risk of myocardial infarction (MI), stroke or death within 5 years after TIA [1–4]. But apart from being a marker of an upcoming cardio or cerebrovascular episode, TIA is also linked to the development of such nonfatal conditions as cognitive impairment (CI) and mood disorders by a few Russian and international researchers [5, 6].

Studies of cognitive function in hypertensive post-TIA patients reveal that such patients suffer from CI; they also demonstrate an association between CI and changes to brain morphology induced by elevated blood pressure. Interestingly, CI does not have any clinically or functionally significant impact on the patients before TIA occurs [5]. Among post-TIA patients, CI is more common in men than women [6]. Research into structural and morphological changes to brain matter in patients with TIA and CI has found signs of cerebral atrophy localized to the thalamus, hypothalamus and the dentate gyrus

[5–7]. The researchers suggest that cognitive and emotional impairments in this cohort are a result of brain matter atrophy.

CI is diagnosed in over 40% of post-TIA patients [4]. Researchers are particularly interested in studying the severity and clinical presentations of cognitive and mood disorders, their prognostic value and effect on a patient's daily life.

Microstructural tissue damage induced by TIA causes cortical and subcortical structures to disconnect. Although motor function is spared, the disconnection promotes development of neuropsychological disorders that have no lesser impact on the patient than post-stroke motor disorders. Exploration of and interaction with the outside world rely on intact cognitive function; in post-TIA patients, its deficit is exacerbated by emotional lability [7].

In order to improve the outcome of rehabilitation programs and to reduce the risk of recurrence in post-TIA patients, the following parameters should be factored into: the patterns of neurological and mental disorders that accompany TIA, possible comorbidities, patients' social and hygienic characteristics. This will help physicians to tailor rehabilitation to the individual patient.

The aim of this study was to provide a rationale for introducing psychological counseling into rehabilitation programs for post-TIA patients after studying the presentations of cognitive and emotional impairments in such patients.

METHODS

The study of cognitive and emotional impairments in 351 patients was based on the analysis of out- and inpatient medical records (Forms 0.25/y and 003/y) and medical/social questionnaires. For female participants, the mean age was 59.6 ± 2.3 years; for male participants, 57.6 ± 2.2 years. The mean age of the entire cohort was 58.6 ± 2.2 years.

CI and its severity were inferred from the patients' medical records that included Mini Mental State Examination (MMSE) scores [8]. The severity of mood disorders was evaluated based on the Hospital Anxiety and Depression scale (HADS) [9], which is used in the setting of a GP practice.

Of all female patients, 46.7% were retired but working. Most patients had a college (47.0%; $n = 165$) or university (35.3%; $n = 124$) degree. The majority of the patients were not satisfied with their current job (62.1%; $n = 218$). One in 5 patients was either widowed or unmarried (19.9%; $n = 70$); this subgroup was dominated by women. We discovered that 79.7% ($n = 280$) of the patients lived with their families; 5.6% ($n = 20$) had relatives but lived separately; 14.7% ($n = 51$) did not have a family. Permanent disabilities were observed in 73 patients (20.8%); of them 58 (79.4%) had a 3rd degree disability, and only 15 (20.6%) had a 2nd degree disability.

Information selected from the medical records was entered into special case sheets and processed in *Excel* (Microsoft;

USA) and *Statistica* 8.0 (StatSoft Inc; USA). The results were presented as the mean + the mean error (M ± m) and the median (Me) for normally distributed variables (the Kolmogorov-Smirnov test). Qualitative characteristics were presented as absolute and relative frequencies (%). The significance of differences was assessed using Student's *t*-test and the nonparametric χ2-test. Spearman's rank correlation coefficient was used to measure a correlation between two variables. Differences were considered significant at $p < 0.05$.

RESULTS

Detected comorbidities were categorized according to the International Statistical Classification of Diseases and Related Health Problems (ICD-10). In terms of prevalence, circulatory system diseases ranked first (32.6%), mental disorders ranked second (31.5%) and endocrine disorders ranked third (15.5%). These 3 groups amounted to 79.6% of all pathologies detected in our post-TIA patients. Table 1 summarizes distribution of various circulatory system diseases among the study participants.

We have found that 312 (89%) patients suffered from comorbid conditions of the circulatory system varying in their severity. Two or more comorbid circulatory system diseases were observed in 130 (37.0%) post-TIA patients.

In terms of prevalence, mental disorders ranked second after circulatory system diseases in post-TIA patients (186.8 cases per 100 patients; Table 2).

Fig. 1 shows how mental disorders were distributed in the studied cohort of patients.

Organic anxiety disorder was diagnosed in 72.9% of 351 patients. CI occurred in 31.1% of the patients and was represented by moderate CI (19.9%), mild dementia (7.7%), and moderate dementia (3.4%). Depression was observed in 17.7% of the participants; of them 12.5% had subclinical depression, 3.4% had a mild depressive episode, and 1.7% suffered from moderate depression.

About 1 in every 2 patients (45.7%) was afflicted with a combination of CI and depression or cooccurring depression and anxiety. CI was most common in patients aged over 60 years, with no significant differences in prevalence between males and females. Mood disorders were more frequent in women aged 50–59, whereas depression was more common in men over 70.

Mood disorders were characterized by low mood, sadness, tension, worrying thoughts, and anxiety. The following symptoms were noticed in the majority of patients: low intellectual productivity, lack of goals, decreased motivation to come back to work and resume social contacts, difficulty concentrating, inertia, and reluctance to take part in rehabilitation programs.

The analysis revealed a strong positive correlation between CI and recurrence of an acute cerebrovascular event (TIA,

Table 1. The frequency of circulatory system diseases diagnosed in post-TIA patients

Condition	Number of cases	
	Abs.	%
Cerebrovascular diseases	312	89.0
Hypertensive heart disease	241	68.7
Atherosclerosis	185	73.7
Ischemic heart disease	141	56.2
Atherosclerotic heart disease	82	58.2
Old myocardial infarction	37	26.2
Other forms of chronic ischaemic heart disease	22	15.6
Occlusion and stenosis of cerebral arteries, not resulting in cerebral infarction	20	14.2

ischemic or hemorrhagic stroke) ($r = 0.724$; $p < 0.05$), as well as between depression and recurrence of an acute cerebrovascular event (TIA, ischemic or hemorrhagic stroke) ($r = 0.736$; $p < 0.05$).

Neuropsychological disorders and cardiovascular conditions cooccurred in 213 (60.7%) patients. Hypertension was observed in 161 (75.6%) patients (Tables 3–5). A direct, strong and reliable correlation was established between the severity of CI and hypertension ($r = 0.95$; $p < 0.05$), as well as between the severity of mood disorders and hypertension ($r = 0.95$; $p < 0.05$).

Neuropsychological disorders cooccurred with coronary artery disease (CAD) in 101 (47.4%) patients; MI was observed in 21 cases (20.8% patients with CAD; Table 6). We analyzed a correlation between cognitive/mood disorders and CAD in the presence or absence of MI. The analysis revealed a strong positive correlation between the presence of CAD and CI ($r = 0.87$; $p < 0.05$); in the patients with MI, the correlation was similar ($r = 0.97$; $p < 0.05$). The analysis also yielded a positive and reliable correlation between CAD and MD ($r = 0.93$; $p < 0.05$). The correlation between depression and CAD with MI was stronger than between depression and CAD without MI.

DISCUSSION

A few authors report the presence of vascular CI varying in severity in 70–80% of patients with acute and chronic cerebrovascular conditions [10, 11]. Minor strokes are often

the cause of CI; therefore, every patient who has experienced a TIA or a stroke should have their cognitive function evaluated [12]. Neuropsychological disorders that often have subclinical manifestations can cause emotional distress, behavioral or adjustment disorders in patients with cerebrovascular conditions [12]. CI signals the unfavorable course of a primary cerebrovascular disorder and is an indicator of low cerebral reserve, which increases the risk of a recurrent vascular event in patients with CI [11].

The data on CI and MD presented in both Russian and international literature covers mainly post-stroke patients; that said, the studied cohorts might have also included patients with TIA. So far, there have been no large-scale studies of neuropsychological conditions in post-TIA patients. The data described in the literature was collected from small cohorts of patients (less than 100) [13, 14].

In post-TIA patients, MD can affect the course of the illness, trigger another stroke or impede rehabilitation [15]. In the cited work, emotional disturbances were assessed using the HADS scale. It was hypothesized that the central focus of post-TIA rehabilitation should be on psychological counseling. Some authors believe that post-TIA patients develop anxiety and depression due to vascular damage and a profound psychological response to the event; therefore, a well-structured multidisciplinary multifactorial program that includes control over vascular risk factors as part of risk mitigation will help to bring down HADS scores and reduce the prevalence of depression a year after the vascular event [16]. Another

Table 2. Prevalence of mental disorders in post-TIA patients

| Condition	Abs.	%
Cognitive impairement:	109	31.1
MCD	70	19.9
Mixed cortical and subcortical vascular dementia, mild form	27	7.7
Mixed cortical and subcortical vascular dementia, moderate form	12	3.4
Organic anxiety disorder	256	72.9
Organic mood disorder:	62	17.7
Subclinical depression	44	12.5
Mild depression	12	3.4
Moderate depression	6	1.7
Organic emotionally labile disorder	58	16.5
Total:	656	186.8

Note: MCD — mild cognitive disorder
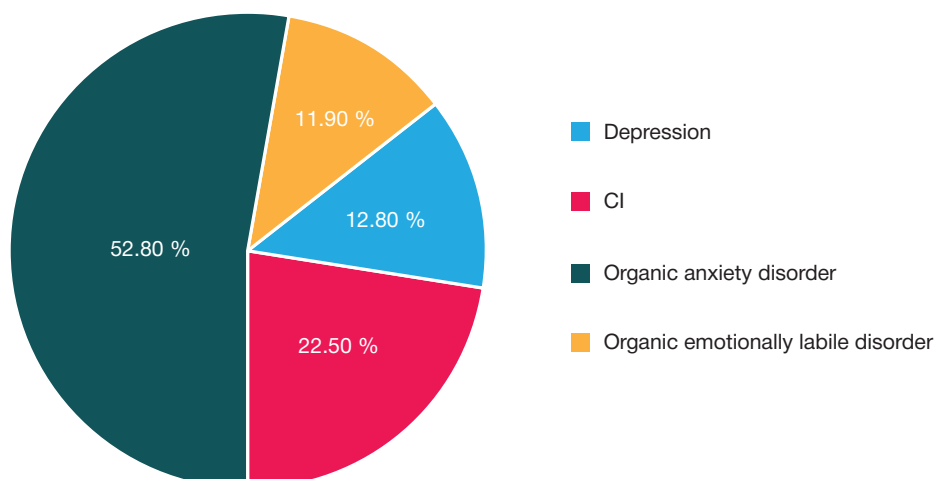
Fig. 1. Distribution of mental disorders in post-TIA patients

Table 3. Prevalence of neuropsychological (cognitive and mood) disorders in post-TIA patients with hypertensive heart disease

Cognitive impairment	Number of cases (abs.)	Number of cases with comorbid hypertensive heart disease
MCD	70	58
Mild dementia	27	22
Moderate dementia	12	12
MD:		
Subclinical depression	44	38
Mild depression	12	8
Moderate depression	6	5

Note: MD — mood disorders

Table 4. Severity of hypertensive heart disease in post-TIA patients with CI

HHD / CI	Stage 1		Stage 2		Stage 3		Total
	Abs.	%	Abs.	%	Abs.	%	Abs.
MCD	38	54.3	12	17.1	8	11.4	58
Mild dementia	5	18.5	10	37	7	26	22
Moderate dementia	1	8.3	2	16.7	9	75	12
Total:	44		24		24		92

Table 5. Severity of hypertensive heart disease in post-TIA patients with mood disorders

HHD / CI	Stage 1		Stage 2		Stage 3		Total
	Abs.	%	Abs.	%	Abs.	%	Abs.
Subclinical MD	30	68.4	5	11.4	3	6.8	38
Mild depression	3	25	4	33.3	1	8.3	8
Moderate depression	0	0	1	16.7	4	66.7	5
Total:	33		9		8		51

Table 6. Prevalence of CI, MD and CAD in post-TIA patients

Cognitive impairment	Number of cases (abs.)	Number of cases of comorbid CI and CAD (abs. / %)		Number of cases of comorbid CI and CAD with MI (abs. / %)	
MCD	70	18	25.7	5	7.1
Mild dementia	27	8	29.6	3	11.1
Moderate dementia	12	4	33.3	2	16.7
MD:					
Subclinical depression	44	32	72.7	8	18.2
Mild depression	12	6	50	5	41.7
Moderate depression	6	4	66.7	2	33.3

study investigated patients' psychosocial response to TIA. The authors were able to identify 6 major reaction patterns, including worrying thoughts about the future/changes in lifestyle, lack of trust, frustration, anxiety, sense of loss, sadness, confusion. Knowledge of such personal reactions to TIA can help to tailor rehabilitation to the needs of an individual patients and transform their usual coping strategies in order to achieve better rehabilitation outcomes [17].

Some authors indicate that CI can occur in patients who have already experienced a TIA or a minor stroke [5, 18, 19]. Within 9 months following TIA, one-third of patients develop CI interfering with their lifestyle [20].

To sum up, MD and CI in post-TIA patients can be used to tailor rehabilitation programs to the needs of an individual patient.

CONCLUSION

CI and MD rank second after cardiovascular diseases among the comorbidities in post-TIA patients (186.8 cases per 100 patients). Mental disorders cooccur with circulatory system diseases in 60.7% of post-TIA patients. We have established direct, strong and reliable correlations between the severity of CI and the presence of hypertensive heart disease ($r = 0.95$; $p < 0.05$), between the severity of mood disorders and hypertensive heart disease ($r = 0.95$; $p < 0.05$) and its stage. A combination of neuropsychological disorders and CAD was observed in 47.4% of post-TIA patients. Therefore, rehabilitation for such patients should be well-structured, multidisciplinary and account for multiple factors, including possible comorbidities among which neuropsychological disorders play a significant role.

References

1. Uchijam Sh. Tranzitornye ishemicheskie ataki. M.: GJeOTAR-Media, 2016; 224 s. Russian.
2. Dzhejms F Tul. Sosudistye zabolevanija golovnogo mozga. M.: GJeOTAR-Media, 2007; 612 s. Russian.
3. Amarenco P. One-Year Risk of Stroke after Transient Ischemic Attack or Minor Stroke. N Engl J Med. 2016; 374 (16): 1533–42. DOI: 10/1056/NEJMoa1412981.
4. Stahovskaya LV. Tranzitornaja ishemicheskaja ataka. Farmateka. Klinicheskie rekomendacii. 2017; (2): 34–45. Russian.
5. Poltavceva OV. Kognitivnye narushenija u pacientov s arterial'noj gipertenziej i tranzitornoj ishemicheskoj atakoj. Sibirskij medicinskij zhurnal. 2014; 29 (1): 39–43. Russian.
6. Bivard A, Lillicrap T, Maréchal B. Transient Ischemic Attack Result in Delayed Brain Atrophy and Cognitive Declaine. Stroke. 2018; 49 (2): 384–90.
7. Lobzin SV, Lobzin VYu, Amurova TR, Mirzaeva LM, Nikishina OA, Nikiforova LG, i dr. Diskussionnye voprosy diagnostiki i patogeneticheskoj terapii hronicheskoj cerebral'noj ishemii s kognitivnymi narushenijami. Medicinskij alfavit. Nevrologija i psihiatrija. 2018; 1 (1): 5–14. Russian.
8. Folstein MF, Folstein SE, McHugh PR. «Mini-mental state»: a practical method for grading the cognitive state of patients for the clinician. Journal of Psychiatric Research. 1975; 12 (3): 189–98.
9. Zigmond AS, Snaith RP. The Hospital Anxiety and Depression scale. Acta Psychiatr Scand. 1983; (67): 361–70.
10. Zaxarov VV, Vaxnina NV. Insul't i kognitivnye narushenija. Zhurnal nevrologii i psihiatrii im. N. N. Korsakova (pril. Insul't). 2008; (22): 6–21. Russian.
11. Damulin IV. Sosudistaja demencija: patogenez, diagnostika i lechenie. Farmateka. 2010; (7): 13–8. Russian.
12. Hachinski V. World Stroke Day 2008: «Little strokes, Big Trouble». Stroke. 2008; 39 (9): 2407–8.
13. Maleina AYu, Kolokolov OV, Lukna EV. Rol' tranzitornoj ishemicheskoj ataki v vozniknovenii kognitivnyh narushenij (obzor). Saratovskij nauchno-medicinskij zhurnal. 2016; 12 (2): 273–7. Russian.
14. Gudkova VV, Shanina TV, Petrova EA, Stahovskaya LV. Tranzitornaja ishemicheskaja ataka-mul'tidisciplinarnaja problema. Nevrologija. Nejropsihiatrija. Psihosomatika. 2012; (3): 20–4. Russian.
15. Spurgeon L, James G, Sackley C. The Hospital Anxiety and Depression Scale: a pilot study to examine its latent structure and the link between psychological state and symptom severity in transient ischaemic attack patients. Psychol Health Med. 2016; 21 (5): 632–8.
16. Ihle-Hansen H, Thommessen B, Fagerland MW, Oksengård AR, Wyller TB, Engedal K, at al. Effect on anxiety and depression of a multifactorial risk factor intervention program after stroke and TIA: a randomized controlled trial. Aging Ment Health. 2014; 18 (5): 540–6.
17. Spurgeon L, James G, Sackley C. Subjective experiences of transient ischaemic attack: a repertory grid approach. Disabil Rehabil. 2013; 35 (26): 2205–12.
18. Boss HM, Van Schaik SM, Deijle IA, de Melker EC, van den Berg BT, Scherder EJ, at al. A randomised controlled trial of aerobic exercise after transient ischaemic attack or minor stroke to prevent cognitive decline: the MoveIT study protocol. BMJ. Open. 2014; 4 (12): e007065.
19. Boss HM, Van Schaik SM, Deijle IA, de Melker EC, van den Berg BT, Scherder EJ, at al. Safety and feasibility of post-stroke care and exercise after minor ischemic stroke or transient ischemic attack: MotiveS & MoveIT. NeuroRehabilitation. 2014; 34 (3): 401–7.
20. Kjörk E, Blomstrand C, Carlsson G, Lundgren-Nilsson Å, Gustafsson C. Daily life consequences, cognitive impairment, and fatigue after transient ischemic attack. Acta Neurologica Scandinavica. 2016; 133 (2): 103.

Литература

1. Учиям Ш. Транзиторные ишемические атаки. М.: ГЭОТАР-Медиа, 2016; 224 с.
2. Джеймс Ф. Тул. Сосудистые заболевания головного мозга. М.: ГЭОТАР-Медиа, 2007; 612 с.
3. Amarenco P. One-Year Risk of Stroke after Transient Ischemic Attack or Minor Stroke. N Engl J Med. 2016; 374 (16): 1533–42. DOI: 10/1056/NEJMoa1412981.
4. Стаховская Л. В. Транзиторная ишемическая атака. Фарматека. Клинические рекомендации. 2017; (2): 34–45.
5. Полтавцева О. В. Когнитивные нарушения у пациентов с артериальной гипертензией и транзиторной ишемической атакой. Сибирский медицинский журнал. 2014; 29 (1): 39–43.
6. Bivard A, Lillicrap T, Maréchal B. Transient Ischemic Attack Result in Delayed Brain Atrophy and Cognitive Declaine. Stroke. 2018; 49 (2): 384–90.
7. Лобзин С. В., Лобзин В. Ю., Амурова Т. Р., Мирзаева Л. М., Никишина О. А., Никифорова Л. Г. и др. Дискуссионные вопросы диагностики и патогенетической терапии хронической церебральной ишемии с когнитивными нарушениями. Медицинский алфавит. Неврология и психиатрия. 2018; 1 (1): 5–14.
8. Folstein MF, Folstein SE, McHugh PR. «Mini-mental state:» a practical method for grading the cognitive state of patients for the clinician. Journal of Psychiatric Research. 1975; 12 (3): 189–98.
9. Zigmond AS, Snaith RP. The Hospital Anxiety and Depression scale. Acta Psychiatr Scand. 1983; (67): 361–70.
10. Захаров В. В., Вахнина Н. В. Инсульт и когнитивные нарушения. Журнал неврологии и психиатрии им. Н. Н. Корсакова (прил. Инсульт). 2008; (22): 6–21.
11. Дамулин И. В. Сосудистая деменция: патогенез, диагностика и лечение. Фарматека. 2010; (7): 13–8.
12. Hachinski V. World Stroke Day 2008: «Little strokes, Big Trouble». Stroke. 2008; 39 (9): 2407–8.
13. Малеина А. Ю., Колоколов О. В., Лукна Е. В. Роль транзиторной ишемической атаки в возникновении когнитивных нарушений (обзор). Саратовский научно-медицинский журнал. 2016; 12 (2): 273–7.
14. Гудкова В. В., Шанина Т. В., Петрова Е. А., Стаховская Л. В. Транзиторная ишемическая атака-мультидисциплинарная проблема. Неврология. Нейропсихиатрия. Психосоматика. 2012; (3): 20–4.
15. Spurgeon L, James G, Sackley C. The Hospital Anxiety and Depression Scale: a pilot study to examine its latent structure and the link between psychological state and symptom severity in transient ischaemic attack patients. Psychol Health Med. 2016; 21 (5): 632–8.
16. Ihle-Hansen H, Thommessen B, Fagerland MW, Oksengård AR, Wyller TB, Engedal K, at al. Effect on anxiety and depression of a multifactorial risk factor intervention program after stroke and TIA: a randomized controlled trial. Aging Ment Health. 2014; 18 (5): 540–6.
17. Spurgeon L, James G, Sackley C. Subjective experiences of transient ischaemic attack: a repertory grid approach. Disabil Rehabil. 2013; 35 (26): 2205–12.
18. Boss HM, Van Schaik SM, Deijle IA, de Melker EC, van den Berg BT, Scherder EJ, at al. A randomised controlled trial of aerobic exercise after transient ischaemic attack or minor stroke to prevent cognitive decline: the MoveIT study protocol. BMJ. Open. 2014; 4 (12): e007065.
19. Boss HM, Van Schaik SM, Deijle IA, de Melker EC, van den Berg BT, Scherder EJ, at al. Safety and feasibility of post-stroke care and exercise after minor ischemic stroke or transient ischemic attack: MotiveS & MoveIT. NeuroRehabilitation. 2014; 34 (3): 401–7.
20. Kjörk E, Blomstrand C, Carlsson G, Lundgren-Nilsson Å, Gustafsson C. Daily life consequences, cognitive impairment, and fatigue after transient ischemic attack. Acta Neurologica Scandinavica. 2016; 133 (2): 103.

DYNAMICS OF SECRETORY IGA IN PATIENTS WITH GENERALIZED CHRONIC PERIODONTITIS

Sashkina TI, Runova GS, Abdullaeva AI, Bozhedomov AYu ✉, Saldusova IV, Zaychenko OV, Faskhutdinov DK, Sokolova SI

Pirogov Russian National Research Medial University, Moscow, Russia

Generalized chronic periodontitis (GCP) is a widespread disease. It has a serious negative impact on the quality of a patient's life, posing a challenge to dentists all over the world. At present, standard therapy regimens for GCP adopted in the Russian Federation do not account for the mucosal barrier state, which is determined by a number of various factors, including the levels of secretory immunoglobulin A (sIgA). In our study, we attempted to assess the functional state of the mucosal barrier in patients with GCP and to provide a rationale for using immunotherapy aimed at restoring the effective barrier function of the oral mucosa. SIgA concentrations, which served as an indicator of the mucosal barrier state, were measured with ELISA. We found that patients with GCP had significantly lower sIgA concentrations in the oral fluid in comparison with healthy individuals. Although therapeutic procedures did help to increase sIgA levels, they still were much lower after therapy than in healthy volunteers (54.6 ± 30.5 µg/ml vs 151.2 ± 105.2 µg/ml). Increased permeability of the mucosal barrier caused sIgA to leak into the peripheral blood serum, where its concentration grew from 0.21 ± 0.28 µg/ml to 0.35 ± 0.47 µg/ml during the treatment course, suggesting damage to the mucosal integrity. This fact needs to be accounted for when treating patients with GCP.

Keywords: generalized chronic periodontitis, mucosal barrier, sIgA

ДИНАМИКА СЕКРЕТОРНОГО IGA У БОЛЬНЫХ ХРОНИЧЕСКИМ ГЕНЕРАЛИЗОВАННЫМ ПАРОДОНТИТОМ СРЕДНЕЙ ТЯЖЕСТИ

Т. И. Сашкина, Г. С. Рунова, А. И. Абдуллаева, А. Ю. Божедомов ✉, И. В. Салдусова, О. В. Зайченко, Д. К. Фасхутдинов, С. И. Соколова

Российский национальный исследовательский медицинский университет имени Н. И. Пирогова, Москва, Россия

Хронический генерализованный пародонтит (ХГП) широко распространен во всем мире. У больных снижается качество жизни, поэтому лечение данного заболевания является актуальной проблемой стоматологии. В настоящий момент терапию ХГП в Российской Федерации проводят по стандарту, не учитывающему важнейшую составляющую пародонта — мукозный барьер. Его состояние зависит от многих факторов, в том числе уровня секреторного иммуноглобулина А (s-IgA). Целью исследования было оценить состояние мукозного барьера для обоснования применения методов терапии, позволяющих восстановить его эффективность. В качестве инструмента для оценки эффективности слизистого барьера мы использовали уровень s-IgA, который определяли методом иммуноферментного анализа. Мы показали, что в ротовой жидкости у больных ХГП уровень s-IgA значительно снижен по сравнению со здоровыми. Проведенная стандартная терапия повышает его уровень, но он остается достоверно ниже, чем у здоровых (54,6 ± 30,5 мкг/мл; 151,2 ± 105,2 мкг/мл соответственно). Увеличение проницаемости слизистого барьера приводит к появлению s-IgA в сыворотке периферической крови, причем его концентрация возрастает после проведенной терапии с 0,21 ± 0,28 мкг/мл до 0,35 ± 0,47 мкг/мл, что свидетельствует о значительных нарушениях целостности мукозного барьера у больных ХГП и о необходимости учитывать эти нарушения при проведении терапевтических мероприятий.

Ключевые слова: хронический генерализованный пародонтит, мукозный барьер, s-IgA

A healthy oral mucosal barrier is critical for protecting periodontal tissue against inflammation. Its functional state is determined by a variety of specific and nonspecific humoral and cellular factors including those that promote continuous renewal of the epithelial surface. Periodontitis is characterized by the loss of integrity and abnormal blood flow in periodontal tissue. The tissue gets infiltrated by immune cells and pathogenic bacteria, which eventually causes damage to the mucosal barrier, affects its protective properties and promotes inflammation. Secretory immunoglobulin A (sIgA) is one of the crucial components of the mucosal barrier. This immunoglobulin is synthesized in lymphoid tissue associated with salivary glands and lymphocytes underlying the epithelium in the *lamina propria*. There are a few factors that interfere with tissue healing and can be observed in patients with periodontal pathology: hypoxia, immune imbalance, abnormal neutrophil activity, elevated proinflammatory cytokines, and aberrant sIgA levels. The barrier function of the oral mucosa can be

assessed by measuring sIgA concentrations. Such tests are particularly relevant in dentistry and other medical fields that involve the study of oral mucous membranes. According to recent publications, local immunity is compromised in patients with congenital or acquired susceptibility to chronic periodontitis. This refers to sIgA levels in the first place. Therefore, adding immunotherapy to the treatment regimens would be beneficial for such patients [1–7]. The aim of the present work was to assess the dynamics of sIgA levels as an indicator of the mucosal barrier state in patients with generalized chronic periodontitis (GCP) and to provide a rationale for using immunotherapy aimed at restoring the effective barrier function of the oral mucosa.

METHODS

The study was conducted at the facilities of the Department of Clinical Pathophysiology of Pirogov Russian National Research Medical University. We examined 178 patients with GCP and identified those suffering from a moderate form of the disease. The age of the selected patients was 37 to 52 years. Severity of periodontitis was graded according to the criteria of Russian Dental Association (RDA, 2012). SIgA was measured in the samples of oral fluid collected from 25 participants. Oral fluid samples collected from healthy volunteers aged 25 to 49 years were used as a control.

The following inclusion criteria were applied: voluntary consent to participate, no decompensated conditions, no severe occlusal diseases, arch integrity (except for single dental crowns), and no removable dentures.

The study excluded patients with other types of pathological inflammation of the oral cavity, systemic inflammatory or autoimmune disorders, severe decompensated chronic conditions, those undergoing exposure to occupational hazards, suffering from decompensated occupational diseases, severe metabolic disorders (diabetes mellitus, obesity, gout, etc.), acute inflammation (acute respiratory infection, pneumonia, bronchitis, etc.), menopausal disorders, smoking, alcohol/drug abuse, as well as pregnant patients and those unwilling to comply with the study rules.

The study group received standard therapy against moderate GCP recommended by RDA: the oral cavity was rinsed with chlorhexidine, miramistin or triclosan; full mouth debridement was performed (plaques and calculus were removed) and metronidazole was applied locally. On average, the course of treatment lasted 10 to 14 days.

SIgA concentrations were measured in the samples of oral fluid and peripheral blood serum before and after the treatment using ELISA. For the analysis, we used monoclonal antibodies specific to the secretory immunoglobulin component (Seramun Diagnostica GmbH; Germany). Saliva samples were either fasting or collected no sooner than one hour after meals.

The obtained data was analyzed using Student's t-test for normal distribution. Normality of data distribution was assessed with the Shapiro-Wilk test: if the yielded value was over 0.05, distribution was considered normal. Sample variance was calculated before and after the treatment. If the obtained values were equal, means (M) and the standard deviation (σ) were computed and compared to the reference values, considering that differences were significant at $p < 0.05$. The results were presented as M ± σ.

Statistical analysis was performed in *Statistica* v10.0 (*StatSoft*; USA).

RESULTS

Secretory immunoglobulin A is produced by plasma cells arising from the differentiation of B lymphocytes associated with major and minor salivary glands or present in the *lamina propria* of the oral mucosa. The immunoglobulin is released into the cavities lined with mucosa and is not expected to be found in the peripheral blood. So, we hypothesized that damage to the oral mucosa would result in the "leakage" of sIgA into the blood serum.

We found that sIgA was present in the serum and oral fluid of patients with GCP. SIgA concentrations in the oral fluid were significantly lower in the diseased individuals than in the healthy volunteers both before and after the treatment. Before the treatment, sIgA levels in the blood serum of the patients were 0.21 ± 0.28 µg/ml, exceeding the values demonstrated by the healthy participants (0.11 ± 0.06 µg/ml).

Before the treatment, sIgA concentrations measured in the oral fluid of the patients were 36.5 ± 28.6 µg/ml, whereas after the treatment the figures changed to 54.6 ± 30.5 µg/ml, which was significantly lower ($p < 0.05$) than in the healthy volunteers (151.2 ± 105.2 µg/ml). SIgA was present in the serum of patients with GCP both before and after the treatment. Upon completing the treatment course, SIgA concentrations were found to have increased from 0.21 ± 0.28 to 0.35 ± 0.47 µg/ml. This is not typical, but considering that sIgA levels in the oral fluid and in the serum had risen by 52% and 50%, respectively, by the end of the treatment course, we can assume that the mucosal barrier did not recover and its permeability remained high. Therefore, the rise in sIgA concentrations both in the oral fluid and blood serum was almost identical (Fig. 1 and 2).

DISCUSSION

By the end of the treatment course, sIgA had increased by 51% relative to its initial concentrations, but the increase amounted to only 35% of the reference values, which is apparently not enough to ensure effective protection, regeneration and stability of periodontal tissue in the presence of other factors promoting susceptibility to periodontitis. Under such

s-IgA in the oral fluid (µg/ml)	36.5 ± 28.4	54.6 ± 30.5**

■ Before treatment ■ After treatment

Fig. 1. SIgA concentrations in the oral fluid of patients with GCP before and after the standard treatment (** $p < 0.05$)

s-IgA in the blood serum (µg/ml)	0.21 ± 0.28	0.35 ± 0.47

■ Before treatment ■ After treatment

Fig. 2. SIgA concentrations in the blood serum of patients with GCP before and after the standard treatment

s-IgA in the oral fluid (µg/ml)	151.2 ± 105.2	54.6 ± 30.05**

■ Healthy volunteers ■ Patients with GCP after treatment

Fig. 3. Comparison of SIgA concentrations in the oral fluid of patients with GCP after the standard treatment and in healthy volunteers (** $p < 0.05$)

s-IgA in the blood serum (µg/ml)	0.11 ± 0.06	0.35 ± 0.47**

■ Healthy volunteers ■ Patients with GCP after treatment

Fig. 4. Comparison of SIgA concentrations in the blood serum of patients with GCP after the standard treatment and in healthy volunteers (** $p < 0.05$)

conditions, microorganisms thrive, continuing to colonize the periodontium of the patients with compromised innate and acquired (lysozyme, interferons, lactoferrin, etc.) immunities (Fig. 3) [8].

Our hypothesis about damage to the mucosal barrier in patients with GCP is supported by the results of sIgA measurements in the blood serum of such patients. After the treatment, sIgA was elevated. Increased sIgA in the oral fluid can be explained by the fact that standard therapies rely on the use of antimicrobial drugs and professional dental cleaning, which reduces bacterial burden in periodontal tissue. As the bacterial population shrinks, sIgA concentrations grow since sIgA is utilized by the organism less intensively; however, its synthesis does not increase (Fig. 4).

In addition, our study demonstrates that conventional therapy causes only temporary improvement in the periodontal tissue state, ensuing from the use of antimicrobial agents and professional dental cleaning procedures. Recovery of the mucosal barrier does not occur because its permeability remains abnormally high even after the treatment. We observed an increase in sIgA levels both in the oral fluid and blood serum of the patients who underwent the full treatment course.

Therefore, in spite of positive dynamics of periodontal indices and mitigated symptoms of inflammation (reduced swelling and bleeding, alleviated pain, partial or full resolution of discomfort in the mouth), the efficacy of treatment for chronic periodontal inflammation should be improved further. The applied therapies should account for all known mechanisms of pathology, including damage to the mucosal barrier.

CONCLUSIONS

The standard treatment regimen for GCP includes professional dental cleaning procedures, antimicrobial and anti-inflammatory drugs. It does not have a healing effect on the mucosal barrier, which largely determines the ability of periodontal tissue to regenerate. This conclusion was drawn from the increased sIgA concentrations in the blood serum of patients with GCP after completing the full therapy course. When the integrity of the mucosal barrier breaks, pathogenicity factors damage periodontal tissue, leaving it remodeled and unresponsive to treatment. In patients with periodontal inflammation, treatment outcomes can be improved by using a comprehensive approach that accounts for all known mechanisms of this pathology.

References

1. Sashkina TI, Volozhin AI, Atakanova ZA, Shevchenko TV. Povyshenie mestnogo immuniteta v polosti rta s pomoshh'ju zhevatel'nyh tabletok Kolostrum (molozivo novozelandskih korov). Cathedra. Stomatologicheskoe obrazovanie. 2007; 6 (3): 30–3. Russian.
2. Horuzhaya RE, Horuzhij ME, Isakov SV. Sostojanie slizistoj obolochki polosti rta i tkanej parodontal'nogo kompleksa u pacientov kardiologicheskogo profilja. Vestnik neotlozhnoj i vosstanovitel'noj mediciny. 2011; 12 (2): 287–90. Russian.
3. Kim MI. Vospalitel'nye zabolevanija parodonta kak projavlenie sistemnoj disfunkcii jendotelija. Krims'kij terapevtichnij zhurnal. 2012; (2): 38–40. Russian.
4. Dmitrieva LA, redaktor. Parodontit. Uchebnoe posobie. M.: MEDpresInform, 2007; 25 s. Russian.
5. Shatohin AI. Parodontopatii pri VICh-infekcii kak prognosticheskij pokazatel' immunosupressii. Parodontologija. 2012; 17 (3): 3–6. Russian.
6. Strobel S. Oral tolerance, systemic immunoregulation and autoimmunity. Ann N Y Acad Sci. 2002; (958): 47–58.
7. Sugawara S, Uehara A, Tamai R, Takada H. Innate immune responses in oral mucosa. J Endotoxin Res. 2002; 8 (6): 465–8.
8. Churilov LP, Vasilyev AG. Patofiziologija immunnoj sistemy. SPb.: Foliant, 2014; 664 s. Russian.

Литература

1. Сашкина Т. И., Воложин А. И., Атаканова З. А., Шевченко Т. В. Повышение местного иммунитета в полости рта с помощью жевательных таблеток Колострум (молозиво новозеландских коров). Cathedra. Стоматологическое образование. 2007; 6 (3): 30–3.
2. Хоружая Р. Е., Хоружий М. Е., Исаков С. В. Состояние слизистой оболочки полости рта и тканей пародонтального комплекса у пациентов кардиологического профиля. Вестник неотложной и восстановительной медицины. 2011; 12 (2): 287–90.
3. Ким М. И. Воспалительные заболевания пародонта как проявление системной дисфункции эндотелия. Кримський терапевтичний журнал. 2012; (2): 38–40.
4. Дмитриева Л. А., редактор. Пародонтит. Учебное пособие. М.: МЕДпресИнформ, 2007; 25 с.
5. Шатохин А. И. Пародонтопатии при ВИЧ-инфекции как прогностический показатель иммуносупрессии. Пародонтология. 2012; 17 (3): 3–6.
6. Strobel S. Oral tolerance, systemic immunoregulation and autoimmunity. Ann N Y Acad Sci. 2002; (958): 47–58.
7. Sugawara S, Uehara A, Tamai R, Takada H. Innate immune responses in oral mucosa. J Endotoxin Res. 2002; 8 (6): 465–8.
8. Чурилов Л. П., Васильев А. Г. Патофизиология иммунной системы. СПб.: Фолиант, 2014; 664 с.

HYPOGRAVITY AS A RISK FACTOR FOR INCREASED INTRAOCULAR PRESSURE

Valyakh MA[1], Kats DV[1], Glazko NG[2], Baranov MV[3]

[1] Pirogov Russian National Research Medical University, Moscow, Russia

[2] Filatov City Clinical Hospital № 15, Moscow, Russia

[3] Research Institute for Space Medicine, Moscow, Russia

Space medicine has long studied the impact of reduced gravity on the human body. Increasing complaints of insufficient visual acuity during and after space flights have been recently drawing a lot of attention to the effects of hypogravity on astronauts' vision. Abnormally high intraocular pressure (IOP) is one of the most clinically important changes occurring during space missions. It is a serious condition that often causes irreversible damage to the optic nerve and blindness. The aim of this study was to explore the effect of reduced gravity on IOP. The study recruited 48 young healthy men with the mean age of 22 years, who formed 2 equally sized groups. In the experimental group, hypogravity was simulated by placing the subjects into the orthostatic position for 21 days. IOP was measured at 4 time points using a Maklakov tonometer. Z-approximation of the Wilcoxon T test was applied. The average increase in IOP in the experimental group was 3.42 ± 0.03 mmHg ($p < 0.01$). The changes were, however, transient, and IOP levels went back to normal right after the exposure to hypogravity conditions was terminated.

ГИПОГРАВИТАЦИЯ КАК ФАКТОР РИСКА ПОВЫШЕНИЯ УРОВНЯ ВНУТРИГЛАЗНОГО ДАВЛЕНИЯ

М. А. Валях[1]✉, Д. В. Кац[1], Н. Г. Глазко[2], М. В. Баранов[3]

[1] Российский национальный исследовательский медицинский университет имени Н. И. Пирогова, Москва, Россия

[2] Городская клиническая больница № 15 имени О. М. Филатова, Москва, Россия

[3] Научно-исследовательский институт космической медицины, Москва, Россия

Космическая медицина давно занимается исследованием воздействия условий измененной гравитации на организм человека. За последнее время все больше внимания исследователи уделяют изменениям со стороны органа зрения. В первую очередь, это связано с увеличением жалоб космонавтов на недостаточную остроту зрения во время и после окончания космических полетов. Среди наиболее важных изменений у них было обнаружено повышение внутриглазного давления (ВГД) — наиболее опасная патология, нередко приводящая к необратимой слепоте за счет поражения зрительного нерва. Целью исследования было выяснить влияние измененной гравитации на офтальмотонус. Для этого 48 здоровых мужчин, средний возраст которых не превышал 22 года, были разделены на две равные по численности группы: группу контроля и группу, в которой моделировали условия гипогравитации путем помещения испытуемых в ортостатическое положение на время всего эксперимента (21 сутки). Измерение ВГД проводили в четырех контрольных точках эксперимента с помощью тонометра Маклакова. Была использована Z-аппроксимация Т-критерия Уилкоксона. Среднее увеличение ВГД в группе моделирования гипогравитации составило 3,42 ± 0,03 мм рт. ст. ($p < 0,01$). Стоит отметить, что данные изменения носили транзиторный характер и после окончания воздействия условий измененной гравитации показатели вернулись к исходным значениям.

The impact of extraterrestrial gravity on the human body during space missions has long been the subject of scientific research. But it was not until recently that researchers started to look into its effects on the vision of astronauts. There have been reports of elevated intraocular pressure (IOP) following exposure to hypogravity, or a decreased gravitational field. This type of gravity has been discovered on the Moon and is believed to be present on other planets of the Solar System [1–5].

The earliest evidence of elevated IOP during a space flight was obtained using a manual applanation tonometer: it showed a 20–25% increase in IOP within the first hour after takeoff [6].

Other researchers reported elevated IOP in more than half of astronauts during an orbital flight; the measurements were taken with a Tono-pen tonometer [7].

The following study was inspired by the reports of our foreign colleagues about changes to the eye structure and vision during space flights, the growing number of space missions, and the fact that elevated IOP can cause irreversible damage to the optic nerve head, eventually leading to visual impairment or blindness. The aim of the study was to explore how hypogravity affects intraocular pressure. It should be noted that our overseas colleagues also point to other changes that occur to the eye in space; however, none of such changes are as pronounced as an increase in intraocular pressure.

METHODS

The study was conducted in July 2016 at the facilities of the Department of Ophthalmology (Nesterov Faculty of General Medicine, Pirogov Russian National Research Medical University), Filatov State Clinical Hospital No. 15 and Research Institute for Space Medicine

The study recruited 48 male participants (96 eyes) aged 18–35 years who were in good physical shape, had no refractive errors (i.e. were emmetropic) or had mild or moderate myopia (up to –6 diopters). Individuals with acute eye conditions, corneal dystrophy, severe myopia (–6 diopters or more), previous corneal surgery, other pathologies, as well as females or males of different age were excluded from the study. The participants were divided into 2 equally sized groups using sealed envelopes (open-label controlled randomization).

Statistical analysis was carried out in *Statistica* 8.0 (StatSoft Inc.; USA). Variables that had normal distribution are presented below as M ± *m*, where M is the mean, *m* is the standard error. For pairwise comparison of two independent samples, the Mann–Whitney U test was applied. For repeated intragroup comparison, the Wilcoxon T test was used. Significance threshold was < 0.05.

In group 1, hypogravity was simulated at daytime by placing the participants into an orthostatic position so that an angle between the upper part of the body and the horizontal axis was +9.6°; at night the participants took a horizontal position. The experiment lasted for 21 days. To minimize exposure to any external stimuli, the rooms where the subjects were staying were sound-proof; the windows were locked tight. Only medical staff were allowed into the rooms; visits from family and friends were forbidden. Group 1 could use their phones or computers or read books according to the schedule. Medical tests and personal hygiene procedures could be performed with the participants lying horizontally. Meals could also be taken in bed.

Group 2 was the control group. No limitations were imposed on the body position in group 2 at daytime. At night (from 11 pm to 8 am) the participants lay in bed in the horizontal position. Medical tests were the same as in group 1 and were scheduled on the same days. Group 2 were allowed to take walks on the premises and receive visits from their family and friends. Their rooms were not sound-proof, the windows could be opened any time (Table 1).

For measurements and examinations, 4 basic time points were defined: 1) the time point of initial measurements, which was 1 day before the actual start of the experiment (i.e. before the participants were placed under simulated hypogravity conditions); 2) day 11 of the experiment; 3) day 21 of the experiment; 4) day 1 after the experiment was over (i.e. after the participants were allowed to leave the premises).

IOP was measured in the morning, because it is when it reaches its maximum, on the days specified above.

Besides, all study participants underwent ophthalmoscopy on the days specified above, as well as computerized perimetry before and after the experiment in order to detect possible damage to the optic nerve.

IOP measurements

IOP was measured with an applanation Maklakov tonometer (Krasnogvardeets; Russia) that had a 10 g plunger weight. The obtained data were converted into mmHg (P_0) using the Nesterov-Egorov conversion ruler. Normal IOP (P_0) is 10–22 mmHg when measured with a Maklakov tonometer with a 10 g plunger weight.

Direct ophthalmoscopy

Direct ophthalmoscopy of the ocular fundus was performed using a ВХα ophthalmoscope (certificate No. 2005/1022; NEITZ; Japan). During the experiment, no eyedrops were used, so the pupils were left undilated for the procedure However, mydriasis was induced to take measurements before the experiment and 1 day after it was over.

Computerized perimetry

Visual fields were measured by static perimetry using a Humphrey Field Analyzer II 750i (certificate No. 2008/02964; Zeiss; Germany). The analysis of the obtained data accounted for the number of false-positive and false-negative responses and the loss of fixation.

RESULTS

We observed a statistically significant increase in IOP (3.33 ± 0.08 mmHg) in all members of group 1 (the hypogravity model) on day 11. On day 21, IOP continued to grow (the increase was 3.42 ± 0.03 mmHg) relative to its value before the experiment. Still, it should be noted that on day 1 after the experiment was completed, IOP dropped to the level comparable to its values before the experiment (Table 2).

Direct ophthalmoscopy revealed no abnormalities in any of the participants in the course of the experiment. The optic disc head was pale pink, excavation was physiological (0.3–0.4). The vascular bundle was localized to the center. The trajectory

Table 1. Characteristics of the groups

Groups	Parameter		
	Number of patients/eyes	Spatial body position	Mean age, years
Group 1: hypogravity model	24/48	The orthostatic position with a +9.6° body tilt at day time alternated with the horizontal position at night (days 1 through 21 of observation)	21.75 ± 3.83
Group 2: control	24/48	No limitations on the body position (days 1 through 21 of observation)	21.21 ± 2.54

Table 2. Intraocular pressure in the experimental group

Time points	Parameter	
	Mean IOP + standard error, mmHg	
Initial	15,75 ± 0,72	
Day 11	19,08 ± 0,64	
	Δ initial — day 11 of the experiment	3.33 ± 0.08 $p < 0.01$
Day 21	19.17 ± 0.69	
	Δ initial — day 21 of the experiment	3.42 ± 0.03 $p < 0.01$
Day 1 after the experiment was completed	15.67 ± 0.62	
	Δ initial — day 1 after the experiment	0.08 ± 0.1 $p > 0.05$

Table 3. Intraocular pressure in the control group

Time points	Parameter	
	Mean IOP + standard error, mmHg	
Initial	15.75 ± 0.72	
Day 11	15.79 ± 0.73	
	Δ initial — day 11 of the experiment	0.04 ± 0.01 $p > 0.05$
Day 21	15.71 ± 0.71	
	Δ initial — day 21 of the experiment	0,04 ± 0.01 $p > 0.05$
Day 1 after the experiment was completed	15.77 ± 0.71	
	Δ initial — day 1 after the experiment	0.02 ± 0.01 $p > 0.05$

and caliber of blood vessels was unchanged. No abnormalities were observed in the macular zone. No peripheral ruptures or dystrophy were noticed.

Computerized perimetry revealed no absolute scotomas or significant enlargement of the blind spot in group 1.

In the control group, IOP was stable throughout the experiment and upon its completion. Its values fell within the normal reference range in all members of group 2 (Table 3). Similar to group 1, no pathologies were detected during direct ophthalmoscopy and computerized perimetry.

Statistical analysis of IOP changes assisted by the Mann–Whitney U test for two independent samples showed that $U_{emp.}$ was 0 in both groups whereas U_{crt} was 834 ($p < 0.01$), suggesting statistical significance and reliability of the obtained results.

DISCUSSION

Hypogravity causes elevated intraocular pressure. We discovered a reliable and statistically significant increase in IOP that rose by an average of 3.42 ± 0.03 mmHg. However, this effect was transient because a day after the experiment was over, IOP was restored to normal values.

Such changes can be explained by a fluid shift in the body leading to an increased blood flow to the head and neck, including the choroid. The fluid shift causes the ocular volume to shrink and IOP to rise. As the body adapts to the conditions simulating a space flight, fluid and electrolytes are reabsorbed by renal tubules, the rate of glomerular filtration increases and urination becomes more frequent, speeding up clearance of osmotically active agents from the body. This brings IOP to its normal values [8]. Another possible explanation for our findings is that the fluid shift induces increased secretion of intraocular fluid but its drainage worsens [9].

CONCLUSIONS

1. Throughout the entire experiment that modelled hypogravity we observed a statistically significant and reliable increase in IOP ($p < 0.01$). 2. IOP increase under hypogravity conditions was transient, and IOP values went back to normal after the experiment was completed. 3. Direct ophthalmoscopy revealed no changes to the ocular fundus and the optic nerve head during the experiment. 4. Computerized perimetry also revealed no abnormalities induced by hypogravity.

References

1. Rastegar N, Eckart P, Mertz M. Radiation — induced cataract in astronauts and cosmonauts. Graefes Arch Clin Exp Ophthalmol. 2002; (240): 534–47.
2. Thomas H, Mader C, Robert OD, Anastas F. Optic Disc Edema, Globale Flattening, Choroidal Folds, and Hyperopic Shifts Observed in Astronauts after Long — duration Space Flight.

American Academy of Ophthalmology Published by Elsevier Inc. 2011; 2058–70.
3. Chylack BE, Peterson LE, Feiveson AH, et al. NASA study of cataract is astronauts (NASA). Report 1: Cross — sectional study of the relationship of exposure to space radiation and risk of lens opacity. Radiat Res. 2009; (172): 10–20.

4. Cucinotta FA, Manuel FK, Jones J, et al. Space radiation and cataracts in astronauts. RADIAT Res. 2001; 460–6.
5. Frey MA. Radiation health: mechanism of radiation — induced cataracts in astronauts. Aviat Space Environ Med. 2009; 575–6.
6. Draeger J. Tonometry under microgravity conditiions. Norderney Symposium on Scentific Results of the German Spacelab Mission D1. 1986; 503–9.
7. Mekjavic PJ, Eiken O, Mekjavic IB. Visual function after prolonged bed rest. J Gravit Physil. 2002; (9): 31–2.

8. Kergoat H, Lovasik JV. Seven-degree head-down tilt reduces choroidal pulsatile ocular blood flow. Aviation, Space and Enviromental Medicine. 2005; 76 (10): 930–5.
9. Mader TH, Gibson GR, Pass AF, et al. Optic disc edema globe flattening, choroidal folds, and hyperopic shifts observed in astronauts after long-dyration space flight. Ophthalmology. 2011; (118): 2058–69.

Литература

1. Rastegar N, Eckart P, Mertz M. Radiation — induced cataract in astronauts and cosmonauts. Graefes Arch Clin Exp Ophthalmol. 2002; (240): 534–47.
2. Thomas H, Mader C, Robert OD, Anastas F. Optic Disc Edema, Globale Flattening, Choroidal Folds, and Hyperopic Shifts Observed in Astronauts after Long — duration Space Flight. American Academy of Ophthalmology Published by Elsevier Inc. 2011; 2058–70.
3. Chylack BE, Peterson LE, Feiveson AH, et al. NASA study of cataract is astronauts (NASA). Report 1: Cross — sectional study of the relationship of exposure to space radiation and risk of lens opacity. Radiat Res. 2009; (172): 10–20.
4. Cucinotta FA, Manuel FK, Jones J, et al. Space radiation and cataracts in astronauts. RADIAT Res. 2001; 460–6.

5. Frey MA. Radiation health: mechanism of radiation — induced cataracts in astronauts. Aviat Space Environ Med. 2009; 575–6.
6. Draeger J. Tonometry under microgravity conditiions. Norderney Symposium on Scentific Results of the German Spacelab Mission D1. 1986; 503–9.
7. Mekjavic PJ, Eiken O, Mekjavic IB. Visual function after prolonged bed rest. J Gravit Physil. 2002; (9): 31–2.
8. Kergoat H, Lovasik JV. Seven-degree head-down tilt reduces choroidal pulsatile ocular blood flow. Aviation, Space and Enviromental Medicine. 2005; 76 (10): 930–5.
9. Mader TH, Gibson GR, Pass AF, et al. Optic disc edema globe flattening, choroidal folds, and hyperopic shifts observed in astronauts after long-dyration space flight. Ophthalmology. 2011; (118): 2058–69.

A BIONIC EYE: PERFORMANCE OF THE ARGUS II RETINAL PROSTHESIS IN LOW-VISION AND SOCIAL REHABILITATION OF PATIENTS WITH END-STAGE RETINITIS PIGMENTOSA

Takhchidi KhP[1], Kachalina GF[2], Takhchidi NKh[2], Manoyan RA[2], Gliznitsa PV[1] ✉

[1] Pirogov Russian National Medical Research University, Moscow, Russia

[2] Scientific Clinical Center of Otorhinolaryngology, FMBA of Russia, Moscow, Russia

The death of outer retinal layers occurring in retinitis pigmentosa causes severe visual impairment and often leads to total blindness. Inner retinal layers are spared, though, which provides a possibility of inducing visual perception by direct electrical stimulation of intact retinal cells. This article presents clinical outcomes of two patients who were the first in Russia to have received the Argus II Retinal Prosthesis System. Both implantations were successful. No complications were reported throughout the entire follow-up period. Upon completing 3 rehabilitation sessions, the patients were able to navigate indoors and outdoors, locate small high-contrast objects, discern contours of large objects and people's silhouettes.

Keywords: bionic eye, artificial vision, retinal prosthesis, implant, Argus II, retinitis pigmentosa, retinal abiotrophy

БИОНИЧЕСКИЙ ГЛАЗ: ВОЗМОЖНОСТИ ЭПИРЕТИНАЛЬНОЙ ПРОТЕЗНОЙ СИСТЕМЫ ARGUS II В ЗРИТЕЛЬНОЙ И СОЦИАЛЬНОЙ РЕАБИЛИТАЦИИ СЛЕПЫХ ПАЦИЕНТОВ С ТЕРМИНАЛЬНОЙ СТАДИЕЙ ПИГМЕНТНОГО РЕТИНИТА

Х. П. Тахчиди[1], Г. Ф. Качалина[2], Н. Х. Тахчиди[2], Р. А. Маноян[2], П. В. Глизница[1] ✉

[1] Российский национальный исследовательский медицинский университет имени Н. И. Пирогова, Москва, Россия

[2] Научно-клинический центр оториноларингологии ФМБА, Москва, Россия

При пигментном ретините происходит гибель наружных слоев сетчатки, сопровождающаяся значительными нарушениями зрительных функций вплоть до слепоты. Сохранность внутренних слоев сетчатки при данной патологии позволила разработать специальные устройства, использующие прямую электрическую стимуляцию для получения зрительного восприятия. В работе представлены результаты впервые проведенных в Российской Федерации двух операций по имплантации эпиретинальной протезной системы Argus II. Обе операции прошли успешно, осложнения отсутствовали на протяжении всего периода наблюдения. После прохождения трех курсов реабилитации пациенты приобрели навыки перемещения внутри помещения и на открытых пространствах, способны определять локализацию высококонтрастных мелких предметов, контуры больших предметов, силуэты людей.

Ключевые слова: бионический глаз, искусственное зрение, эпиретинальный протез, имплантат, Argus II, пигментный ретинит, абиотрофия сетчатки

Retinitis pigmentosa is a group of inherited disorders characterized by progressive degeneration of the retinal pigment epithelium and photoreceptors. Patients with retinitis pigmentosa gradually lose their side and night vision, suffer from decreased visual acuity and can eventually develop total blindness [1]. However, inner retinal layers (bipolar neurons, ganglion cells and the optic nerve layer) are not affected by the pathology [2, 3]. This provides a possibility of inducing visual perception in such patients by direct electrical stimulation of spared retinal cells using an implantable device [4, 5]. To date, about 10 such projects have been launched worldwide.

The Argus II Retinal Prosthesis System is the most in-demand retinal implant. So far, over 350 Argus devices have been implanted. Argus II has been approved for commercial use by the European Union. It has also received approval from the American Food and Drug Association (FDA) as a humanitarian use device [6, 7]. Argus II consists of externally worn equipment (a pair of glasses with an integrated video camera and a video processing unit) and an implantable unit (a scleral band, an electronics case, a receiving coil and an array of 60 electrodes, which is affixed to the retina). The video camera captures the scene; the obtained video signals are transformed

by the processing unit and transmitted to the implant, which electrically stimulates intact retinal cells. The emitted pulses are perceived by the patient as patterns of light [8]. Ideally, one electrode will activate only its neighboring cells and induce visual perception in the form of circular spots of light, which is important for perceiving the shape of objects [9].

This study aimed to assess the use of the Argus II Retinal Prosthesis System in low-vision and social rehabilitation of blind patients with end-stage retinitis pigmentosa.

METHODS

The study was carried out at the facilities of the Scientific Research Center for Ophthalmology of Pirogov Russian National Medical Research University and the Scientific Clinical Center of Otorhinolaryngology. Two patients were selected from a list of 20 candidates with retinitis pigmentosa. Those 2 individuals were the first Russian patients to receive the Argus II Retinal Prosthesis System (Second Sight Inc.; USA). One patient underwent surgery on June 30, 2017; the other, on December 4, 2017.

The following implantation eligibility criteria were applied: end-stage retinitis pigmentosa; bare light perception; a previous history of useful form vision; age over 25 years. Contraindications for implantation included corneal opacity in the optical zone; optic nerve diseases; choroidal neovascularization; the axial eye length < 20.5 mm and > 26 mm.

Case 1

Patient U., aged 58, was diagnosed with end-stage retinitis pigmentosa of both eyes and referred to our Clinical Research Center. His visual acuity was (1/∞) pr. l. incertae for both eyes. Based on electroretinography findings, the right eye (OD) was selected as a better candidate for implantation.

Before surgery, visual acuity in OD was (1/∞) pr. l. incertae and intraocular pressure was 16 mmHg. Biomicroscopy revealed no abnormalities in the anterior segment. Opacities were starting to form in the central zone of the lens. In the ocular fundus, the optic disc was pale, waxy, with sharp margins; blood vessels were attenuated. The anatomy of the macula was intact but a depigmented ring-shaped area was observed

on the periphery. The macular reflex was absent. Perivascular bone spicule pigment deposits were noticed in the periphery; the retina was atrophied (Fig. 1A).

Retinal atrophy was confirmed by a crossline optical coherence tomography (OCT) scan performed with Spectralis OCT (Heidelberg Engineering, Inc.; Germany). The atrophy was the most pronounced in the outer layers. Measured by electroretinography, the perceptual threshold (PT) was 800 μA and the flicker fusion rate was 60 Hz.

Surgery was performed according to the protocol recommended by the manufacturer of the retinal prosthesis. It lasted 5 hours and consisted of the following stages: the natural lens was removed and an artificial intraocular lens was implanted; the scleral band with the electronics case was passed under the recti muscles, encircling the globe, and secured in place; subtotal vitrectomy was performed followed by the implantation of the intraocular segment of the prosthesis; the electrode array was secured to the retina in the macular zone with a retinal tack; the scleral wound and the conjunctiva were then closed.

Case 2

Female patient Z., aged 56, was diagnosed with end-stage retinitis pigmentosa of both eyes. Her visual acuity was (1/∞) pr. l. incertae in both eyes. The OCT scan of the retina revealed that the patient was able to fix the gaze with her right eye. Therefore, the worse-seeing left eye was selected for surgery as recommended by the manufacturer of Argus II.

Before surgery, the patient's visual acuity was (1/∞) pr. l. incertae in both eyes and intraocular pressure was 16 mmHg. Biomicroscopy revealed no abnormalities in the anterior segment. Opacities were starting to form in the central zone of the lens. In the ocular fundus, the optic disc was pale, waxy, with sharp margins; blood vessels were attenuated. The anatomy of the macula was intact; a depigmented ring-shaped area was observed on the periphery. The macular reflex was absent. Perivascular bone spicule pigment deposits were noticed in the periphery; the retina was atrophied (Fig. 2A). A crossline OCT scan revealed retinal atrophy that was very pronounced in outer retinal layers. Measured by electroretinography, the perceptual threshold (PT) was 500 μA and the flicker fusion rate was 75 Hz.
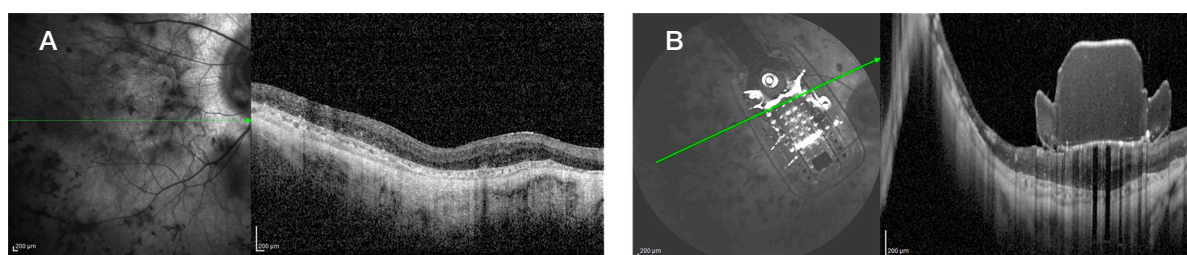

Fig. 1. OCT scans of patient U.'s right eye before (**A**) and after (**B**) implantation of Argus II show the correct position of the implant secured to the retina
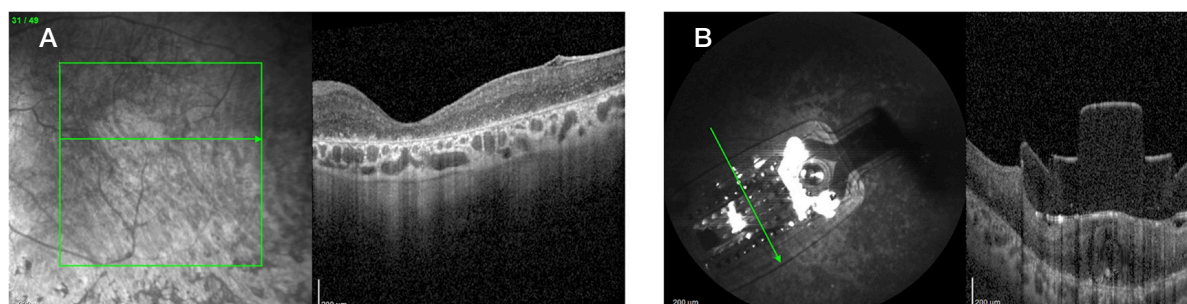

Fig. 2. OCT scans of patient Z.'s left eye before (**A**) and after (**B**) implantation of Argus II show the correct position of the implant secured to the retina

Surgery, which lasted 4 hours, was performed according to the protocol described above.

RESULTS

The patients received 3 post-operative rehabilitation sessions each. During the sessions, they were trained to use the device both indoors and outdoors. Their visual function was assessed by 3 tests that were conducted in a darkened room using software and a touch screen monitor supplied by Second Sight (Fig. 3). In the Grating Visual Acuity test, black and white lines varying in width appeared on the screen. The lines were moving in different directions. The patient had to identify the direction of each line. In the Motion of Direction test, a white line was moving across the black screen in different directions. The task was to identify the direction of movement. In the third test called the Square Localization test differently sized white squares appeared in different parts of the black screen; the patient was asked to locate the square on the screen.

Patient 1 had no complications during or after implantation in the follow-up period. The medication therapy he received conformed to the guidelines provided by the implant's manufacturer. Two weeks after surgery, primary wound healing was observed; the wound showed no discharge or signs of inflammation. The scleral band and the electronics case were securely held in place. Ocular mobility was normal. The scleral and conjunctival wounds did not leak. Intraocular pressure measured by an Icare® PRO tonometer (iCare PRO; Finland) was 17–18 mmHg. The cornea was transparent. The deep anterior chamber was filled with transparent fluid. The intraocular lens was well-centered. The electrode array was also held in place, fitting snugly against the retina (Fig. 1B).

The implant was activated 2 weeks after surgery as planned. Diagnostic testing revealed that all 60 electrodes conducted electric current. OCT showed that the array was fitted snugly against the retina. Impedance was measured for each electrode. Perceptual thresholds were determined from instrumentation readings and the patient's feedback. Because their values fell within the acceptable range, all 60 electrodes could be used to induce visual perception (Fig. 4A).

Once the implant was activated for custom fitting, the patient reported seeing flashes of light (phosphenes) of different shapes and shades. The first training session was conducted a month after surgery. During the session, the patient was taught basic skills needed to use the system. Two months after surgery, during the second session, the patient was trained to navigate indoors. He learnt to locate small high-contrast objects, identify contours of large objects, human silhouettes,

etc. (Fig. 5A). The third session was held in month 6 following the surgical procedure. The patient's visual function assessed by a number of tests continued to improve. Now he was able to navigate both indoors and outdoors. Tests showed that the patient performed better with the Argus 2 system on (Fig. 6).

Patient 2 also had no complications during or after implantation in the follow-up period. The medication therapy she received conformed to the guidelines provided by the implant's manufacturer. Two weeks after surgery, primary wound healing was observed; the wound showed no discharge or signs of inflammation. The scleral band and the electronics case were securely held in place. Ocular mobility was normal. The scleral and conjunctival wounds did not leak. Intraocular pressure measured by an Icare® PRO tonometer (iCare PRO; Finland) was 16–17 mmHg. The cornea was transparent. The deep anterior chamber was filled with transparent fluid. The intraocular lens was well-centered. The electrode array was also held in place, fitting snugly against the retina (Fig. 2B).

The implant was activated 2 weeks after surgery as planned. Diagnostic testing revealed that all 60 electrodes conducted electric current. OCT showed that the array was fitted snugly against the retina. Impedance was measured for each electrode. Perceptual thresholds were determined from instrumentation readings and the patient's feedback. Three electrodes failed to induce visual perception at acceptable perceptual thresholds, so only the remaining 57 electrodes were used to stimulate spared retinal cells (Fig. 4B). Once the implant was activated, the patient reported seeing flashes of light of different shades and shapes. The patient was also immediately able to discern people's silhouettes (Fig. 5B).

In the first training session, the patient learnt basic skills needed to use the device. The second session took place in month 6 after surgery. The patient was taught to navigate indoors, locate small high-contrast objects, contours of large objects, people's silhouettes, etc. Tests showed that she performed better with the Argus 2 system on (Fig. 7).
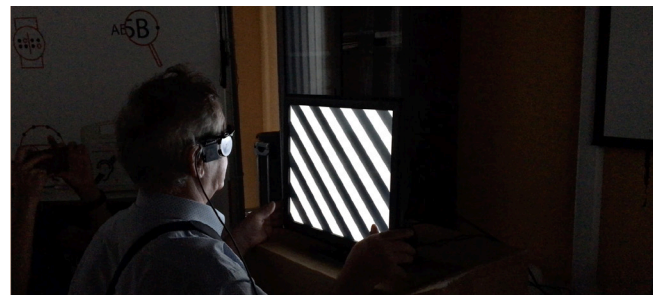

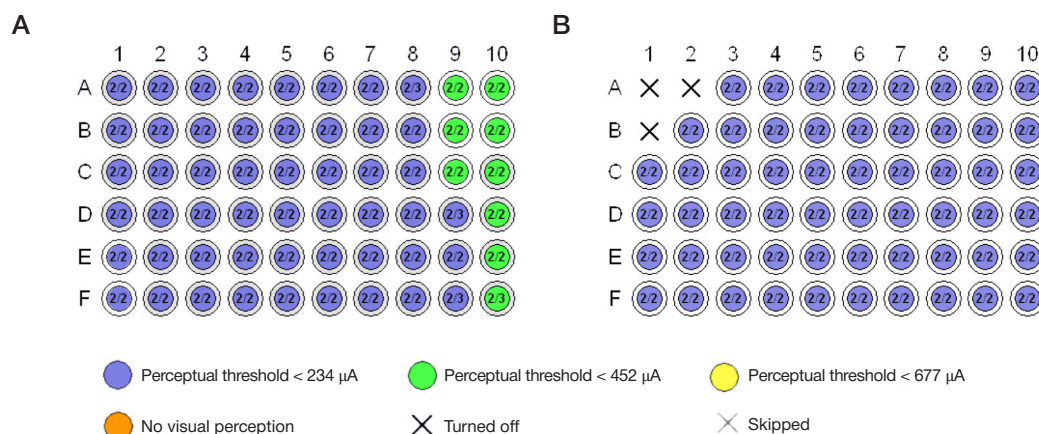**Fig. 3.** Patient U. is taking a Grating Visual Acuity test

Fig. 4. Stimulation charts of the implants showing perceptual thresholds for each of 60 electrodes in patient U. (**A**) and patient Z. (**B**)
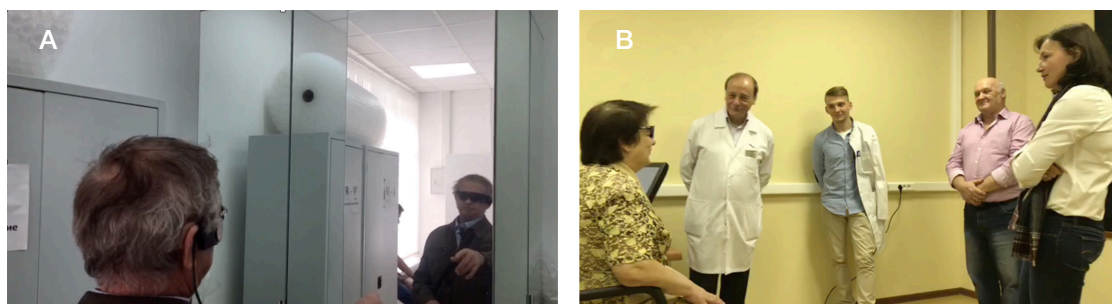
Fig. 5. Patient U. identifies a mirror before him and recognizes his own reflection (**A**). Patient Z. can correctly tell the number of people standing in front of her during the custom fitting session (**B**)
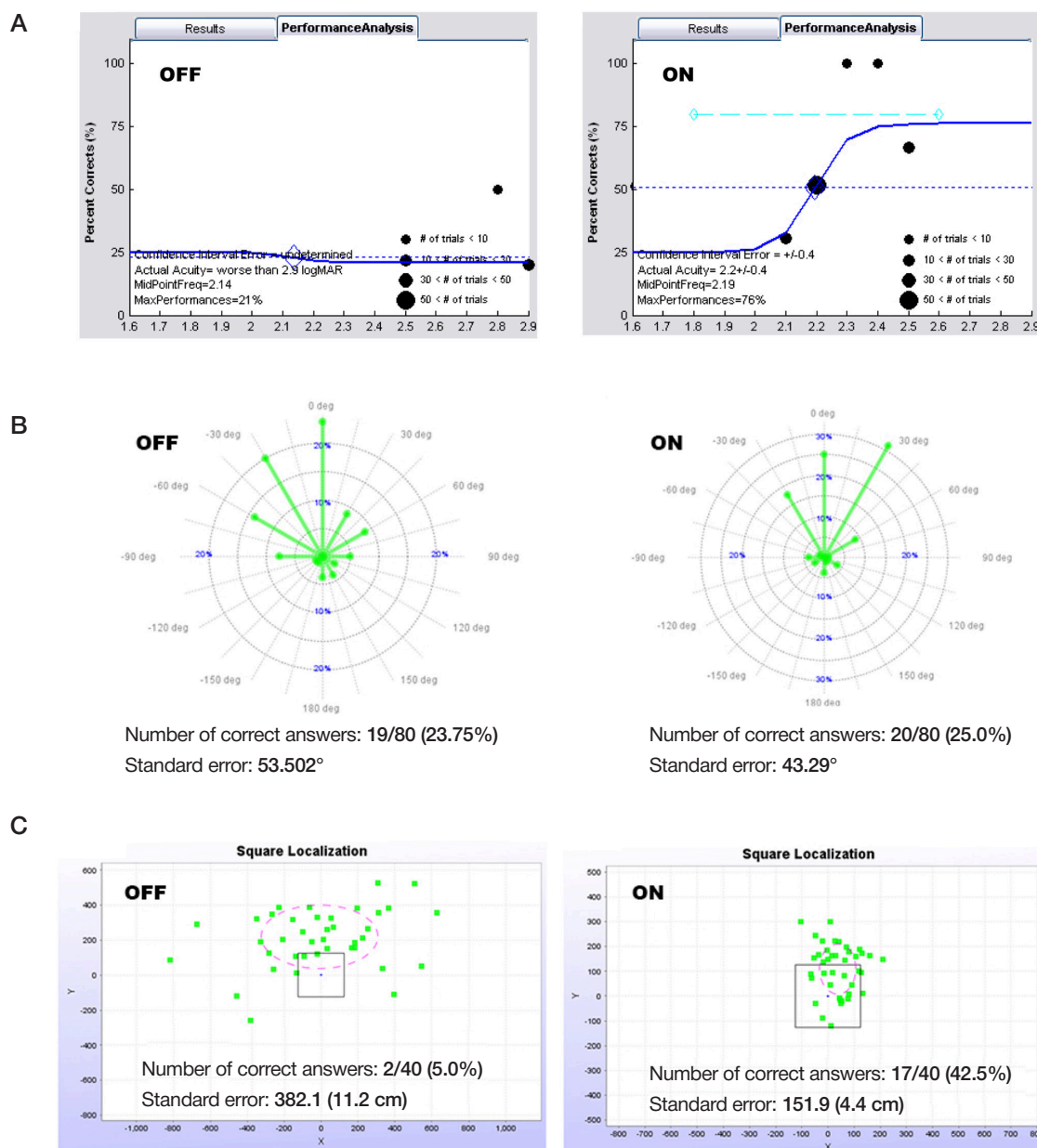

Fig. 6. Results of visual assessment computer tests done by patient U. with Argus II off and on: the Grating Visual Acuity Test (**A**); the Direction of Motion test (**B**); the Square Localization test (**C**)

After completing the basic rehabilitation course, both patients felt they did not require assistance at home: they were able to locate eating utensils and household appliances, could go from one room to another, etc. They could use public transport, take walks outdoors, go shopping, etc on their own. For safety reasons, the patients were accompanied by family or friends when taking new or long routes. At present, patient U. performs in his own magic show together with his dog all over Russia (Fig. 8A). Patient Z. has taken part in a Moscow fashion show (Fig. 8B). Both patients attend conferences on the problems of vision rehabilitation.
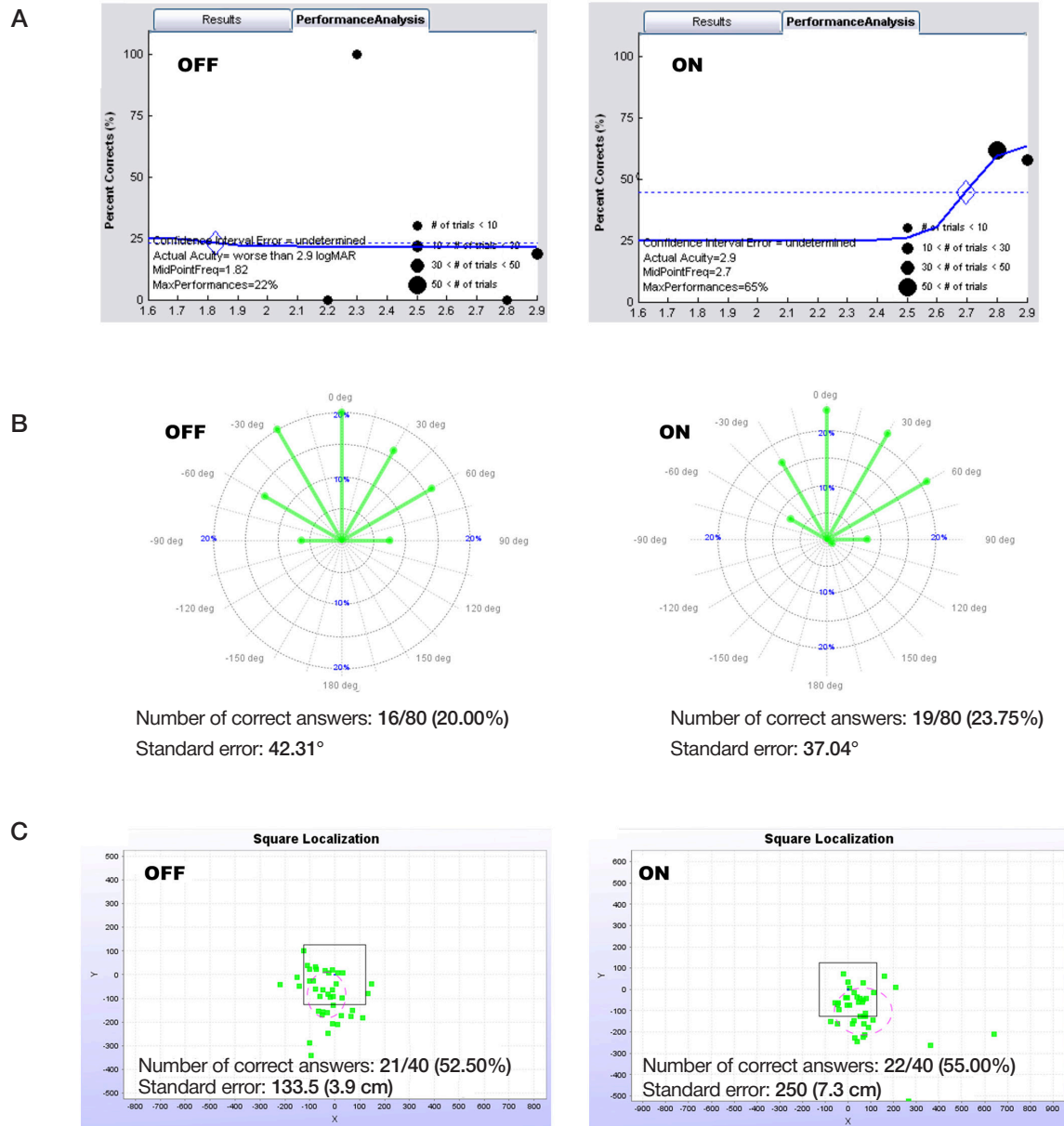
Fig. 7. Results of visual assessment computer tests done by patient Z. with Argus II off and on: the Grating Visual Acuity Test (**A**); the Direction of Motion test (**B**); the Square Localization test (**C**)
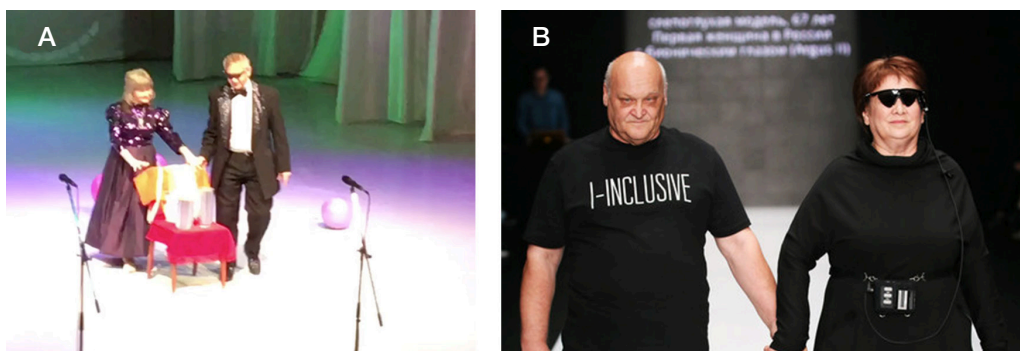

Fig. 8. Patient U. is giving a magic show in Chelyabinsk (**A**); patient Z. on a catwalk during a fashion show in Moscow (**B**)

DISCUSSION

A 5-year multicenter clinical efficacy and safety trial of Argus II in patients with retinitis pigmentosa has yielded the following results: visual perception was induced in 100% of patient implanted with Argus II right upon activation of the implant; 96% of patients performed better in the Square Localization test with Argus II on; 57% of patients performed better in the Direction of Motion test with Argus II on; 23% of patients had measurable grating visual acuity with the implant on; post-operatively, the average number of functional electrodes in those patients was 43 [10, 11]. Our

patients performed better in each of the 3 tests with Argus II on, which places them in the group of individuals with the best clinical outcomes. No complications were observed in both patients during surgery and post operatively; all 60 electrodes were functional after implantation. Visual perception was successfully induced in both patients by activating 60 and 57 electrodes, respectively. In the second patient, 3 electrodes were turned off because they failed to induce visual perception at an acceptable perceptual threshold. Given that only 23% of all patients with an implanted Argus II prosthesis had measurable grating visual acuity over 2.9 LogMAR (Vis = 0.001) and that in patient U. grating visual acuity was 2.2 LogMAR (Vis = 0.006) (Fig. 6A), we believe in the case of our patient, the clinical outcome was one of the best possible [8, 12].

Significant positive changes in the patients' social life were driven by their desire to see again, which encourage them to work hard on a daily basis to improve their Argus II skills. Socially, patients have benefited greatly from increasing

attention to this unique technology that allows blind people to restore some vision.

CONCLUSIONS

The Argus II Retinal Prosthesis System is a robust tool that facilitates social and low-vision rehabilitation of blind patients with end-stage retinitis pigmentosa. Both patients are very satisfied with the results they have achieved. They are able to navigate indoors and outdoors without assistance and report that their quality of life has significantly improved. Success of Argus II demonstrates that 1) an interaction between a retinal implant and the natural retina can be effective in transmitting the collected video data into the visual cortex; 2) these data can be perceived by the cortex as visual in response to electrical stimulation of retinal neurons; 3) these visual data can be successfully used by patients with end-stage retinitis pigmentosa helping them to become less dependent on other people in their daily life, improve their social adaptation and ultimately enjoy a better quality of life.

References

1. Grüsser O-J, Hagner M. On the history of deformation phosphenes and the idea of internal light generated in the eye for the purpose of vision. History of Ophthalmology book series. ACOI. 1990; (3): 57–85.
2. Loewenstein JI, Montezuma SR, Rizzo JF. Outer retinal degeneration: an electronic retinal prosthesis as a treatment strategy. Arch Ophthalmol. 2004; 122 (4): 587–96.
3. Brelen ME, Duret F, Gerard B, Delbeke J, Veraart C. Creating a meaningful visual perception in blind volunteers by optic nerve stimulation. J Neural Eng. 2005; (2): 22–8.
4. Ghodasra DH, Chen A, Arevalo JF, et al. Worldwide Argus II implantation: recommendations to optimize patient outcomes. BMC Ophthalmol. 2016; 16 (1): 52.
5. Humayun MS, de Juan E, Jr, Dagnelie G, Greenberg RJ, Propst RH, Phillips DH. Visual perception elicited by electrical stimulation of retina in blind humans. Arch Ophthalmol. 1996; 114 (1): 40–6.
6. Mills JO, Jalil A, Stanga PE. Electronic retinal implants and artificial vision: journey and present. Eye (Lond). 2017 Oct; 31 (10): 1383–98.
7. Yue L, Weiland JD, Roska B, Humayun MS. Retinal stimulation strategies to restore vision: Fundamentals and systems. Prog Retin Eye Res. 2016 Jul; 53: 21–47.
8. da Cruz L, Dorn JD, Humayun MS, Dagnelie G, Handa J, Barale P-O, et al. Five-Year Safety and Performance Results from the Argus II Retinal Prosthesis System Clinical Trial. Ophthalmology. 2016 Oct; 123 (10): 2248–54.
9. Chader GJ, Weiland J, Humayun MS. Artificial vision: needs, functioning, and testing of a retinal electronic prosthesis. Prog Brain Res. 2009; (175): 317–32.
10. Tran BK, Wolfensberger TJ. Retina-Implant Interaction after 16 Months Follow-up in a Patient with an Argus II Prosthesis. Klin Monbl Augenheilkd. 2017 Apr; 234 (4): 538–40.
11. de Balthasar C, Patel S, Roy A, et al. Factors a ec ng perceptual thresholds in epirenal prostheses. Invest Ophthalmol Vis Sci. 2008; 49 (6): 2303–14.
12. Besch D, Sachs H, Szurman P, et al. Extraocular surgery for implantation of an active subretinal visual prosthesis with external connections: feasibility and outcome in seven patients. Br J Ophthalmol. 2008; (92): 1361–8.

Литература

1. Grüsser O-J, Hagner M. On the history of deformation phosphenes and the idea of internal light generated in the eye for the purpose of vision. History of Ophthalmology book series. ACOI. 1990; (3): 57–85.
2. Loewenstein JI, Montezuma SR, Rizzo JF. Outer retinal degeneration: an electronic retinal prosthesis as a treatment strategy. Arch Ophthalmol. 2004; 122 (4): 587–96.
3. Brelen ME, Duret F, Gerard B, Delbeke J, Veraart C. Creating a meaningful visual perception in blind volunteers by optic nerve stimulation. J Neural Eng. 2005; (2): 22–8.
4. Ghodasra DH, Chen A, Arevalo JF, et al. Worldwide Argus II implantation: recommendations to optimize patient outcomes. BMC Ophthalmol. 2016; 16 (1): 52.
5. Humayun MS, de Juan E, Jr, Dagnelie G, Greenberg RJ, Propst RH, Phillips DH. Visual perception elicited by electrical stimulation of retina in blind humans. Arch Ophthalmol. 1996; 114 (1): 40–6.
6. Mills JO, Jalil A, Stanga PE. Electronic retinal implants and artificial vision: journey and present. Eye (Lond). 2017 Oct; 31 (10): 1383–98.
7. Yue L, Weiland JD, Roska B, Humayun MS. Retinal stimulation strategies to restore vision: Fundamentals and systems. Prog Retin Eye Res. 2016 Jul; 53: 21–47.
8. da Cruz L, Dorn JD, Humayun MS, Dagnelie G, Handa J, Barale P-O, et al. Five-Year Safety and Performance Results from the Argus II Retinal Prosthesis System Clinical Trial. Ophthalmology. 2016 Oct; 123 (10): 2248–54.
9. Chader GJ, Weiland J, Humayun MS. Artificial vision: needs, functioning, and testing of a retinal electronic prosthesis. Prog Brain Res. 2009; (175): 317–32.
10. Tran BK, Wolfensberger TJ. Retina-Implant Interaction after 16 Months Follow-up in a Patient with an Argus II Prosthesis. Klin Monbl Augenheilkd. 2017 Apr; 234 (4): 538–40.
11. de Balthasar C, Patel S, Roy A, et al. Factors a ec ng perceptual thresholds in epirenal prostheses. Invest Ophthalmol Vis Sci. 2008; 49 (6): 2303–14.
12. Besch D, Sachs H, Szurman P, et al. Extraocular surgery for implantation of an active subretinal visual prosthesis with external connections: feasibility and outcome in seven patients. Br J Ophthalmol. 2008; (92): 1361–8.